



University  
of Glasgow

Dong, Zhaoyang (2024) *Investigating the phosphorylation of free fatty acid receptor 4 and free fatty acid receptor 2*. PhD thesis.

<https://theses.gla.ac.uk/84441/>

Copyright and moral rights for this work are retained by the author

A copy can be downloaded for personal non-commercial research or study, without prior permission or charge

This work cannot be reproduced or quoted extensively from without first obtaining permission from the author

The content must not be changed in any way or sold commercially in any format or medium without the formal permission of the author

When referring to this work, full bibliographic details including the author, title, awarding institution and date of the thesis must be given

Enlighten: Theses

<https://theses.gla.ac.uk/>  
[research-enlighten@glasgow.ac.uk](mailto:research-enlighten@glasgow.ac.uk)

# Investigating the phosphorylation of free fatty acid receptor 4 and free fatty acid receptor 2

Zhaoyang Dong

MSc BSc

Submitted in fulfilment of the requirements for the Degree of  
**Doctor of Philosophy**

School of Molecular Biosciences

College of Medical, Veterinary and life Science

University of Glasgow

June 2023



University  
of Glasgow

## Abstract

G protein-coupled receptors (GPCRs), as a large receptor family, are involved in many physiological and pathological processes. Almost all GPCRs are regulated by phosphorylation, which is a complex process and a key event in determining the downstream signal transduction. However, it is difficult to detect the phosphorylation status of the receptors in living individuals.

Free fatty acids are considered not only as dietary nutrients but also as signalling molecules because of their ability to activate the family of G protein-coupled free fatty acid receptors. Among the GPCRs for free fatty acids, free fatty acid receptor 4 (FFA4, also known as GPR120) is known to respond to long-chain fatty acids such as docosahexaenoic acid (DHA) and eicosapentaenoic acid (EPA). FFA4 was found to regulate gut incretin glucagon-like peptide-1 (GLP-1) secretion in enteroendocrine L cells as well as insulin-sensitizing and antidiabetic effects of omega-3 polyunsaturated fatty acids. The therapeutic potential of FFA4 agonists is drawing great attention in the treatment of diabetes. Recent studies have also shown the anti-inflammatory effects of FFA4 in lung resident macrophages, as well as the mediation of airway smooth muscle relaxation. Therefore, it is vital to understand details of the identification and regulation of phosphorylation in FFA4 response to ligands. This thesis aimed to integrate phosphorylation sites of FFA4 by using novel phospho-specific antibodies, and applying the antibodies to probe phosphorylation *in vivo*. Additionally, this thesis also investigated the GPCR kinase (GRK) isoforms involved in the regulation of the phosphorylation of FFA4.

To verify phosphorylation sites of FFA4, we first characterised the phospho-site specific antibodies, anti-pThr<sup>347</sup> and anti-pThr<sup>349</sup>/Ser<sup>350</sup>. These antibodies were derived from phosphorylated peptide containing phosphorylation phosphate on residue Thr<sup>347</sup> (GAILDTSVK) and Thr<sup>349</sup>/Ser<sup>350</sup> (ILTDTSVKRND). The antibodies identified the phosphorylated FFA4 in Flp-In TERx 293 cells transformed with human FFA4 (hFFA4), and this was stopped by Lambda Protein Phosphatase. The immunoblots showed that the phosphorylation of FFA4 at Thr<sup>347</sup> and Thr<sup>349</sup>/Ser<sup>350</sup> was in an agonist-dependent way. We further treated the cells with agonists and antagonists and lysed the cells at different time points. The cell lysates were immunoprecipitated and analysed by western blot. The results demonstrated

that phosphorylation of FFA4 was regulated by agonists and antagonists in time-dependent patterns. The images from immunocytochemistry demonstrate the distribution of phosphorylated FFA4 in hFFA4 cells. These images also display FFA4 internalization with long-time exposure to agonist. Previous studies have reported that phosphorylation was regulated by GRKs and  $\beta$ -arrestins. Thus, hFFA4 cells were treated with GRK inhibitors to verify which GRKs are involved in mediating the phosphorylation of FFA4. Our results revealed that FFA4 phosphorylation is inhibited by GRK6 inhibitor compound 19. However, the  $\beta$ -arrestin 2 recruitment signal was highly inhibited by a combination of compound 19 and compound 101 (GRK 2/3 inhibitor) suggesting that phosphorylation of FFA4 may be regulated by multiple GRKs. To investigate the phosphorylation profile of FFA4 in real tissues, I collected lung tissues from FFA4 wild type mice and FFA4 knock out mice, treated them with FFA4 agonist and analysed with western blot. However, translating these findings to endogenously expressed FFA4 in lung tissue was challenging and will require further studies to optimize conditions. As our lab also has the phosphor-site specific antibodies of FFA2, and FFA2 shows effects on metabolism and immune process, I then turned to study FFA2.

FFA2 is able to activated by short chain fatty acids, and widely express in cells and tissues, such as immune cells, adipose, and colon. FFA2 is related to metabolism and immune process, which makes it a potential target to obesity, type 2 diabetes and anti-inflammatory. To investigate whether phospho-site specific antibodies were able to identify the phosphorylated form of FFA2 in vivo, it is confirmed that the agonist-mediated phosphorylation of hFFA2-DREADD was identified by anti-pSer<sup>296</sup>/Ser<sup>297</sup> and anti-Thr<sup>306</sup>/Thr<sup>310</sup> FFA2 in cells stably expressing hFFA2-DREADD (hFFA2-DREADD means designer receptor exclusively activated by designer drug variant of huma FFA2). Attempts were made to translate the in vitro findings described above to hFFA2-DREADD expressed in mouse tissues. Our results illustrate that hFFA2-DREADD was phosphorylated at Ser<sup>296</sup>/Ser<sup>297</sup> in white adipose tissue but not in Peyer's patches. In contrast, hFFA2-DREADD was phosphorylated at Thr<sup>306</sup>/Thr<sup>310</sup> in Peyer's patches, but not in phosphorylated white adipose tissue. Meanwhile the residues were all phosphorylated in colonic epithelium. These findings provide evidence to GPCR phosphorylation bar-code theory.



In summary, this thesis showed the phosphorylation of FFA4 sites Thr<sup>347</sup> and Thr<sup>349</sup>/Ser<sup>350</sup> were agonist induced and play a time-dependent manner. The regulation of phosphorylation of FFA4 was mainly responsible by GRK6. As for FFA2, I showed that anti-pSer<sup>296</sup>/Ser<sup>297</sup> and anti-Thr<sup>306</sup>/Thr<sup>310</sup> identified the agonist-induced phosphorylation on specific sites in human FFA2-DREADD cells. moreover, FFA2 showed distinct phosphorylation profile in different tissues from hFFA2-DREADD mouse. These findings contribute to understanding the phosphorylation behaviours of FFA4 and FFA2, and confirm phospho-sites specific antibodies as probes to detect phosphorylation of the receptor. Conclusions drawn from these studies may help advance future efforts to validate the therapeutic potential of targeting FFA4 and FFA2.

## Table of Contents

Abstract.....	ii
Table of Contents .....	v
List of Tables.....	viii
List of Figures.....	ix
List of Publications.....	xi
Acknowledgement.....	xii
Author's Declaration.....	xiii
Abbreviations .....	xiv
Chapter 1 Introduction.....	1
1.1 G protein-coupled receptors .....	1
1.1.1 Classification of GPCRs .....	1
1.1.2 Heterotrimeric G protein dependent signalling .....	3
1.1.3 G protein independent signalling .....	5
1.1.3.1 Arrestins in G protein independent signalling .....	5
1.1.3.2 G Protein-Coupled Receptor Kinases G protein independent signalling .....	6
1.1.3.3 GPCR regulation by phosphorylation .....	6
1.1.3.4 Desensitization and internalization of GPCR .....	7
1.2 Free fatty acid (FFA) receptors .....	8
1.2.1 Structural architecture of free fatty acid receptors .....	9
1.2.2 Ligands at free fatty acids .....	10
1.2.2.1 Agonists of long-chain fatty acids.....	10
1.2.2.2 Antagonists of long-chain fatty acids.....	12
1.2.2.3 Agonists of short-chain fatty acids.....	14
1.2.3 Expression and function of free fatty acid receptors .....	16
1.2.4 Signalling of free fatty acid receptors .....	18
1.2.4.1 G protein dependent signalling.....	18
1.2.4.2 Phosphorylation in FFA4 .....	20
1.2.5 FFA4 isoforms.....	21
1.2.6 Therapeutic target for FFA4 .....	22
1.2.6.1 Type 2 diabetes .....	22
1.2.6.2 Cancer .....	23
1.2.6.3 Lung diseases .....	24
1.2.7 Therapeutic of FFA2.....	24
1.2.8 Unique model facilitates study of FFA2.....	错误!未定义书签。
1.3 Application of protein phosphorylation.....	26
1.4 Aims.....	27
Chapter 2 Materials and methods.....	28
2.1 Chemicals and reagents .....	28
2.2 Compounds preparation .....	28
2.3 Cell culture .....	29
2.3.1 Flp-In TREx 293 cells .....	29
2.3.2 Chinese hamster ovary (CHO) cells .....	29
2.4 Cell harvesting .....	29
2.5 Isolation of cellular lysates .....	30
2.6 Protein quantification using the Bradford assay .....	30
2.7 Immunoprecipitation.....	31
2.7.1 GFP-trap.....	31
2.7.2 HA-trap .....	31
2.8 Antibody characterization using phosphatase treatment .....	31

2.9	Lambda Protein Phosphatase (LPP) treatment .....	32
2.10	N-glycosidase F (N-GF) treatment .....	32
2.11	Western blot assay .....	32
2.12	Immunocytochemistry .....	33
2.13	B-arrestin 2 recruitment .....	34
2.13.1	Luria-Bertani (LB) agar plates .....	34
2.13.2	Bacterial transformation .....	34
2.13.3	Maxipreps .....	34
2.13.4	B-arrestin 2 recruitment assay .....	35
2.14	Experimental animals .....	37
2.14.1	Animal maintenance .....	37
2.14.2	Tissue harvest and Treatment .....	38
2.14.3	Tissue homogenisation .....	38
2.14.4	Membrane extract preparation .....	38
2.15	Statistical analysis .....	39
Chapter 3	Characterisation of FFA4 phospho-site antibodies .....	41
3.1	Introduction .....	41
3.2	Results .....	42
3.2.1	Characterisation of antibodies raised against pThr <sup>347</sup> FFA4 and pThr <sup>349</sup> /Ser <sup>350</sup> on human FFA4 .....	42
3.2.2	Lambda Protein Phosphatase dephosphorylates hFFA4-eYFP cell extracts .....	45
3.2.3	Anti-pThr <sup>347</sup> and anti-pThr <sup>349</sup> /Ser <sup>350</sup> identify de-glycosylated FFA4 receptor .....	46
3.3	Discussion .....	49
Chapter 4	Investigation of FFA4 phosphorylation pattern .....	52
4.1	Introduction .....	52
4.2	Results .....	53
4.2.1	Other FFA4 ligands participate in regulation of FFA4 phosphorylation .....	53
4.2.1.1	Agonist 2 promotes regulation of FFA4 phosphorylation	53
4.2.1.2	An FFA4 antagonist prevents TUG-891 mediated receptor phosphorylation .....	55
4.2.2	FFA4 ligands regulate phosphorylation of FFA4 in a time-dependent manner .....	57
4.2.2.1	FFA4 becomes phosphorylated in a time-dependent manner	57
4.2.2.2	AH-7614 inhibits FFA4 phosphorylation in a time-dependent manner .....	58
4.2.2.3	Phosphorylation and internalization of FFA4 in Flp-In TReX 293 cells .....	59
4.2.3	GRKs participate in the regulation of FFA4 phosphorylation ....	64
4.2.3.1	GRK inhibitors affect FFA4 phosphorylation .....	64
4.2.3.2	Interactions between FFA4 and B-arrestin 2 in the presence of GRK inhibitors .....	67
4.2.4	Investigation of phosphorylation status of mouse FFA4 .....	70
4.2.4.1	Anti-pThr <sup>349</sup> /Ser <sup>350</sup> identified mFFA4 in CHO cells .....	70
4.2.4.2	Characterisation of anti-pThr <sup>349</sup> /Ser <sup>350</sup> in lung tissue ...	73
4.2.4.3	FFA4 expression in membrane preparations from mouse lung	74
4.3	Discussion .....	75
Chapter 5	Investigation of phosphorylation status of FFA2 <i>ex vivo</i> .....	79

5.1	Introduction .....	79
5.1.1	From FFA4 to FFA2 .....	79
5.1.2	Pharmacological tools to study function of FFA2 .....	79
5.1.3	Aims .....	80
5.2	Results .....	82
5.2.1	Characterisation of anti-pSer <sup>296</sup> /Ser <sup>297</sup> hFFA2 and anti-pThr <sup>306</sup> /Thr <sup>310</sup> hFFA2.....	82
5.2.1.1	Characterisation of anti-pSer <sup>296</sup> /Ser <sup>297</sup> hFFA2 and anti-pThr <sup>306</sup> /Thr <sup>310</sup> hFFA2 in cell lines .....	82
5.2.2	Investigation of phosphorylation status of FFA2 <i>ex vivo</i> .....	86
5.2.2.1	Investigation of phosphorylation status of hFFA2-DREADD using anti-pSer <sup>296</sup> /Ser <sup>297</sup> hFFA2 and anti-pThr <sup>306</sup> /Thr <sup>310</sup> hFFA2 in Peyer's patches and mesenteric lymph nodes. ....	86
5.2.2.2	Investigation of phosphorylation status of FFA2-DREADD using anti-pSer <sup>296</sup> /Ser <sup>297</sup> FFA2 and anti-pThr <sup>306</sup> /Thr <sup>310</sup> FFA2 in white adipose tissue .....	90
5.2.2.3	Investigation of phosphorylation status of FFA2-DREADD-HA using anti-pSer <sup>296</sup> /Ser <sup>297</sup> hFFA2 and anti-pThr <sup>306</sup> /Thr <sup>310</sup> hFFA2 in colonic epithelium .....	92
5.3	Discussion .....	94
Chapter 6	Final discussion.....	97
References	.....	103

## List of Tables

Table 1-1 Structures and chemical names of FFA4 compounds .....	14
Table 2-1 List of primary antibodies .....	39
Table 2-2 List of secondary antibodies used for western blot .....	40
Table 2-3 List of secondary antibodies used for immunocytochemistry ....	40
Table 4-1 IC50 of GRK5/6 inhibitors.....	65
Table 4-2 IC50 of GRK inhibitors in $\beta$ -arrestin2 recruitment assay .....	69
Table 5-1 Ligands at wild type human FFA2. ....	81

## List of Figures

Figure 1.1 Classification of GPCRs .....	3
Figure 1.2 G protein dependent signalling pathways .....	5
Figure 1.3 GPCR signalling mediated by $\beta$ -arrestin. ....	8
Figure 1.4 G protein dependent signalling pathway of FFA4 .....	19
Figure 1.5 Primary amino acid sequence of human FFA4 short isoform .....	22
Figure 1.6 Signalling pathways of hFFA2-DREADD .....	26
Figure 2.1 The mechanism of BRET assay .....	37
Figure 3.1 Anti-pThr <sup>347</sup> and anti-pThr <sup>349</sup> /Ser <sup>350</sup> identify FFA4 phosphorylation induced by TUG-891. ....	44
Figure 3.2 Anti-pThr <sup>347</sup> and anti-pThr <sup>349</sup> /Ser <sup>350</sup> failed to identify FFA4 phosphorylation removed by Lambda Protein Phosphatase (LPP). ....	46
Figure 3.3 Anti-pThr <sup>347</sup> and anti-pThr <sup>349</sup> /Ser <sup>350</sup> identify FFA4 phosphorylation with the presence of N-glycosidase F (N-GF). ....	49
Figure 4.1 Anti-pThr <sup>347</sup> and anti-pThr <sup>349</sup> /Ser <sup>350</sup> identify FFA4 phosphorylation induced by Agonist 2. ....	55
Figure 4.2 Agonist-induced FFA4 phosphorylation is inhibited by AH-7614. ....	56
Figure 4.3 FFA4 becomes phosphorylated in a time-dependent manner. ....	58
Figure 4.4 FFA4 antagonist AH-7614 inhibits agonist-induced FFA4 phosphorylation in a time-dependent manner. ....	59
Figure 4.5 immunocytochemistry of FFA4 phosphorylation induced by TUG-891. ....	61
Figure 4.6 Immunocytochemistry of FFA4 phosphorylation induced by TUG-891 in a time- dependent manner. ....	63
Figure 4.7 Identification of GRK inhibitors regulation of hFFA4 phosphorylation status using phospho-site specific antibody anti-pThr <sup>349</sup> /Ser <sup>350</sup> FFA4. ....	66
Figure 4.8 Identification of GRK inhibitors regulation of hFFA4 phosphorylation status using phospho-site specific antibody anti-pThr <sup>347</sup> FFA4. ....	67
Figure 4.9 $\beta$ -arrestin 2 recruitment affected by TUG-891 and GRK inhibitors. ....	68
Figure 4.10 $\beta$ -arrestin 2 recruitment inhibited by a combination of compound 19 and compound 101. ....	69
Figure 4.11 $\beta$ -arrestin 2 recruitment inhibited by a combination of compound 19 and 10 $\mu$ M of compound 101. ....	70
Figure 4.12 Characterisation of anti-pThr <sup>349</sup> /Ser <sup>350</sup> in CHO cells .....	72
Figure 4.13 Characterisation of anti-pThr <sup>349</sup> /Ser <sup>350</sup> FFA4 in lung. ....	74
Figure 4.14 FFA4 expression in membrane protein extract from lung. ....	75
Figure 5.1 Primary amino acid sequence of human FFA2 .....	82
Figure 5.2 Identification of agonist regulation of hFFA2-DREADD phosphorylation status using phospho-site specific antibodies. ....	84
Figure 5.3 Phosphorylated hFFA2-DREADD is identified in immunocytochemical studies. ....	86
Figure 5.4 Histology slice of small intestine in cross section .....	88
Figure 5.5 Identification of agonist regulation of hFFA2-DREADD-HA phosphorylation status in Peyer's patches and MLNs using phospho-specific antibodies. ....	89
Figure 5.6 Identification of agonist regulation of hFFA2-DREADD-HA phosphorylation status in white adipose tissue using phospho-specific antibodies. ....	91

Figure 5.7 Identification of agonist regulation of hFFA2-DREADD phosphorylation status in colonic epithelium using phospho-specific antibodies. ....	93
--	----

## List of Publications

Prihandoko, R., Kaur, D., Wiegman, C.H., Alvarez-Curto, E., Donovan, C., Chachi, L., Ulven, T., Tyas, M.R., Euston, E., Dong, Z., Alharbi, A.G.M., Kim, R.Y., Lowe, J.G., Hansbro, P.M., Chung, K.F., Brightling, C.E., Milligan, G. and Tobin, A.B. (2020) 'Pathophysiological regulation of lung function by the free fatty acid receptor FFA4', *Science Translational Medicine*, 12(557), pp. 1-14.



## Acknowledgement

First and foremost, I would like to express my deepest and sincerest gratitude to my supervisor, Professor Andrew Tobin. Thanks for all of the support over the last four years. I also would like to appreciate Professor Graeme Milligan. The invaluable guidance, encouragement and support from them throughout my PhD study. I am grateful for the opportunity to learn from such outstanding scientists. Thanks all of the postdocs and technicians, especially Rudi, Natasja and Laura for their enthusiasm and kindness, which have provided me with a great deal of encouragement. The care and support they provided enabled me to complete my lab work and thesis. Elios and Abdul, thank you for always being there as a FFA4 team with me.

I would also like to thank my friends Yilin, Mengyi, Xing, and Yan for their support over the years. Thank you for celebrate every Chinese New Year with me, which prevent me from being homesick. You are my family in Glasgow. I would like to extend a special thanks to Yilin for helping me so much and take care of me when I had Covid-19.

Last but not least, I would like to thank my family for their unconditional love and support. Thank you for always encouraging me and having confidence in me. I could not have done it without you all. In addition, thanks for the financial support from my father. It would not have been possible for me to study in the UK and meet such wonderful people without your assistance

I would also like to thank all the warm and welcoming people of Glasgow all the people I It would not have been possible for me to study in the UK and meet such wonderful people without you.

## **Author's Declaration**

“I declare that, except where explicit reference is made to the contribution of others, this dissertation is the result of my own work and has not been submitted for any other degree at the University of Glasgow or any other institution.”

Zhaoyang Dong

## Abbreviations

<b>5-HT</b>	5-hydroxytryptamine
<b>Akt</b>	Protein Kinase B
<b>Ala</b>	Alanine
<b>ALA</b>	$\alpha$ -linolenic acid
<b>ANOVA</b>	Analysis of variance
<b>Arg</b>	Arginine
<b>Asn</b>	Asparagine
<b>Asp</b>	Aspartic acid
<b>AT1R</b>	Angiotensin Receptor
<b>B2AR</b>	Beta-2 adrenergic receptor
<b>BIMII</b>	Bisindolylmaleimide II
<b>BRET</b>	Bioluminescence resonance energy transfer
<b>BSA</b>	Bovine serum albumin
<b>cAMP</b>	Cyclic adenosine monophosphate
<b>CCK</b>	Cholecystokinin
<b>CCSs</b>	Clathrin-coated structures
<b>CHO</b>	Chinese hamster ovary
<b>Cpd 101</b>	compound 101
<b>Cpd 15</b>	compound 15
<b>Cpd 18</b>	compound 18
<b>Cpd 19</b>	compound 19
<b>CpdA</b>	Compound A
<b>CRD</b>	cysteine-rich domains
<b>CXCR4</b>	C-X-C Motif Chemokine Receptor 4
<b>Cys</b>	cysteine
<b>DAG</b>	Diacylglycerol
<b>DHA</b>	Docosahexaenoic acid
<b>DMEM</b>	Dulbecco's modified Eagle's medium
<b>DMSO</b>	Dimethyl sulfoxide
<b>DREADD</b>	designer receptors exclusively activated by designer drug
<b>EC50</b>	Effective concentration at 50% maximal response of activation
<b>ECD</b>	Extracellular domain
<b>ECL2</b>	Extracellular loop 2
<b>ECLs</b>	Extracellular loops

<b>EPA</b>	eicosapentaenoic acid
<b>eYFP</b>	Enhanced yellow fluorescent protein
<b>FBS</b>	Fetal bovine serum
<b>FFA</b>	Free fatty acid
<b>FFA1</b>	Free fatty acid receptor 1
<b>FFA2</b>	Free fatty acid receptor 2
<b>FFA3</b>	Free fatty acid receptor 3
<b>FFA4</b>	Free fatty acid receptor 4
<b>FRET</b>	Fluorescent resonance energy transfer
<b>GABAB</b>	$\gamma$ -aminobutyric acid
<b>GAIN</b>	GPCR autoproteolysis-inducing domain
<b>GFP</b>	Green fluorescent protein
<b>GIP</b>	Glucose-dependent insulinotropic peptide
<b>GLP-1</b>	Secreted glucagon-like peptide 1
<b>Glu</b>	Glutamic acid
<b>Gly</b>	Glycine
<b>GPCRs</b>	G protein-coupled receptors
<b>GRKs</b>	G Protein-Coupled Receptor Kinases
<b>GSIS</b>	Glucose-stimulated insulin secretion
<b>Gai/o</b>	G $\alpha$ proteins of the inhibitory class
<b>HA</b>	Human influenza hemagglutinin
<b>HBSS</b>	Hanks' balanced salt solution
<b>hFFA4</b>	Human FFA4
<b>HTS</b>	High throughput screening
<b>IC50</b>	Effective concentration at 50% maximal response of inhibition
<b>ICL</b>	Intracellular loop
<b>ICL3</b>	Intracellular loop 3
<b>ICLs</b>	Intracellular loops
<b>IKK</b>	I $\kappa$ B kinase
<b>Ile</b>	Isoleucine
<b>IP3</b>	Inositol triphosphate
<b>JNK</b>	c-Jun N-terminal Kinase
<b>KO</b>	Knock out
<b>LB</b>	Luria-Bertani
<b>LCFAs</b>	Long chain fatty acids
<b>Leu</b>	Leucine

<b>LPP</b>	Lambda Protein Phosphatase
<b>mAChR</b>	muscarinic acetylcholine receptor
<b>mGlu</b>	Metabotropic glutamate
<b>MLNs</b>	mesenteric lymph nodes
<b>MMP-9</b>	Matrix metalloproteinase-9
<b>MOMBA</b>	4-methoxy-3-methyl-benzoic acid
<b>N-GF</b>	N-glycosidase F
<b>PBS</b>	Phosphate buffered saline
<b>PD</b>	Phospho-deficient
<b>PEI</b>	Polyethylenimine
<b>PET</b>	positron emission tomography
<b>Phe</b>	Phenylalanine
<b>PI3K</b>	Phosphoinositide 3-kinase
<b>PKA</b>	Protein kinase A
<b>PKC</b>	Protein kinase C
<b>PLC</b>	Phospholipase C
<b>PMA</b>	Phorbol-12-myristate-13-acetate
<b>PP1</b>	Protein phosphatase 1
<b>PP2A</b>	Protein phosphatase 2A
<b>PPAR-<math>\gamma</math></b>	Peroxisome proliferator-activated receptor- $\gamma$
<b>PPAR<math>\gamma</math>2</b>	Peroxisome proliferator-activated receptor- $\gamma$ 2
<b>PTM</b>	Post-translational modification
<b>PTX</b>	Pertussis toxin
<b>PYY</b>	Peptide YY
<b>RH</b>	G-protein signalling homology domain
<b>RIPA buffer</b>	Radioimmunoprecipitation assay buffer
<b>SA</b>	Sorbic acid
<b>SAR</b>	Structure-Activity Relationship
<b>SCFAs</b>	Short chain fatty acids
<b>SDS-PAGE</b>	Sodium dodecyl sulphate-polyacrylamide gel electrophoresis
<b>SEM</b>	Standard error
<b>Ser</b>	Serine
<b>T2DM</b>	type 2 diabetes
<b>TAK1</b>	Transforming growth factor- $\beta$ -activated kinase 1
<b>Thr</b>	Threonine
<b>TLR4</b>	Toll-like receptor 4

<b>TMD</b>	Transmembrane domain
<b>Trp</b>	Tryptophan
<b>Tyr</b>	Tyrosine
<b>V2R</b>	Vasopressin 2 receptor
<b>Val</b>	Valine
<b>VFD</b>	Venus fly-trap domain
<b>VFTM</b>	Venus flytrap module
<b>WT</b>	Wild type
<b>B2AR</b>	$\beta$ 2-adrenergic receptors

# Chapter 1 Introduction

## 1.1 G protein-coupled receptors

G protein-coupled receptors (GPCRs) comprise the largest class of membrane proteins in the human genome (Lagerström and Schiöth, 2008). To date, over 800 different GPCRs have been found (Liapakis et al., 2012). They are widely distributed in the central nervous system, immune system, cardiovascular system, retina, and other organs and tissues, and are involved in the development and normal functioning of the body. These receptors transmit extracellular information into cells and lead to subsequent cellular responses via coordination between ligands, GPCRs, effector proteins (G proteins, arrestin, etc.) and downstream signalling pathways (Rosenbaum et al., 2009, Gurevich and Gurevich, 2019). Thus, GPCRs are considered as regulators of various pathological processes and important drug targets for many diseases.

### 1.1.1 Classification of GPCRs

The majority of GPCRs consist of 7-segment  $\alpha$ -helical structures that span the cytoplasmic membrane. The N-terminus and three loops are located extracellularly and are involved in the interaction between receptors and their ligands. The C-terminus and three loops are located intracellularly, and are involved in the interaction and mediation between GPCR proteins and downstream G proteins. The GPCRs are classified into three sub-families based on their structure and function, that is classes A, B, and C which include frizzled receptors (Katritch et al., 2013).

Class A consists of rhodopsin-like receptors, which include approximately 700 GPCRs in humans (Fredriksson et al., 2003). These receptors have a wide range of ligands. Common endogenous ligands for rhodopsin-like receptors include amine-bearing neurotransmitters (i.e., epinephrine, histamine, and acetylcholine) polypeptides (i.e., ghrelin), opioids (i.e., enkephalin and endorphins) and chemokines. Receptors in this family have a relatively simple structural composition and a short N-terminus (Venkatakrisnan et al., 2013). Despite that the overall sequence identity for the family A receptors is low, there are still several highly conserved key residues shared in the family. These

## Chapter 1

residues have important roles in the structural and functional integrity of receptors. An arginine (Arg) located between TM3 and ECL2 has been confirmed as a conserved residue (Arg<sup>3.50</sup>). This Arg forms a salt bridge with Aspartic (Asp) or Glutamic (Glu) located in a nearby acidic side chain. The bridge exists only in inactive receptor structures (Vogel et al., 2008). Other conserved residues are NPXXY motif. This is highly conserved in 92% of family A GPCRs and it changes its rotamer conformation in activated receptors (Katritch et al., 2013). Alanine (Ala<sup>2.47</sup>) and serine (Ser<sup>4.53</sup>) are two conserved residues found in two clusters promoting tight transmembrane helix association (Sanchez-Reyes et al., 2017). To determine the information of TM region of GPCRs, Ballesteros and Harel Weinstein developed a universal numbering scheme used to determine the information of TM region of GPCRs. The numbering scheme provides information on the relative position of each amino acid, and the true position number in a specific GPCR. In each TM region, the position of the most conservative amino acids is considered as 50, and the next position towards (to the C-terminus) is 51. For example, the amino acid backwards (to the N-terminus) is 49. For example, the most conservative amino acid in TM3 is an arginine, then this position is Arg<sup>3.50</sup>.

Class B GPCRs are divided into two subfamilies: B1 secretin receptors (secretin) and B2 class adhesion receptors (adhesion). They are activated by peptide hormones, and coordinate the regulation of metabolic homeostasis, as well as, neural and endocrine activity in the body (Lagerström and Schiöth, 2008, Hollenstein et al., 2014). Compared with class A receptors, those in class B family have longer N-terminal extracellular domain (ECD) and transmembrane domain (TMD). These two domains are important in G protein signalling. The N-terminal contains two disulfide bonds, which maintain the stability of ECD (Unson et al., 2002).

Class C GPCRs include metabotropic glutamate receptors with various of endogenous ligands such as glutamate (mGlu),  $\gamma$ -aminobutyric acid (GABAB), taste receptors and calcium-sensitive receptors. Receptors in this family are distinguished by constitutive dimerization and a large extracellular domain. This extracellular domain contains a venus flytrap module (VFTM) and a cysteine (Cys) rich domain. Moreover, the orthosteric binding sites of class C GPCRs are



## Chapter 1

found in the VFTM (Gether, 2000). Members in frizzled receptors have a cysteine rich domain (CRD), which is composed of approximately 120 amino acids. This GPCR family is involved in tissue homeostasis and individual development (Dann et al., 2001).

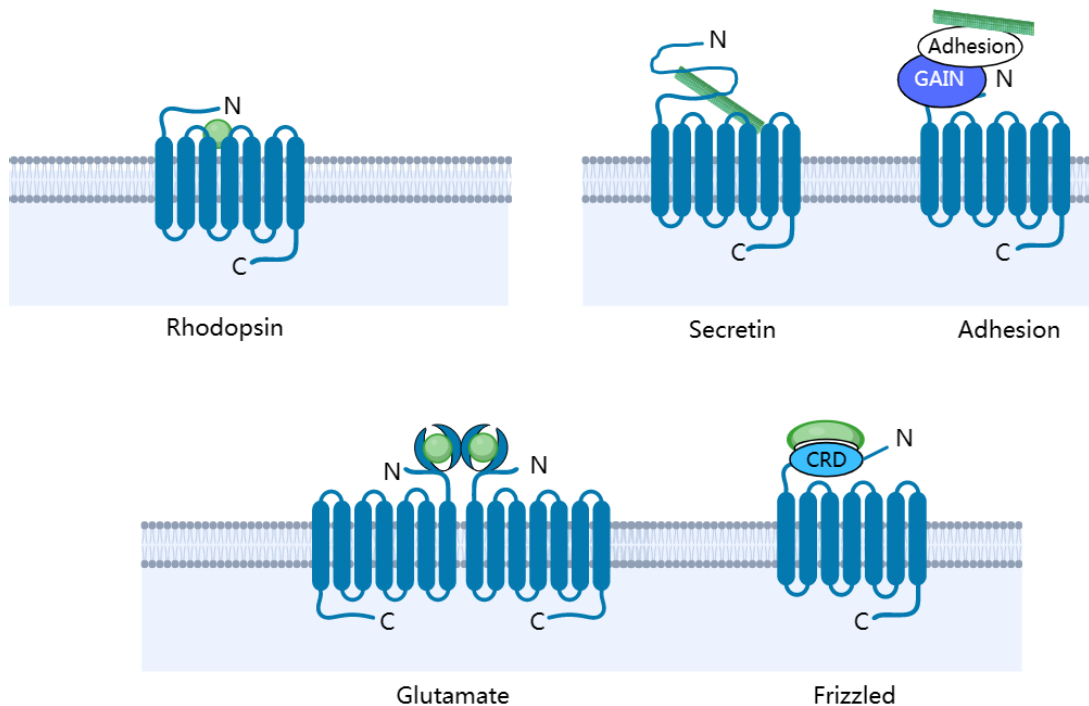


**Figure 1.1 Classification of GPCRs**

All G protein-coupled receptors (GPCRs) share a 7-transmembrane helix arrangement with an extracellular N-terminus and an intracellular C-terminus. However, they have diverse extracellular regions. Rhodopsin receptors (Class A) have a small N-terminus and their natural ligands directly bind to the transmembrane domains, whereas, secretin receptors have a longer N-terminus. Adhesion receptors contain GPCR autoproteolysis-inducing (GAIN) domains, which catalyse the cleavage of the N terminus, resulting in non-covalent association of ligands. Glutamate family exist in dimeric form and bind ligands by employing their venus fly trap domain (VFD). Frizzled receptors show cysteine-rich domains (CRD) to bind ligands with the help of palmitoyl group. Agonist is shown in green.

### 1.1.2 Heterotrimeric G protein dependent signalling

GPCRs transduce extracellular signals into cells, in which process heterotrimeric G proteins play important roles. Heterotrimeric G proteins are typically composed of three subunits,  $G\alpha$ ,  $G\beta$  and  $G\gamma$ .  $G\alpha$  is the largest subunit and is divided into subgroups:  $G\alpha_i$ ,  $G\alpha_q$ ,  $G\alpha_s$ , and  $G\alpha_{12}$  (Simon et al., 1991).  $G\alpha$  subunits have binding sites to GDP/GTP and have enzymatic activity.  $G\beta$  and  $G\gamma$

## Chapter 1

generally exist as dimers and are the anchoring sites for the  $G\alpha$  subunit (Dingus et al., 2005). When the receptor is in inactive state, the  $G\alpha$  subunits bound with GDP. When the receptor is activated,  $G\alpha$  release GDP and associate with GTP and separates from the other two subunits. The activated receptors then relay the signal to other components in the signalling cascades. As GTP is hydrolysed to GDP by guanine nucleotide triphosphatase (GTPase). This step is accelerated by binding of another protein called regulator of G Protein Signalling (RGS). The three subunits then reassociate, and heterotrimeric G proteins return to the inactive state (Lambright et al., 1996). For the receptors, the intracellular effector enzymes are activated, inducing changes in second messengers that cause the cell to respond to stimuli. One of the common effector enzymes is adenylyl cyclase (AC), which produces cAMP as a second messenger. Another effector enzyme is phospholipase C (PLC), which produces inositol triphosphate (IP3) and diacylglycerol (DAG).  $G\alpha_s$  activated adenylyl cyclase catalyses the production of cyclic adenosine monophosphate (cAMP), a second messenger that stimulates protein kinase A (PKA) activity (Arshavsky et al., 2002). PKA can further activate or inhibit downstream proteins depending on the type of  $G\alpha$  protein in different cell lines. Generally, activation of PKA results in receptor phosphorylation or protein synthesis. Cyclic adenosine monophosphate is inhibited when  $G\alpha_i$  is activated. Another pathway mediated by PLC can promote the intracellular synthesis of inositol triphosphate and diglyceride as second messengers. This pathway is activated by  $G\alpha_q$ . In this process, phosphatidylinositol (PI) is phosphorylated on specific hydroxyl, and turn to phosphoinositide (PIP) and phosphatidylinositol 4,5-bisphosphate (PIP2). PIP2 is hydrolysed into IP3 and DAG by PLCB (the isomer of PLC). This raises IP3 intracellular calcium concentration, resulting in a series of cellular responses and DAG is able to activate PKC that leads to the intercellular pH increase (Rhee, 2001).

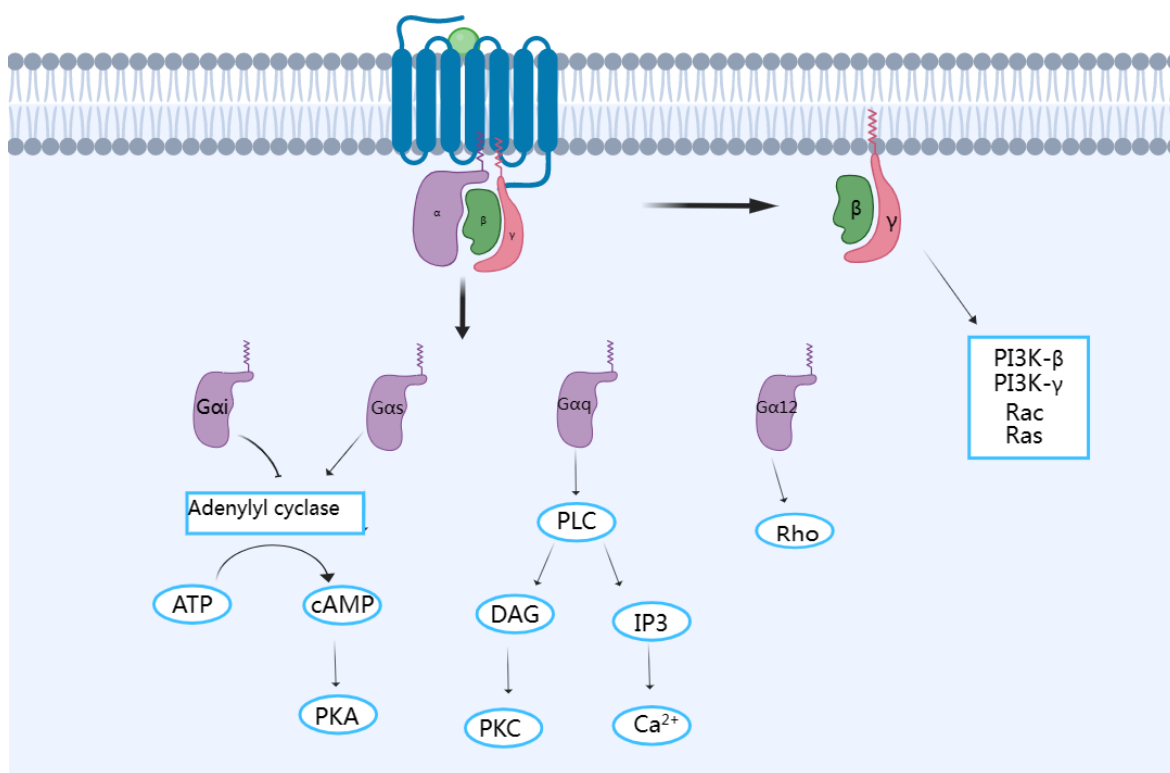


**Figure 1.2 G protein dependent signalling pathways**

When the receptor is activated, G $\alpha$  subunit binds with GPCRs and separates from the other two subunits. Different downstream effectors are activated depending on the type of G $\alpha$  subunit. G $\alpha$ s and G $\alpha$ i families regulate adenylate cyclase activity. G $\alpha$ q subunits activate PKC via PLC signalling. The G $\alpha$ q subunits also stimulate PLC signalling resulting in an increase of intracellular Ca<sup>2+</sup>. The G $\alpha$ 12 subunits activate Rho GTPases. The G $\beta\gamma$  subunits are also able to engage a range of different signalling cascades. PLC, phospholipase-C; PKC, Protein kinase C.

### 1.1.3 G protein independent signalling

#### 1.1.3.1 Arrestins in G protein independent signalling

The signalling pathways of GPCRs depend on the activation of G proteins, but there are still some pathways that are independent of G protein activation. Arrestins are a group of protein widely involved in mediating G protein independent signalling (Luttrell and Gesty-Palmer, 2010). There are four members of the arrestin family. Arrestin 1 and arrestin 4 express only in rod and cone photoreceptors, and interaction with activated rhodopsin results in termination of phototransduction (Luttrell and Lefkowitz, 2002). Arrestin 2 and arrestin 3, also called  $\beta$ -arrestin 1 and  $\beta$ -arrestin 2, are able to regulate the activity of the many hundreds of non-visual GPCRs (Gurevich and Gurevich, 2006). Apart from activating ERK via G proteins, GPCRs also activate ERK via  $\beta$ -arrestins. The activation of ERK1/2 induced by B2-adrenergic receptor has been

## Chapter 1

found via both G protein-dependent and  $\beta$ -arrestin pathways. G protein-mediated ERK activation is transient, localized in the nucleus and promotes gene transcription, whereas  $\beta$ -arrestin-dependent ERK is slowly activated but long-lasting. It is localized in clathrin-coated structures (CCSs) and stabilized in endosomes (Eichel et al., 2016, Shenoy et al., 2007). The Angiotensin Receptor (AT1R) and the vasopressin type-2 receptor (V2R) which form a stable complex with either  $\beta$ -arrestin isoform, promote sustained ERK signalling in endosomes, whereas the  $\beta$ 2-Adrenergic receptor ( $\beta$ 2AR) forms a transient complex with  $\beta$ -arrestins and induces transient ERK activity (Tohgo et al., 2003).

### 1.1.3.2 G Protein-Coupled Receptor Kinases G protein independent signalling

G Protein-Coupled Receptor Kinases (GRKs) are a group of serine/threonine protein kinases, that belong to the AGC kinase family. These kinases are divided into three subgroups based on their sequence similarities. The GRK1 subgroup consists of GRK1 and GRK7, the GRK2 subgroup consists of GRK2 and GRK3, and the GRK4 subgroup contains GRK4,5, and 6 (Komolov and Benovic, 2018). The GRK4 subgroup are widely expressed in mammalian tissues and GRK1, 4, and 7 are identified only in specific organs (Gurevich et al., 2012). GRK1 and GRK7 are expressed in the rods and cones of the retina, respectively. GRK4 is found in the cerebellum, kidney, and testis (Sterne-Marr et al., 2013). GRKs share a common architecture with a conserved central catalytic domain, an N-terminal domain, and a variable carboxy terminal lipid-binding region (Ribas et al., 2007). The N-terminal domain contains a catalytic region in the regulator of G protein signalling homology (RH) domain, and it is important to intracellular membrane in receptor recognition. However, only the RH domain of GRK2 and GRK3 is functional, those of other GRKs are not able to interact with G proteins because of the lack of key residues (Lodowski et al., 2006, Picascia et al., 2004, Sterne-Marr et al., 2004).

### 1.1.3.3 GPCR regulation by phosphorylation

Most GPCRs undergo phosphorylation as a receptor regulation when stimulated by agonists (Lefkowitz, 2004). This is a rapid process which makes the receptor to undergo uncoupling from G proteins and the recruitment of arrestins to the

## Chapter 1

receptor (Lefkowitz and Shenoy, 2005). Both desensitization and internalization are associated with GPCRs phosphorylation.

As described earlier, GRKs and arrestins are key adapter and scaffold molecules that can mediate the actions of a variety of distinct GPCRs (Luttrell and Gesty-Palmer, 2010). GRKs engaging different conformations of  $\beta$ -arrestins results in various downstream effects (Ribas et al., 2007). Phosphorylation of GPCRs was described as a bar-code theory which suggests that ligands could differentially regulate signalling outcomes in different cells and tissues by promoting different arrestin-mediated effects (Tobin, 2008).  $\beta_2$ -adrenergic receptor could be an example. When the receptors are at low levels of ligand occupancy, they are phosphorylated in sites in the third intracellular loop and C-terminal tail becoming phosphorylated by the second messenger PKA (Seibold et al., 2000, Tran et al., 2004). However, at high agonist occupancy, the receptors are phosphorylated at the same sites by members of the GRK family (Seibold et al., 2000). A recent study has provided a structural model, which is helpful to understand the receptor phospho-coding mechanism. The model phosphate-binding pockets on arrestins recognized the receptor phosphorylation patterns and translated them into distinct conformations. These selective conformations are recognized by various effector molecules downstream of arrestins (Yang et al., 2017). The phospho-barcoding mechanism might regulate GPCR phosphorylation together with arrestin conformations.

### **1.1.3.4 Desensitization and internalization of GPCR**

GPCR activation is dynamic and reversible however long-time stimulation the receptors would desensitisation. In this case the receptor binds with high affinity to  $\beta$ -arrestins.  $\beta$ -arrestins physically occupy G protein coupling site to inactivate the receptors, meanwhile, the level of downstream second messengers of activated receptors are reduced (Shenoy and Lefkowitz, 2011, Lefkowitz and Shenoy, 2005).  $\beta$ -arrestins also recruit the phosphorylated receptors to clathrin from where the receptors are endocytosed. GRKs phosphorylation and binding with arrestins promote receptor internalization (Gurevich et al., 2012). The internalized receptors are either degraded or recycled to the cell membrane for next activation (Jean-Charles et al., 2017).

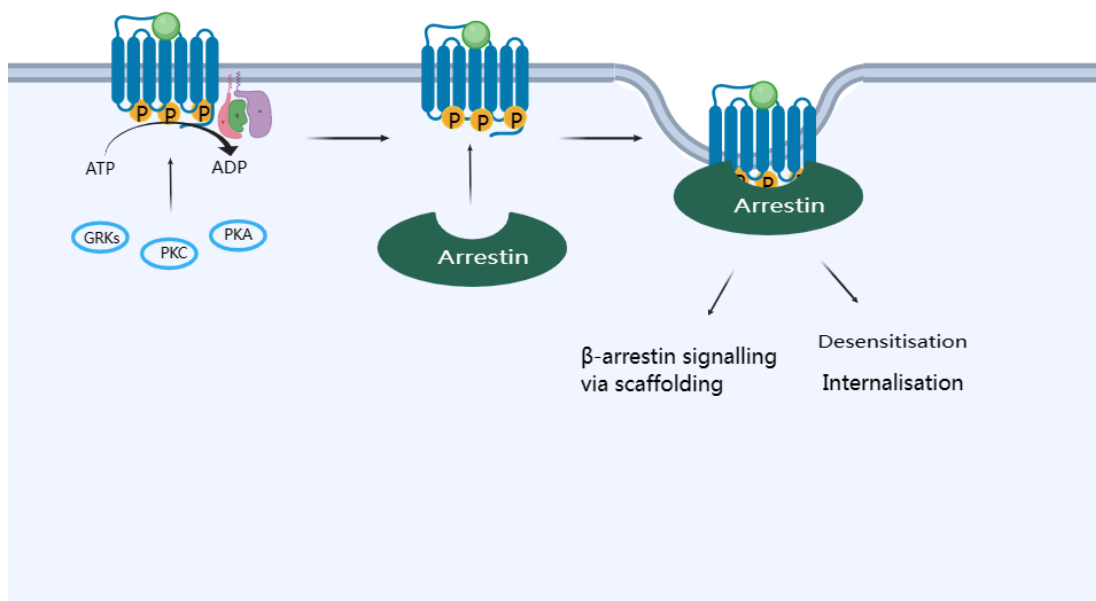


**Figure 1.3 GPCR signalling mediated by  $\beta$ -arrestin.**

Following agonist binding and G protein signalling (agonist is shown as a green ball), kinases such as GRKs, PKA, and PKC, phosphorylate intracellular residues of the activated GPCR.  $\beta$ -arrestin is recruited to the receptor and this sterically hinders G protein binding and activation. The receptor will then be desensitised and internalised.  $\beta$ -arrestin also acts as a scaffold.

## 1.2 Free fatty acid (FFA) receptors

Free fatty acid (FFA) receptors are a group of GPCRs, which are identified to bind endogenous free fatty acids. There are five members in the free fatty acid receptors family. The free fatty acid receptor 1 (FFA1) and free fatty acid receptor 4 (FFA4) are activated by long chain fatty acids (LCFAs). The free fatty acid receptor 2 (FFA2) and free fatty acid receptor 3 (FFA3) are activated by short chain fatty acids (SCFAs), and GPR84 binds medium chain fatty acids. Free fatty acids are not only an important source of energy in animals and human beings but are a group of signal molecules with a variety of physiological roles (Roy et al., 2006). The free fatty acid signalling system has been found to impact glucose level stabilization, adipose tissue development and differentiation and affect immune response (Yates et al., 2014, Font-Burgada et al., 2016). Accordingly, these signal molecules are considered to contribute in treating type

## Chapter 1

2 diabetes (T2DM), obesity, and metabolic disease and are anti-inflammatory (Stoddart et al., 2008b, Hidalgo et al., 2021).

### 1.2.1 Structural architecture of free fatty acid receptors

The free fatty acid receptors share the typical structure of GPCR: seven transmembrane helices, three extracellular loops (ECLs) and an amino terminus, as well as three intracellular loops (ICLs) and a carboxyl terminus (Venkatakrisnan et al., 2013).

FFA1 was crystallized to verify the mechanism of action and the interactions with TAK-875, an ago-allosteric modulator. This is thought to be the first structural X-ray crystallography among free fatty acid receptors, and three binding pockets were revealed. According to the crystallography, TAK-875 binding pocket was between transmembrane helices 3-5 and the extracellular loop 2 (ECL2) regions, and ECL2 was considered as the roof of the binding cavity. Glu<sup>172</sup> on ECL2 hydrogen bonded to Arg<sup>258</sup> was also involved in the pocket structure (Srivastava et al., 2014). This is consistent with the prediction confirmed by site-directed mutagenesis twelve amino acids from the putative binding pocket (Sum et al., 2007). The results of calcium flux showed that the response to GW9508 4-[[[(3-Phenoxyphenyl) methyl] amino] benzene propanoic acid] had completely disappeared in Arg<sup>183</sup> or Arg<sup>258</sup> mutations, and significantly decreased Asn<sup>244</sup> mutation (Srivastava et al., 2014). The interaction between the carboxylate moiety of agonist ligands with Arg<sup>183</sup> and Arg<sup>258</sup> was also observed in the TAK-875 combination (Sum et al., 2009). The other two binding pockets were found by visual inspection of the receptor surface. One was located between transmembrane helix 1 and transmembrane helix 7, near the traditional GPCR orthosteric site. Another one was between transmembrane helix 4 and transmembrane helix 5, probably to allow a ligand to pass (Srivastava et al., 2014).

FFA1, FFA2 and FFA3 are a class of receptors accidentally found in the search for new galanin receptor subtypes (Sawzdargo et al., 1997). Comparing the amino acid sequence, FFA1 has 30% sequence identity with FFA2 and FFA3 (Tikhonova, 2017). However, FFA2 and FFA3 bind to short chain acids instead of long chain fatty acids. Ligands were placed in the cavity comprising transmembrane helices

## Chapter 1

3, 5, and 6, anchored by residues Arg<sup>5.39</sup> and Arg<sup>7.35</sup> in FFA2 and FFA3 (Schmidt et al., 2011, Stoddart et al., 2008a). An allosteric site was found binding with 4-CMTB at Lys<sup>65</sup> in FFA4 (Smith et al., 2011, Hudson et al., 2012b). Compared to FFA2, FFA3 has a larger binding pocket. When FFA2 residues Glu<sup>166</sup>, Leu<sup>183</sup>, and Cys<sup>184</sup> were mutated by the corresponding FFA3 residues Leu, Met, and Ala, the volume of the orthosteric site increased (Schmidt et al., 2011)

FFA4 structure was investigated by a variety of methods, such as molecular modelling, receptor mutagenesis and ligand SAR studies, since no crystal structure exists. Arg<sup>99</sup>, Trp<sup>104</sup> (Tryptophane), Phe<sup>303</sup> (phenylalanine), Phe<sup>304</sup>, and Thr<sup>310</sup> (Threonine) mutations resulted in response to TUG 891 and GW9850 reductions in the BRET assay, and the binding site located in TM helical 2, 3, 5 and 7. The typical Arg residues have been shown to form ionic interactions with the carboxylate of endogenous fatty acids and synthetic ligands (Tikhonova et al., 2007, Stoddart et al., 2008a). The ortho-biphenyl part is incorporated into a narrow hydrophobic binding pocket lined by Phe<sup>88</sup>, Thr<sup>119</sup>, Gly<sup>122</sup>, Trp<sup>277</sup>, Thr<sup>310</sup>, Asn<sup>215</sup>, Val<sup>212</sup>, Phe<sup>211</sup>, Ile<sup>281</sup>, and Ile<sup>280</sup> (Hudson et al., 2014).

For GPR84, the putative binding site is created by aromatic residues, Phe<sup>170</sup>, Phe<sup>101</sup>, Phe<sup>335</sup> and Trp<sup>360</sup>, and aliphatic residues, Leu<sup>73</sup> and Leu<sup>100</sup>, which locating in binding cavity in the helical bundle (Nikaido et al., 2015).

## 1.2.2 Ligands at free fatty acids

### 1.2.2.1 Agonists of long-chain fatty acids

FFA1 also known as GPR40 (G protein-coupled receptor 40) was the first receptor orphanized in the fatty acid group (Sawzdargo et al., 1997). It was found highly expressed in pancreatic  $\beta$  cells (Itoh et al., 2003). Glucose-stimulated insulin secretion from pancreatic  $\beta$  cells was amplified as a result of long-chain FFAs activated GPR40. Itoh and colleagues established a method to select FFA1 ligands via measuring intercellular  $[Ca^{2+}]_i$  response in CHO cells expressing the G $\alpha_q$ /i-responsive Gal4-Elk1 reporter system (Itoh et al., 2003). The results indicated that C12-C16 saturated fatty acid and C18/C20 unsaturated fatty acid activated FFA1. Carbon chain length less than 6 had no activation effect (Briscoe et al., 2003, Kotarsky et al., 2003b). The endogenous agonists of FFA1 include



## Chapter 1

docosahexaenoic acid (DHA),  $\alpha$ -linolenic acid (ALA), oleic acid and palmitic acid, and agonistic activities decrease as the carbon chain gets shorter (Le Poul et al., 2003). To obtain high affinity and selective ligands, various synthetic compounds were selected by high-throughput screening and characterized by *in vitro* and *in vivo* experiments. GW9508 was considered a partial agonist of FFA1 with good chemical stability and pharmacokinetics (McKeown et al., 2007, Garrido et al., 2006).

GW9508 increased insulin secretion in MIN6 B-cells (Briscoe et al., 2006). It also affected matrix metalloproteinase-9 (MMP-9) release via PLC and PKC in bovine neutrophils and elevated chemotaxis response to IL-8 (Mena et al., 2016, Manosalva et al., 2015). Hydrogen bonding and  $\pi$ - $\pi$  conjugation have effects on the interaction between receptors and ligands (Itoh et al., 2003). After a series of syntheses and screening, TAK-875 becomes a representative compound, which has high water solubility and bioavailability (Negoro et al., 2012). Studies from clinical trials showed that TAK-875 enhanced glucose-stimulated insulin secretion (GSIS) without inducing hypoglycaemia (Kaku et al., 2015). However, the clinical trial was stopped because of its hepatotoxicity (Menon et al., 2018). Full agonist AM-1638 was developed from AM-837, and both of them showed ability to enhance GSIS (Houze et al., 2012, Brown et al., 2012). Another compound AM-5625 showed improved effect compared to AM-1638 (Wang et al., 2013, Hauge et al., 2015). Apart from phenyl propionic acid compounds, compounds with other chemical structure, such as diphenyl pyridine carboxylic acids also activated FFA1 (Zhou et al., 2010).

Like FFA1, FFA4 is also activated by LCFAs. The similarities to FFA1 make it easy to deorphanize; in the meantime, high selectivity over FFA1 becomes a necessary requirement of FFA4 ligands. In 2005, Hirasawa and his colleagues found GPR 120 activated by saturated fatty acid with a carbon chain length from C14 to C18, and unsaturated fatty acid with a carbon chain length from C16 to C22 via measuring changes in intracellular calcium ion concentration (Hirasawa et al., 2005). After this, the receptor was named FFA4. The endogenous agonists include DHA, ALA and palmitic acid. High throughput screening (HTS) has found some synthetic agonists, such as NCG21, TUG-891, and GSK137647A. All of them

## Chapter 1

showed similar effects on FFA4 activation (Suzuki et al., 2008, Hudson et al., 2013b, Sparks et al., 2014).

NCG21 (4-{4-[2-(phenyl-pyridin-2-yl-amino)-ethoxy]-phenyl}-butyric acid), which is obtained from peroxisome proliferator-activated receptor- $\gamma$  (PPAR- $\gamma$ ) agonist derivatives showed 10-fold higher selectivity for FFA4 over the FFA1 (Suzuki et al., 2008). TUG-891 (3-(4-{[5-fluoro-2-(4-methylphenyl) phenyl] methoxy}phenyl) propanoic acid) was the first ligand reported with nanomolar potency at human FFA4 receptors, and although it could also activate FFA1 receptors, its selectivity to FFA4 is much higher (Shimpukade et al., 2012). TUG-891 induced calcium mobilization, receptor phosphorylation,  $\beta$ -arrestin-1 and  $\beta$ -arrestin-2 recruitment, GLP-1 secretion and anti-inflammation. TUG-891 could also activate mouse FFA1 and FFA4 as a potent agonist, though the selectivity of ligands for FFA4 cannot be thought to be equivalent between human and mouse (Hudson et al., 2013b). Compound A (CpdA), developed as orally available, showed anti-inflammatory effects in macrophages (Oh et al., 2014). It also improved insulin sensitivity in animal models (Son et al., 2020). Metabolex 36 and metabolex compound B (also known as Agonist 2), were two of the FFA4 agonists developed by the company Metabolex (now Cymabay Therapeutics). Metabolex 36 inhibited glucose-induced somatostatin secretion from murine islets, however, FFA4 KO mice were not affected (Stone et al., 2014). Compound B (Agonist 2) inhibited basal ghrelin secretion from primary gastric mucosal cells in a dose-dependent way, but it had no effect in cells isolated from FFA4 KO mice (Engelstoft et al., 2013). Compounds with sulfonamide also developed FFA4 agonists. GSK137647A[4-methoxy-N-(2,4,6-trimethylphenyl) benzenesulfonamide] is the first non-carboxylic FFA4 receptor agonist, though it showed less potency (Sparks et al., 2014).

### 1.2.2.2 Antagonists of long-chain fatty acids

There are few reports on antagonists. For FFA1, GW1100 was the first one reported to inhibit the calcium increase insulin secretion induced by GW9508 and linoleic acid (Briscoe et al., 2006). Compounds with a sulfonamide structure such as DC260126 inhibited intracellular calcium responses linoleic acid, oleic acid, and palmitic acid in a dose-dependent way (Hu et al., 2009). In addition,

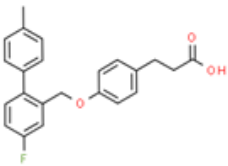
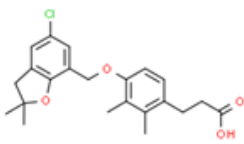
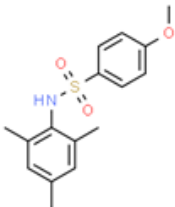
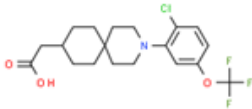
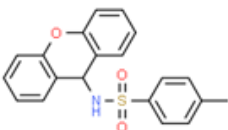
## Chapter 1

DC1260126 improved insulin resistance and prevent pancreatic  $\beta$ -cell dysfunction in obese diabetic db/db mice (Sun et al., 2013).

A sulphonamide AH7614 was considered an FFA4 antagonist by inhibiting FFA4 activation induced by GSK137647A and linoleic acid (Sparks et al., 2014). TUG-891 phosphorylated FFA4 was also inhibited by AH7614 (Watterson et al., 2017). AH7614 treatment reduced the protective effect of DHA on hepatic steatosis, but the reduction was not observed in liver cells from FFA4 receptor-deficient mice (Kang et al., 2018).

## Chapter 1

Table 1-1 Structures and chemical names of FFA4 compounds

Compound	Structure	Chemical Formula
TUG-891		3-{4-[(4-Fluoro-4'-methyl-2-biphenyl)methoxy]phenyl}propanoic acid
Agonist 2		3-{4-[(5-Chloro-2,2-dimethyl-2,3-dihydro-1-benzofuran-7-yl)methoxy]-2,3-dimethylphenyl}propanoic acid
FFA4 agonists		
GSK137647A		N-Mesityl-4-methoxybenzenesulfonamide
Compound A		(3-[2-chloro-5-(trifluoromethoxy)phenyl]-3-azaspiro[5.5]undecane-9-acetic acid)
FFA4 antagonist		
AH 7614		4-Methyl-N-(9H-xanthen-9-yl)benzenesulfonamide

## 1.2.2.3 Agonists of short-chain fatty acids

Short chain fatty acids (SCFAs), which consist of under six carbon atoms, play an important role in physiological processes. They are involved in regulating

## Chapter 1

immune response, affecting cell growth and differentiation, and maintaining glucose homeostasis (Roy et al., 2006, Tedelind et al., 2007). GPR43 was activated by SCFAs and described as the second receptor activated by free fatty acids, also called FFA2 (Le Poul et al., 2003, Nilsson et al., 2003, Brown et al., 2003). The activation level of various fatty acids to the receptors is in order of propionate (C3), acetate (C2), butyrate (C4), and formate (C1) (Nilsson et al., 2003). The synthetic ligands are described as orthosteric ligands and allosteric ligands based on their binding site (Tikhonova and Poerio, 2015). Orthosteric ligands directly binds to orthosteric sites. The orthosteric site is defined as the binding site of the endogenous agonist(s). These sites are often considered as the primary, functional binding pockets for specific targets. Allosteric ligands are defined as ligands that interact at a site of receptor that is distinct from and does not overlap with the orthosteric binding sites. The orthosteric ligands Compound 1 3-benzyl-4-(cyclopropyl-(4-(2,5-dichlorophenyl)thiazol-2-yl)amino)-4-oxobutanoic acid and compound 2 (R)-3(cyclopentylmethyl)-4-(cyclopropyl(4-(2,6-dichlorophenyl)thiazol-2-yl)amino)-4-oxobutanoic acid are orthosteric agonists of FFA2, based on a 4-oxobutanoic acid backbone (Strausberg et al., 2002, Pizzonero et al., 2014). The two compounds have a carboxylate moiety in their structural, which interacts with orthosteric binding sites. [35S]GTPγS and Ca<sup>2+</sup> assays were used to test compound 1 and 2; the results show that two compounds had higher potency than C3. Compound 1 and compound 2 also showed high selectivity over FFA3 (Hudson et al., 2013a). Before compound 1 and compound 2, FFA2 synthetic small molecule agonists were reported allosteric agonists (Wang et al., 2010). In hFFA2-eYFP cells, 4-CMTB treatment received similar response to propionate in [35S]GTPγS assay. Besides, 4-CMTB increased the binding efficacy of SCFAs and activated the FFA2 receptor on its own, so it is also considered ago-allosteric on FFA2 (Smith et al., 2011). AMG-7703 and phenylacetamide 1 and 2 are also act as allosteric agonists (Park et al., 2016). A study on FFA2 described phenylacetamide 1 and 2 as allosteric agonists, which selectively activated FFA2 and inhibited adipose degradation through the Gαi pathway (Lee et al., 2008).

CATPB((S)-3-(2-(3-chlorophenyl) acetamido)-4-(4(trifluoromethyl) phenyl) butanoic acid) and GLPG0974 (4-[[1-(benzo[*b*]thiophene-3-carbonyl)-2-methylazetidine-2-carbonyl]- (3-chlorobenzyl) amino] butyric acid) act as

## Chapter 1

orthosteric antagonists to the FFA2 receptor (Hudson et al., 2012b). GLPG0976 showed inhibition of  $\beta$ -arrestin-2 recruitment and phosphorylation induced by FFA2 agonist compound 1, which was similar to CATPB (Namour et al., 2016). Interestingly, BTI-A-404, and BTI-A-292 reduced the  $\text{Ca}^{2+}$  level via blocking  $\text{G}\alpha_q$  signalling without the presence of agonists (Park et al., 2016). For this reason, they are described as inverse agonists of FFA2.

FFA3, also known as GPR41, activates by endogenous agonist SCFAs (Brown et al., 2003). Compared to FFA2, FFA3 prefer the longer SCFAs (Tikhonova and Poerio, 2015). The corresponding rank order of potencies for FFA3 was propionate (C3) ~ butyrate (C4) ~ valerate (C5) > acetate (C2) > caproate (C6) (Brown et al., 2003, Le Poul et al., 2003). The studies on FFA3 synthetic ligands are still limited. AR420626 N-(2,5-dichlorophenyl)-4-(furan-2-yl)-2-methyl-5-oxo-1,4,5,6,7,8-hexahydro-quinoline-3-carboxamide is an allosteric agonist (Samuel et al., 2008, Tikhonova and Poerio, 2015). It was used in investigating ghrelin and GLP-1 release (Arora et al., 2019).

### 1.2.3 Expression and function of free fatty acid receptors

FFA1 was found expressed in the liver, heart, muscles, pancreas and brains (Briscoe et al., 2003, Kotarsky et al., 2003a). Via measure mRNA level, FFA1 was found highly expressed in the pancreas, and showed 17 folds expression level in pancreatic  $\beta$ -cells throughout the whole pancreas (Itoh et al., 2003). Studies showed that some free fatty acids activated FFA1 increased insulin secretion induced by glucose. Turning FFA1 expression down via small interfering RNA, antisense oligonucleotides in MIN6 cells (Salehi et al., 2005), chemical inhibitors (Briscoe et al., 2006) or with the use of FFA1 KO mice decreased GSIS (Steneberg et al., 2005, Lan et al., 2008, Kebede et al., 2008, Latour et al., 2007).

However, overexpression of FFA1 in high fat diet mice prevented hyperglycemia. These characteristics were relocated to a potential therapeutic target of type 2 diabetes. Secrete glucagon-like peptide 1 (GLP-1), glucose-dependent insulinotropic peptide (GIP) and cholecystokinin (CCK) were released from L, K and I cells after FFA1 was activated, which suggested FFA1 was expressed in enteroendocrine cells and participated in blood glucose mediation in more than one pathway (Edfalk et al., 2008, Sykaras et al., 2012, Liou et al., 2011). Although most FFA1 researches focus on metabolic disease, FFA1 also has a

## Chapter 1

function in other diseases. Apart from the pancreas, brain tissues also express FFA1. FFA1 at a high level and may play roles in anti-inflammatory effects in the hypothalamus (Dragano et al., 2017).

FFA2 intensively expressed in immune cells, such as eosinophils and monocytes, showed maximum expression level in neutrophils, which suggested FFA2 is involved in immune response (Mishra et al., 2020). In colitis, arthritis, and airway inflammatory animal models, FFA2 KO mice failed to be resistant to inflammatory disease, and showed more inflammation (Maslowski et al., 2009). FFA2 also plays important roles in regulating intestinal function. FFA2 was located in the intestine, and activated by SCFAs resulting in GLP-1 release. QRT-PCR studies have shown FFA2 expression in GLP-1 secreting L-cells (Tolhurst et al., 2012). FFA2 was found overexpressed in the white adipose tissue of mice on a high fat diet. FFA2 also increased the activation of proliferator-activated receptor- $\gamma$ 2 (PPAR $\gamma$ 2) in 3T3-L1 cells. The inhibition of FFA2 expression by siRNA decreased PPAR $\gamma$ 2, lead to adipose accumulation in cells (Hong et al., 2005).

Although amino acid homology between FFA2 and FFA3 is 43%, and they are all activated by SCFAs, the distribution of FFA3 is different from FFA2. FFA3 expression is detected in adipose tissue, the spleen, bone marrow, liver, pancreatic  $\beta$ -cells, and brain endothelium (Mishra et al., 2020). The highest expression of FFA3 appears in adipose tissue, whereas FFA2 is in immune cells. However, the functions of FFA3 overlap FFA2 functions in some sections. FFA3 activation increased GLP-1 release in mice colonic crypts (Samuel et al., 2008). GLP-1 and PYY significantly reduced in FFA3 KO mice compared to WT ones (Shimizu et al., 2019). Interestingly, different phenotypes were shown between male and female mice fed by high fat diet. Body fat mass and plasma leptin levels decreased in male mice, which was also observed in human (Bellahcene et al., 2013). FFA3 is also able to reduce inflammatory response (Mishra et al., 2020).

FFA4 is expressed in numerous tissues including those of the intestines, colon, lungs, as well as adipose tissue (Oh et al., 2010). In the lung, it has been suggested that the receptor may play a role in modulating lung inflammation associated with respiratory diseases (Milligan et al., 2017). FFA4 activated by an agonist expanded mouse airways pre-contracted by carbachol (Prihandoko et al.,

## Chapter 1

2020). Studies using animal models showed FFA4 to have a profound role in the modulation of energy homeostasis and metabolism as well as endocrine and immune functions (Oh et al., 2010, Oh et al., 2014). Activation of FFA4 by fatty acid or synthetic ligands caused enhancement of hepatic glucose uptake and decrease steatosis (Hirasawa et al., 2005). Insulin sensitivity in animals was also increased following FFA4 activation (Oh et al., 2014). Like other FFA receptors, FFA4 is also involved in the regulation of intestinal hormone secretion. Ghrelin secretion was inhibited, and GLP-1 and CCK release was increased after FFA4 activation (Hirasawa et al., 2005).

### 1.2.4 Signalling of free fatty acid receptors

#### 1.2.4.1 G protein dependent signalling

Free fatty acids receptors couple to G proteins and transmit physiological signals after being activated by their agonists. Gαq/11 protein has been reported to participate in FFA1 signal transduction (Itoh et al., 2003). FFA1 couples to Gαq/11 proteins, followed by phospholipase C (PLC) hydrolysis. Inositol triphosphate (IP<sub>3</sub>) and diacylglycerol (DAG) are produced. PKC activation increased the level of intracellular Ca<sup>2+</sup>, and insulin was released subsequently (Gilon and Henquin, 2001).

Both FFA2 and FFA3 have been proved to increase the level of IP<sub>3</sub> and reduce cAMP, resulting in the Ca<sup>2+</sup> response and phosphorylation (Le Poul et al., 2003). However, when treated with pertussis toxin (PTX), the Ca<sup>2+</sup> response in FFA3 was fully blocked, while the Ca<sup>2+</sup> response in FFA2 still existed (Le Poul et al., 2003). This suggest that FFA3 mainly couples to Gai/o proteins while FFA2 couples to both Gai/o and Gαq/11.

FFA4 coupling to Gαq/11 protein has been proved by inducing Ca<sup>2+</sup> response but not increasing cAMP when it is activated (Hirasawa et al., 2005). However, several reports have shown that treatment with TPX inhibited the release of ghrelin and somatostatin from delta cells, which suggests Gai/o also participates in FFA4 transduction of signals (Engelstoft et al., 2013). In STC-1 cells, FFA4 enhanced CCK and GLP-1 secretion by IP<sub>3</sub> (produced from PLC hydrolysis) and induced an increase in intercellular Ca<sup>2+</sup> (Hirasawa et al., 2005). PLC is also



## Chapter 1

involved in apoptosis regulated by FFA4. In this system, DAG activated PKC/ERK to inhibit apoptosis. Another pathway via Gαq/11 contains PI3K/AKT (Alvarez-Curto et al., 2016, Katsuma et al., 2005). Akt as a downstream target is activated by PI3K, and plays a role in cell survival and proliferation (Katsuma et al., 2005). β-arrestin 2 is identified to have an important role in FFA4 anti-inflammatory effects (Butcher et al., 2014). After ligand binding to FFA4, internalized β-arrestin-2 would interact with Transforming Growth Factor-β-Activated Kinase 1 (TAK1), which is a point of convergence for TNF-α and TLR4 signal transduction. As a result, the JNK and IKK activation pathways are inhibited and this leads to the inhibition of inflammation (Oh et al., 2010).

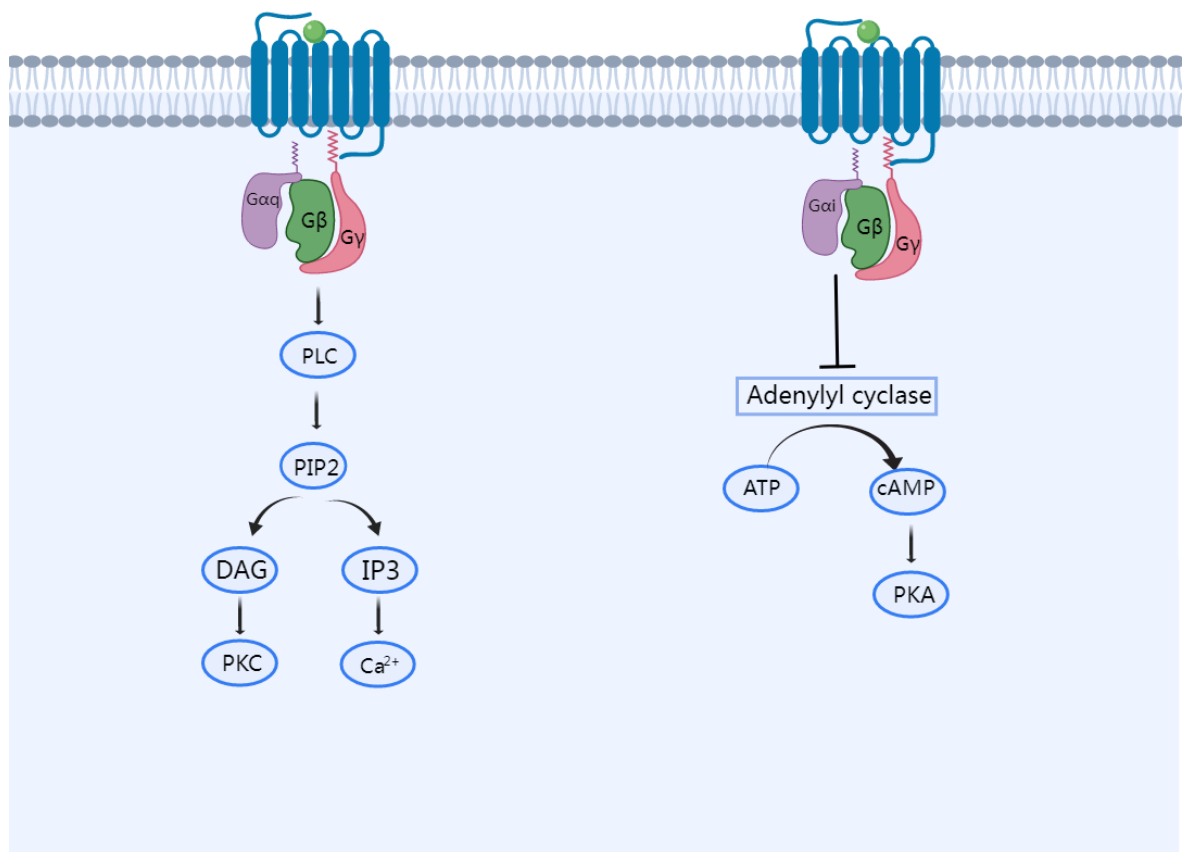


**Figure 1.4 G protein dependent signalling pathway of FFA4**

Agonist-activated FFA4 (agonist is shown as a green ball) bind heterotrimeric G proteins, causing α and βγ subunits to dissociate and signal. Gαq stimulates PLC which cleaves PIP2 to produce DAG and (IP3). DAG activates PKC which feeds into MAPK signalling. IP3 stimulates calcium release from the sarcoplasmic reticulum in endoplasmic reticulum. Gαi signals to inhibit adenylyl cyclase (AC) which is stimulated by Gas signalling. The inhibition also affects PKA activation by cAMP.

## Chapter 1

**1.2.4.2 Phosphorylation in FFA4**

It has been demonstrated that agonism of FFA4 with docosahexaenoic acid (DHA) and alpha-linoleic acid (ALA) facilitates phosphorylation of FFA4 rapidly in HEK 293 cells which were transiently expressed human FFA4 (Burns and Moniri, 2010). Several studies have been focused on the precise mechanisms that promote FFA4 phosphorylation. The mechanisms behind both heterologous and homologous phosphorylation of FFA4 were demonstrated depending on different mediators (Burns et al., 2014). DHA-mediated signal was significantly reduced but not fully blocked in GRK6 knockdown HEK 293 cells, while similar signal levels to scrambled control condition were shown in other GRKs (GRK2, GRK3 and GRK5) knockdown cells. Stimulation with the phorbol ester phorbol-12-myristate-13-acetate (PMA), which is a PKC agonist widely used in in vitro and in vivo experiments, resulted in a significant increase in FFA4 phosphorylation, and the phosphorylation was inhibited by PKC-selective inhibitor bisindolylmaleimide II (BIMII). These results proved heterologous phosphorylation depends on PKC while both GRK6 and PKC contribute to homologous phosphorylation of FFA4 (Burns et al., 2014). However, pre-treatment of cells with BIMII failed to reduce the phosphorylation level induced by TUG-891, which indicated PKC was not involved in agonist-dependent phosphorylation of FFA4 (Butcher et al., 2014).

The phosphorylation sites were determined via a mass spectrometry-based proteomics study. The sequencing revealed four phosphorylation sites Thr<sup>347</sup>, Thr<sup>349</sup>, Ser<sup>350</sup>, and Ser<sup>357</sup>, located in the C-terminal tail in human FFA4. Mutation on all four sites significantly reduced phosphorylation of FFA4 in response to TUG-891, but still showed some phosphorylation. Another mutation in combination with Ser<sup>360</sup> and the other four phosphorylation sites showed no phosphorylation response to TUG 891 treatment, which suggested that the sites of agonist-regulated phosphorylation in human FFA4 were Thr<sup>347</sup>, Thr<sup>349</sup>, Ser<sup>350</sup>, Ser<sup>357</sup>, and Ser<sup>360</sup> (Butcher et al., 2014). Open-source computer algorithms predicted the sites of some other potential phosphorylation sites located on Ser<sup>237</sup>, Thr<sup>242</sup> and Ser<sup>250</sup> in the third intracellular loop (ICL). However, the single mutants on Ser<sup>237</sup>, Thr<sup>242</sup>, and Ser<sup>250</sup> showed the same phosphorylation level as WT FFA4, which demonstrated that these are not significant sites of FFA4 phosphorylation (Burns et al., 2014).

## Chapter 1

In mouse FFA4, five serine and threonine residues were identified as phosphorylation sites. These residues were located on C-terminal and divided into two clusters. Cluster 1 was involved in Thr<sup>347</sup>, Thr<sup>349</sup>, and Ser<sup>350</sup>, and cluster 2 was involved in sites on Ser<sup>357</sup> and Ser<sup>361</sup>. Interestingly, Ser<sup>360</sup> was failed to be identified as a phosphorylation site by mass spectrometry study, but identified by identifying peptides (Prihandoko et al., 2016).

FFA4 interacts effectively with  $\beta$ -arrestin 2 in an agonist-dependent manner (Hudson et al., 2013b). Truncations from the residues on position 340, 345, 350, and 355 to remove the agonist-mediated phosphorylation sites showed progressively increasing response to TUG-891-induced  $\beta$ -arrestin 2 recruitment and receptor internalization. The interaction between phosphorylated FFA4 and  $\beta$ -arrestin 2 was regulated by a series of phosphorylation events (Butcher et al., 2014). Similar results were reported in the mouse orthologue of FFA4 (Prihandoko et al., 2016).

### 1.2.5 FFA4 isoforms

The human FFA4 gene is comprised of a single 1134 nucleotide sequence which encodes a protein of 361 amino acids (GPR120 Short, GPR120-S), but it is found that the human FFA4 gene can be alternatively spliced yielding an isoform of 377 amino acids (GPR120 Long, GPR120-L) (Hirasawa et al., 2005). A study indicated that the long isoform of FFA4 existed only in human beings (Moore et al., 2009). The GPR120-L contains a insertion of 16 additional amino acids between positions 231 and 247 in intracellular loop 3 (ICL3) (Watson et al., 2012). The insertion also contains four phospho-labile serine/threonine residues, which suggests that GPR120-S and GPR120-L could have different phosphorylation profiles (Burns and Moniri, 2010). However, the results failed to detect differences in the rate or degree of agonist-mediated phosphorylation between the two isoforms (Burns and Moniri, 2010). Moreover, both GPR120S and GPR120L receptors recruited  $\beta$ -arrestin2 and internalized stimulated oleic acid. Surprisingly, only the short isoform showed an ability to increase intracellular Ca<sup>2+</sup> concentration in HEK293 cells, which suggested that GPR120-L was not involved in Ca<sup>2+</sup> mobilization (Watson et al., 2012).

## Chapter 1

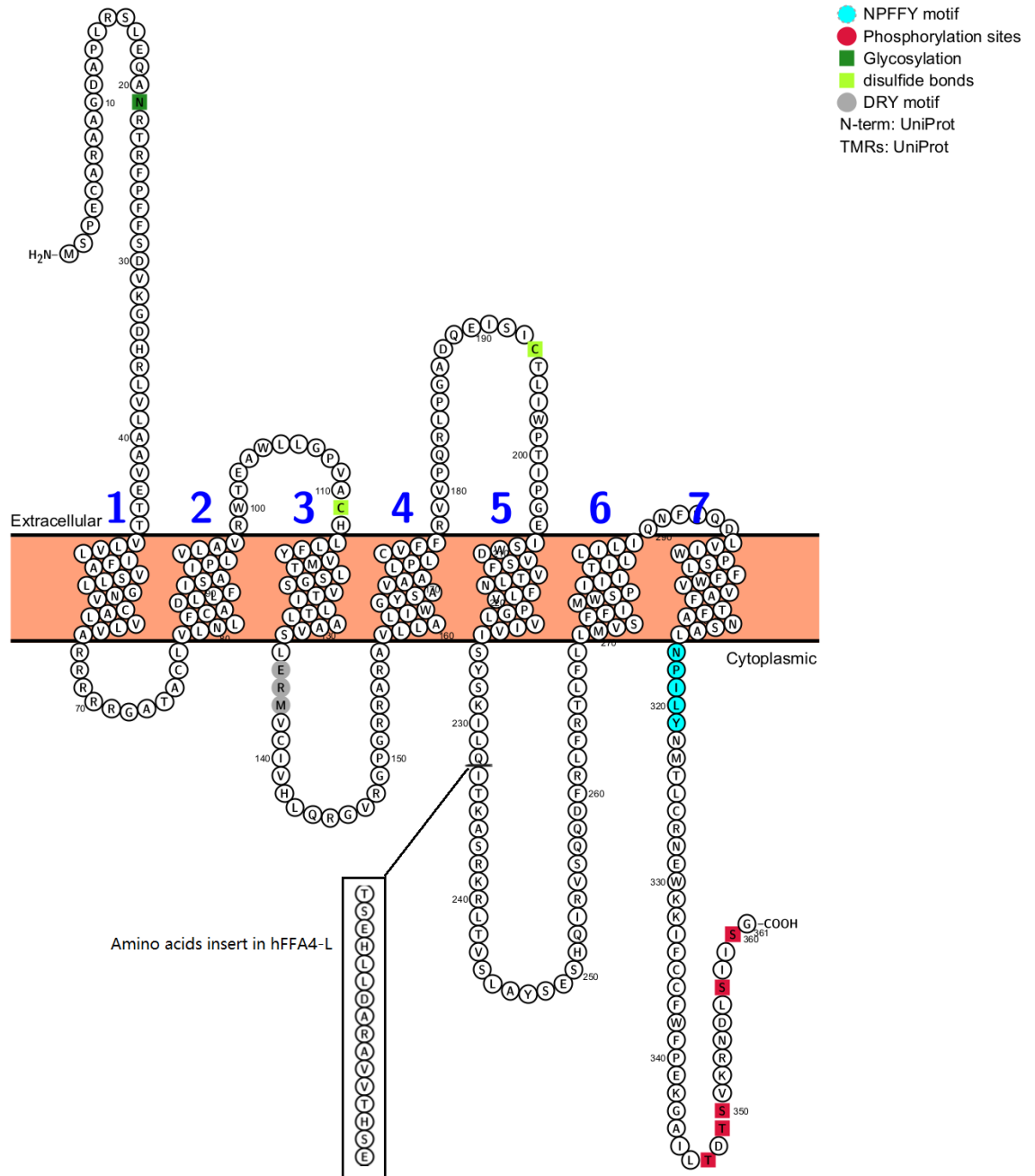


**Figure 1.5 Primary amino acid sequence of human FFA4 short isoform**

Amino acid residues from the human FFA4 short form isoform are displayed as a snake plot. The location of a 16 amino acid insertion in the third intercellular loop, which forms the FFA4 long isoform, is marked. The phosphorylation sites in C-terminals are shown in red. The residue in N-terminal which is able to be N-link glycosylated is shown in green.

## 1.2.6 Therapeutic target for FFA4

### 1.2.6.1 Type 2 diabetes

Type 2 diabetes (T2DM) is a metabolic disease caused by the decrease of insulin secretion in  $\beta$  cells in islets, or insulin resistance in target cells. Early-stage type 2 diabetes can be monitored by controlling the diet or by using chemical

## Chapter 1

medicine, until intervention by insulin treatment (Kahn et al., 2014). The main drugs used were able to enhance insulin secretion, sensitize the target organs of insulin, and impair glucose absorption (Kahn et al., 2014). The FFA4 receptor is related to complex pharmacological activity and has different effects on metabolic disorders, which make it a potential therapeutic focus for type 2 diabetes. FFA4 is highly expressed in enteroendocrine cells and increases GLP-1 secretion, which results in insulin release (Tanaka et al., 2008). It was found in WT mice that peripheral free fatty acids facilitated glucose intake and insulin sensitivity in tissues, but this was not found in FFA4 KO mice (Zhang and Leung, 2014). Moreover, insulin resistance was found in FFA4 KO mice fed a high fat diet (Zhang and Leung, 2014). These evidences proved that FFA4 could be targeted to treat T2DM. A recent study illustrated that the combined use of the PPAR $\gamma$  agonist Rosiglitazone and the GPR120 agonist CpdA produced an additive effect to improve glucose tolerance and insulin sensitivity (Paschoal et al., 2020). The combination also requires a lower dose of rosiglitazone, which is helpful to avoid its side effects (Paschoal et al., 2020).

### 1.2.6.2 Cancer

Beyond T2DM, the therapeutic area in which FFA4 has perhaps attracted the greatest attention to date is cancer. Many studies have shown interest in this area (Houthuijzen, 2016). A previous study demonstrated that omega-3 fatty acids such as DHA inhibited proliferation and migration in human prostate cell lines DU145 and PC-3 (Liu et al., 2015). FFA4 agonist TUG-891 showed similar ability in this inhibitory effect, however the inhibitory effect was not observed in FFA4 knockdown prostate cell lines. The comparison between cancer tissue and normal tissue from breast cancer patients pointed out that FFA4 showed a higher expression in cancer tissue (Zhu et al., 2018). However, the inhibitory effect in breast cancer cells was considered to be mediated by FFA1 rather than FFA4 (Hopkins et al., 2016). Apart from the inhibitory effect related to fatty acids, FFA4 contributed to the development of systemic resistance to cisplatin-based chemotherapy (Milligan et al., 2017). A previous study has indicated that the platinum-induced fatty acid 16:4(n-3) induced an FFA4 signalling cascade in splenic macrophages to promote chemotherapy resistance (Houthuijzen et al., 2017). This result suggested that FFA4 antagonists might be able to limit development of chemotherapy resistance.

## Chapter 1

### 1.2.6.3 Lung diseases

It has been shown that FFA4 is abundantly expressed in lung epithelial cells, especially in club cells (Miyachi et al., 2009, Lee et al., 2017). A study indicated FFA4 had a positive effect on mediating the recovery from naphthalene-induced airway injury. The role that FFA4 might play in lung physiology was revealed by a study by Prihandoko and his colleagues (Prihandoko et al., 2020). In this study, FFA4 was proved to promote airway relaxation, and relieve airway inflammation in the presence of agonist TUG-891 (Prihandoko et al., 2020). The roles of FFA4 in lung diseases are only beginning to be addressed. Despite that precise pharmacological properties of clinically effective human FFA4 agonists have not been fully understood, the research gave evidence that pharmacological activation of lung FFA4 had beneficial effects on lung diseases (Prihandoko et al., 2020). This suggests that it may be a target for the treatment of airway diseases associated with bronchoconstriction and inflammation.

### 1.2.7 Therapeutic relevance of FFA2

FFA2 was found activated by short chain fatty acid in 2003 (Brown et al., 2003). It is widely expressed throughout the body and has been suggested to play a role in immune system and metabolism. High expression of FFA2 has been reported in enteroendocrine cells, activation of which results in the release of the incretin GLP-1 and the satiety hormone peptide YY (PYY) (Tolhurst et al., 2012, Chambers et al., 2015). The mice overexpressing FFA2 in adipose kept lean on a high fat diet, while the FFA2 KO mice were observed increase on weight (Kimura et al., 2013). This demonstrated the expression of FFA2 receptor was able to effect on adiposity. However, other studies showed contradictory results. FFA2 showed inhibition on isoproterenol-induced lipolysis in adipose tissue, and this inhibition was absent in FFA2-KO mice (Ge et al., 2008). The inhibition was PTX-sensitive, which suggested the inhibition of lipolysis by FFA2 was mediated by G $\alpha$ i/o (Ohira et al., 2013). FFA2 also participates in the resolution of inflammation, leading to neutrophil apoptosis at infection sites and mediates IgA and IgG responses induced by cholera toxin (Galvão et al., 2018, Yang et al., 2019). All the reports suggest that FFA2 modulation could be of use as a therapeutic target in inflammatory diseases and in metabolic diseases such as diabetes or obesity. In fact, a FFA2 antagonist had been tested in clinical trial,

## Chapter 1

but was terminated because of no beneficial effects (Namour et al., 2016, Bolognini et al., 2016b).

### **1.2.8 Unique mouse model facilitates study of physiological role of FFA2**

Previous studies from our group developed a unique mouse model called hFFA2-DREADD. It is a Designer Receptor Exclusively Activated by Designer Drug (DREADD) variant of human FFA2 generated by substitution of two amino acids (Cys4.57Gly and His6.55Gln). Some molecules such as sorbic acid (SA) and MOMBA (4-methoxy-3-methyl-benzoic acid) were then identified as agonists for hFFA2-DREADD (Bolognini et al., 2019, Barki et al., 2022). Because hFFA2-DREADD is unresponsive to natural SCFAs, but is activated by sorbic acid and MOMBA makes it possible to differentiate actions of FFA2 from other free fatty acid receptors, especially FFA3 (Bolognini et al., 2019, Hudson et al., 2012a) in tissue from the hFFA2-DREADD mice. Interestingly, human-specific antagonists of FFA2 GLPG0974 and CATPB are still able to inhibit the activity of hFFA2-DREADD (Bolognini et al., 2019). Signalling pathways of hFFA2-DREADD are displayed in Figure 1.6. The signalling through hFFA2-DREADD is indistinguishable from that of wild-type hFFA2. Activation of hFFA2-DREADD has been shown to promote the migration of neutrophils, the release of GLP-1 and PYY, and to inhibit lipolysis in hFFA2-DREADD mice (Bolognini et al., 2019, Milligan et al., 2021). Additionally, to detect the receptor in tissues in these animals hFFA2-DREADD is C-terminally tagged with the HA sequence.

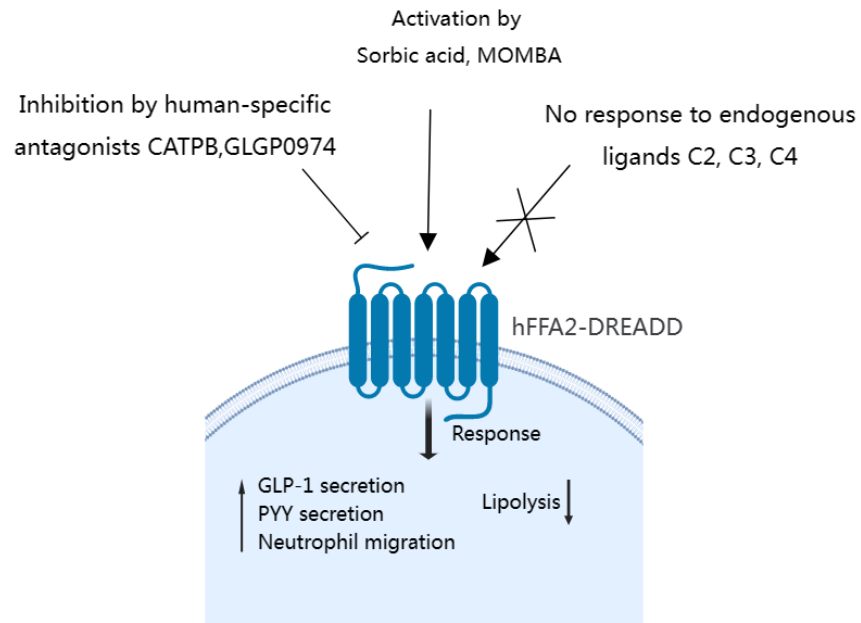


**Figure 1.6 Signalling pathways of hFFA2-DREADD**

hFFA2-DREADD is activated by the nonendogenous ligands sorbic acid and MOMBA, but is inert to the endogenous ligand C3. FFA2-DREADD retains high affinity for the human-specific blockers CATPB and GLPG0974.

### 1.3 Application of protein phosphorylation

Protein phosphorylation modification is one of the most common and important post-translational modifications of proteins (Graves and Krebs, 1999). At least 30% of proteins in organisms are phosphorylated and modified by phosphorylation (Ardito et al., 2017). It plays an important role in the regulation of signal transduction, gene expression, cell cycle, development and differentiation and many other processes. It has been shown that the interaction between proteins can be regulated by phosphorylation at multiple sites (Delom and Fessart, 2011, Yang et al., 2017). Abnormal up-regulation or down-regulation of protein phosphorylation levels is closely related to the occurrence of various diseases such as diabetes, metabolic syndrome, Alzheimer's disease, etc (Ardito et al., 2017, Hampel et al., 2010). Therefore, exploration the characteristics of protein phosphorylation is necessary for understanding the functions of proteins.



## Chapter 1

### 1.4 Aims

Previous studies have shown that the phosphorylation of GPCR is a complex mechanism in organisms. This process involves various proteins and kinases and ligand-specific phosphorylation patterns of a receptor to direct its distinct functional outcomes. GRKs are essential mediators, and homologous and heterologous phosphorylation of FFA4 has been shown to be mediated by GRK6 and PKC respectively (Burns et al., 2014). However, FFA4 phosphorylation caused by synthetic ligands is still unclear. Moreover, although the FFA phosphorylation sites have been identified, the interactions between these sites and arrestin remains to be further investigated.

Here are three main aims of this thesis are:

- i ) To characterize the phospho-specific antibodies Anti-Thr<sup>347</sup> FFA4 and anti-Thr<sup>349</sup>/Ser<sup>350</sup> FFA4;
- ii ) Utilizing the phospho-specific antibodies and GRK inhibitors to investigate the roles of GRKs in the phosphorylation of FFA4;
- iii) Trying to use the antibodies in samples from animal models and investigate the possibilities of these phospho-specific antibodies in translational pharmacology.

## Chapter 2 Materials and methods

### 2.1 Chemicals and reagents

Unless otherwise specified, all chemicals and reagents were supplied by Sigma Aldrich (Dorset, UK) and Thermo Fisher Scientific (Loughborough, UK). Mammalian cell culture reagents such as various cell culture media, phosphate buffered saline (PBS), Hanks' balanced salt solution (HBSS), Dulbecco's modified Eagle's medium (DMEM), Nutrient Mixture F-12, foetal bovine serum (FBS), penicillin/streptomycin solution, poly-D-lysine, were purchased from Gibco (Thermo Fisher Scientific, Loughborough, UK). Primary antibody Anti-Thr<sup>347</sup> FFA4 and anti-Thr<sup>349</sup>/Ser<sup>350</sup> FFA4 were purchased from (7TM Antibodies, Jena, Germany). Anti-HA was purchased from Roche Applied Science (Penzberg, Germany). Secondary antibodies used for western blot were purchased from LI-COR Biosciences (Cambridge, UK). Secondary antibodies used for immunocytochemistry were purchased from Invitrogen (Carlsbad, US). Details of the antibodies were showed in Table 2-1, Table 2-2 and Table 2-3.

### 2.2 Compounds preparation

TUG-891 (3-(4-{{[5-fluoro-2-(4-methylphenyl) phenyl] methoxy} phenyl} propanoic acid), 4-CMTB (4-chloro- $\alpha$ -(1-methylethyl)-N-2-thiazolylbenzeneacetamide) AZ1729 (N-[3-(2-Carbamimidamido-4-methyl-1,3-thiazol-5-yl) phenyl]-4-fluorobenzamide), and CATPB ((S)-3-(2-(3-chlorophenyl)acetamido)-4-(4-(trifluoromethyl) phenyl)butanoic acid) were purchased from Tocris (Bristol, UK). Agonist 2 (4-[(5-Chloro-2,3-dihydro-2,2-dimethyl-7benzofuranyl) methoxy]-2,3-dimethylbenzenepropanoic acid), AH 7614 (4-methyl-N-9H-xanthen-9-yl-benzenesulfonamide) and Compound 101 (3-[(4-methyl-5-pyridin-4-yl-1,2,4-triazol-3-yl)methylamino]-N-[[2-(trifluoromethyl)phenyl]methyl]benzamide) were purchased from MedChemExpress (New Jersey, USA). Compound 15 ((S)-N4-(3-Ethyl-1H-pyrazol-5-yl)-N2-(1-(5-fluoropyridin-2-yl)- ethyl)-5-methoxyquinazoline-2,4 diamine), Compound 18 (N2-(4-Chloro-2-methoxybenzyl)-N4-(5-ethyl-1H-pyrazol-3-yl)-5-methoxyquinazoline-2,4-diamine), and Compound 19 ((S)-N2-(1-(5-Chloropyridin-2-yl)ethyl)-N4-(5-ethyl-1H-pyrazol-3-yl)-5-methoxyquinazoline-2,4-diamine) were obtained from Ontario Institute for Cancer Research (Ontario, Canada). MOMBA (4-methoxy-3-methyl-

## Chapter 2

benzoic acid) was purchased from Fluorochem (Hadfield, UK). All powdered test compounds except MOMBA were resuspended in dimethyl sulfoxide (DMSO), (Thermo Fisher Scientific, Waltham, US) to a 10 mM working stock solution. MOMBA was resuspended in DMSO to a 100 mM working stock solution.

## 2.3 Cell culture

### 2.3.1 Flp-In TREx 293 cells

Flp-In TREx 293 cells were cultured in DEME (without sodium pyruvate), supplemented with 10% (v/v) fetal calf serum, 1% penicillin/streptomycin mixture (v/v) and 0.2 mg/ml hygromycin B (Roche Applied Science, Penzberg, Germany), at 37°C in a 5% CO<sub>2</sub> humidified atmosphere. The Flp-In TREx cells was induced by treatment with up to 100 ng/ml doxycycline overnight before use if the cells were expected to express FFA4 receptor. Flp-In TREx 293 cells were generated in house.

### 2.3.2 Chinese hamster ovary (CHO) cells

Chinese hamster ovary (CHO) cells were cultured in Nutrient Mixture F-12 medium cells and 1% penicillin/streptomycin mixture (v/v) at 37°C in a 5% CO<sub>2</sub> humidified atmosphere.

CHO cells transfected to express hFFA4-HA were cultured in Nutrient Mixture F-12 medium, with 10% (v/v) fetal calf serum, 1% penicillin/streptomycin mixture (v/v) and 0.2 mg/ml hygromycin B (Roche Applied Science, Penzberg, Germany), at 37°C in a 5% CO<sub>2</sub> humidified atmosphere. These cells were generated in house and express hFFA4-HA stably.

## 2.4 Cell harvesting

Cells were harvest after doxycycline induction overnight and treatment. Medium was aspirated and cells were washed with 5 ml of ice-cold PBS. After washing, 5 ml of ice-cold PBS was added to petri dish. To maintain protein cells were dislodged from plasticware by scraping on ice. Cell suspensions were transferred to ice-cold 15 ml tubes and centrifuged at a speed of 3000 rpm for 5 minutes at

## Chapter 2

4°C to get cell pellets. All supernatant was aspirated and cell pellets were stored at -80°C.

### **2.5 Isolation of cellular lysates**

Isolated cell pellets were resuspended in 500µl lysis buffer (150 mM NaCl, 50 mM Tris-HCl pH 8, 5 mM EDTA, 1% (v/v) IGEPAL CA-630, 0.5% (w/v) Na-Deoxycholat), on the day of use, and supplemented with 1 EDTA-free cOmplete™ protease cocktail inhibitor tablet (Roche Applied Science, Penzberg, Germany) and 1 PhosSTOP™ phosphatases inhibitor (Roche Applied Science, Penzberg, Germany) per 10 mL buffer. Lysates were placed within a rotator and rotated for 30 minutes at 4°C, before centrifugation at 15,000 rpm at 4°C for 15 minutes to pellet cellular debris. All supernatants were collected and measured protein concentration by Bradford protein assay. Samples were then frozen at -80°C until required.

### **2.6 Protein quantification using the Bradford assay**

To control loading amount, the concentration of cell lysates should be measured. Protein concentrations from cell lysates and membrane preparations were determined by measuring absorbance at 595 nm in a spectrophotometer. Bovine Serum albumin (Roche Applied Science, Penzberg, Germany) standards (200 µg/ml-2000 µg/ml) were prepared and mixed with 1 ml of Bradford reagent. The spectrophotometer was blanked with lysis buffer 1:100 diluted in distilled water (1 ml volume) and 1 ml of Bradford reagent (Sigma, Darmstadt, Germany). Protein samples were first 1:10 diluted in lysis buffer, and then diluted (1:1000) in distilled water (1 ml volume). 1 ml Bradford reagent was added to each sample. The absorbance of the protein samples was measured and the protein concentration determined by extrapolating their absorbance with the absorbance of the Bovine Serum albumin (BSA) standards.

The cell lysates were normalized to the same concentration. The concentration depended on the lowest concentration of the cell lysate in one individual experiment, usually between 1.1µg/µl-1.6µg/µl. The normalized cell lysates were immunoprecipitated.

## 2.7 Immunoprecipitation

### 2.7.1 GFP-trap

GFP-trap is a tool to capture GFP fusion proteins. It directly covalently couples alpaca nanoantibodies targeting GFP with solid-phase carriers to precipitate of high-purity GFP fusion protein efficiently and rapidly. Cell lysates (200  $\mu$ l) were added 20  $\mu$ l GFP-trap (ChromoTek, Planegg, Germany) incubated overnight at 4°C. The beads were washed three times with ice-cold 500  $\mu$ l lysis buffer at the speed of 2500 rcf for 5 minutes at 4°C. Immunocomplexes were resuspended in 60 $\mu$ l 2 $\times$ Laemmli buffer (Merck, Glasgow, UK) and placed in a 60°C water bath for 5 minutes. After that, samples were centrifuged at a speed of 2500 rcf for 2 minutes at 4°C and all supernatants were transferred to fresh 1.5ml eppendorf tubes. The supernatants were then separated by the NuPAGE Novex system (Invitrogen, Carlsbad, US) using 4-12% Bis-Tris gels.

### 2.7.2 HA-trap

Cell lysates (1 ml) were cleared by centrifugation (15,000 rpm for 15 minutes at 4°C) and added 50  $\mu$ l Anti-HA Affinity Matrix (Roche Applied Science, Penzberg, Germany) incubated overnight at 4°C. The beads were washed twice with ice-cold 1 ml of lysis buffer at the speed of 1000 rcf for 1 minutes at 4°C. Immunocomplexes were resuspended in 2 $\times$ Laemmli buffer (Merck, Glasgow, UK) and placed in a 60°C water bath for 5 minutes. After that, samples were centrifuged at a speed of 1000 rcf for 2 minutes at 4°C and all supernatants were transferred to fresh 1.5ml eppendorf tubes. The supernatants were separated by the NuPAGE Novex system (Invitrogen, Carlsbad, US) using 4-12% Bis-Tris gels.

## 2.8 Antibody characterization using phosphatase treatment

To characterize potential phosphor-specific antibodies, phosphatase treatment experiments were performed. Flp-In TReX 293 cells were seeded in 10 mm dishes, and incubated to 80% confluence. Cells were serum starved for 1 hour and stimulated with agonists or antagonists for 5 minutes at 37°C. The receptors were purified by immunoprecipitation as described above. The

## Chapter 2

immunoprecipitated receptors were washed three times with 500 $\mu$ l lysis buffer supplemented with protease inhibitors and phosphatase inhibitor. Samples were run on 4-12% SDS-PAGE and analysed by western blotting.

### **2.9 Lambda Protein Phosphatase (LPP) treatment**

After immunoprecipitation overnight, samples were washed three times with ice-cold 500  $\mu$ l lysis buffer at the speed of 2500 rcf for 5 minutes at 4°C. 3  $\mu$ l of Lambda Protein Phosphatase (New England Biolabs, Hitchin, UK), 5  $\mu$ l of 10X NEBuffer Metallo Phosphatases, 5  $\mu$ l of 10 mM MnCl<sub>2</sub>, and 37  $\mu$ l of lysis buffer were added to each sample to make a 50  $\mu$ l reaction system. Samples were incubated at 30°C for 3 hours. After incubation, immunocomplexes were resuspended in 2 $\times$ Laemmli buffer and placed in a 60°C water bath for 5 minutes. Samples were centrifuged at a speed of 2500 rcf for 2 minutes at 4°C and all supernatants were transferred to fresh 1.5ml eppendorf tubes and then run on 4-12% SDS-PAGE and analysed by western blotting.

### **2.10 N-glycosidase F (N-GF) treatment**

3  $\mu$ l of N-glycosidase F (Roche Applied Science, Penzberg, Germany) was added to cell lysate and incubated for 3 hours at 37°C and then immunoprecipitated as described before. Samples were run on 4-12% SDS-PAGE and analysed by western blotting.

### **2.11 Western blot assay**

Receptor proteins were separated by the NuPAGE Novex system (Invitrogen, Carlsbad, US) using 4-12% Bis-Tris gels. The supernatants described in section 2.7 were loaded 20  $\mu$ l per well. The gels were run in NuPAGE™ MOPS SDS Running Buffer (Invitrogen, Carlsbad, US) at 170 V for 20 minutes and then at 200 V until the loading buffer reached the bottom of the gel. When finishing, gels were electroblotted onto nitrocellulose membranes using the wet transfer method at 60 v for 2 hours with Tris-glycine transfer buffer (25 mM Tris, 190 mM glycine, and 20% (v/v) ethanol). Membranes were blocked in TBS (20 mM Tris base, 140mM NaCl,) containing 0.1% Tween-20 (TBS-T) and 5% BSA (w/v) for 1 hour at room temperature, and then incubated in primary antibody dilution (1:1000)

## Chapter 2

with 5% BSA in TBS-T overnight at 4 °C. All primary antibodies are displayed in Table 2-1. The host of the primary antibodies is rabbit. Membranes were washed with TBS-T four times, and each wash was 5 minutes. Then membranes were incubated in secondary antibody (1:10,000 dilution) in dark. Secondary antibody is displayed in Table 2-2. Membranes were washed three times and each wash was 5 minutes, and developed by Odyssey Sa Li-cor. Odyssey Sa Li-cor is an image system to measure fluorescence and analysis the immunoblots.

## 2.12 Immunocytochemistry

Cells were seeded ( $5 \times 10^5$  cells/ml) on poly-D-lysine coated 22 mm round coverslips in 24-well plates and maintained at 37 °C in a 5% CO<sub>2</sub> humidified atmosphere. Cells were treated as described previously, then fixed with 4% (w/v) paraformaldehyde in PBS for 10 min at room temperature. Fixed cells were washed 3 times in PBS, then blocked with blocking buffer (PBS + 1% BSA +3% goat serum) for 2 hours at room temperature. Cells were then before incubating with primary antibody (Anti-Thr<sup>349</sup>/Ser<sup>350</sup> FFA4 and Anti-Thr<sup>306</sup>/Thr<sup>310</sup> FFA2, displayed in Table 2-1) overnight at 4 °C. Subsequently, cells were washed 3 × 15 min in PBS, then incubated with secondary antibody (displayed in Table 2-3) for 2 hours at room temperature. Cells were washed 3 × 15 min in PBS, and coverslips were mounted onto glass slides using VECTASHIELD Mounting Medium with DAPI (Vector laboratories). Imaging was performed using the 63× Plan-Apochromat objective of the Zeiss 880 Axio Observer Z1 Laser Scanning Confocal Microscope (Zeiss). Samples were excited by lasers (at 2.0% power) at 594 nm, 488 nm and 405 nm, inducing emission at 655 nm, 522 nm and 441 nm, respectively. Track 1 (red) detected emission between 604 nm and 706 nm, Track 2 (green) detected emission between 511 nm and 533 nm, Track 3 (blue) detected between 411 nm and 470 nm.

## Chapter 2

### **2.13 $\beta$ -arrestin 2 recruitment**

#### **2.13.1 Luria-Bertani (LB) agar plates**

Luria-Bertani (LB) agar (1% w/v tryptone, 0.5% w/v yeast extract, 1% w/v NaCl, and 1.5% w/v bacteriological agar) was autoclaved and placed in 50 °C oven to cool down. About 25 ml of LB agar was transferred into petri dish and wait until solidification, after ampicillin (final concentration 100 µg/ml) was added into LB agar.

#### **2.13.2 Bacterial transformation**

Hunan FFA4-eYFP plasmid DNA were transformed into XL-1 blue competent (*E.coli*) cells (Agilent Technologies, Santa Clara, US). Cells were incubated on ice for 10 minutes, 25 µl of the cells were aliquoted into pre-chilled 1.5 ml eppendorf tube. 0.5 µg of plasmid DNA was added to the bacterial cells and left on ice to incubate for 30 minutes. The mixture was then heat-shocked at 42 °C for 45 seconds and immediately placed on ice for 2 minutes. The reaction mixture was adjusted to 500 µl with LB broth (1% w/v tryptone, 0.5% w/v yeast extract, and 1% w/v NaCl). The cells were incubated on a shaker at a speed of 200 rpm for 1 hour at 37 °C. 100 µl aliquots were spread onto 10 cm LB agar plates containing ampicillin and incubated at 37 °C overnight. The plates were then sealed with parafilm and stored inverted at 4 °C.

#### **2.13.3 Maxipreps**

The Qiagen plasmid maxi kit (QIAGEN, Manchester, UK) was used to purify large scale DNA samples from bacterial cultures. The clones grown in LB agar plate were picked into 5 ml of LB broth containing ampicillin using tips and incubated for 6 hours shaking with 200 rpm at 37 °C. 100 µl of culture grown transferred into 100 ml LB broth overnight at 37 °C shaking with 200 rpm. Culture grown was transferred to 50 ml tubes and centrifuged at a speed of 3000 rpm for 30 minutes at 4 °C. The supernatant was decanted and the pellet was then resuspended in 10 ml of buffer P1 (resuspension buffer) supplemented with RNase. 10 ml of buffer P2 (lysis buffer) was added and mixed thoroughly and incubated at room temperature for 5 min. 10 ml of cold buffer P3 (neutralisation buffer) was added to the lysed cells, mixed thoroughly and centrifuged (at 3,000



## Chapter 2

rpm, 30 min, 4°C). In the meantime, a QIAGEN-tip was equilibrated with 10 ml buffer QBT, and allowed to empty by gravity flow. The supernatant was then transferred the QIAGEN-tip and allowed to empty by gravity flow. The QIAGEN-tip was then washed twice with wash buffer QC. 50 ml of buffer QF was added to QIAGEN-tip to elute DNA. 10.5 ml of isopropanol was added and mixed thoroughly. The mixture was then centrifuged at a speed of 3000 rpm for 30 minutes at 4°C. The supernatant was decanted and the DNA pellet was washed by 5 ml of 70% ethanol. DNA pallet was centrifuged at a speed of 3000 rpm for 10 minutes at 4°C. The supernatant was decanted and the pellet was air-dried. To redissolve the DNA pellet, a suitable volume of sterilised water. The concentration and purity of DNA samples was quantified using PHERAstar (BMG LABTECH). The DNA plasmid was stored at -20°C.

### **2.13.4      $\beta$ -arrestin 2 recruitment assay**

$\beta$ -arrestin 2 recruitment was measured by bioluminescence resonance energy transfer (BRET) assay. This technology is a technique for detecting protein-protein interactions. Before applying this system, it is necessary to first fuse Renilla reniformis luciferase (Rluc) or eYFP onto the two proteins that need to be detected, respectively. Coelenterazine h is substrate of Rluc, the interaction between them is able to produce light (peak emission at 480nm). When the distance between the energy donor Rluc and the energy receptor eYFP is relatively close, the energy will be transferred from Rluc to eYFP, forming its excitation and emitting an emission light with a wavelength of 530nm (shown as Figure 2.1).

HEK 239T cells were seeded into 10 cm petri-dishes, and incubated to 60-70% confluence. cells were co-transfected with  $\beta$ -arrestin-Renilla luciferase and hFFA4-eYFP plasmids in a 1:4 ratio using PEI. One transfected construct reaction contained 5  $\mu$ g DNA in a ratio of 4:1 hFFA4-eYFP to  $\beta$ -arrestin-Renilla luciferase, 30  $\mu$ l of 1mg/ml PEI and topped up with sterile 150 mM NaCl. The constructs systems were incubated for 10 minutes at room temperature and then dropped into cells. To coat plates, poly-D-lysine was added at 50 $\mu$ l/well to white 96 microplates and stored overnight at 4°C. Pre-coated 96 well plates were warmed to room temperature and washed with media (DMEM with 10% FBS and 1% penicillin/streptomycin mixture) before use. Cells were transferred at

## Chapter 2

100µl/well to poly-D-lysine coated white 96 microplates the next day after transfection and incubated overnight. Cells were then washed with HBSS (Gibco, Life Technologies Ltd, Paisley, UK,) 100 µl/well and incubated in HBSS (80 µl/well for agonist assay or 70 µl/well for GRK inhibitors assay) for 30 minutes. GRK inhibitors was added 10 µl to each well and the plate was incubated for 30 minutes at 37 °C. Coelenterazine h (NanoLight Technology, Pinetop, US) was added to a final concentration of 5 µM and incubated for 10 min at 37 °C before FFA4 agonist was added. Luminescence emissions at 535 and 475 nm were measured using a PHERAstar (BMG Labtech, Offenburg, Germany). The signal was represented as the 535/475 ratio multiplied by 1000 to yield the arbitrary milli-BRET units. Calculated mBRET was plotted against log agonist concentrations using GraphPad Prism Software.

$$\text{mBRET} = \left\{ \frac{\text{sample at } 535\text{nm}}{\text{sample at } 475\text{nm}} - \text{mean} \left( \frac{\text{RLuc control at } 535\text{nm}}{\text{RLuc control at } 475\text{nm}} \right) \right\} \times 1000$$

## Chapter 2

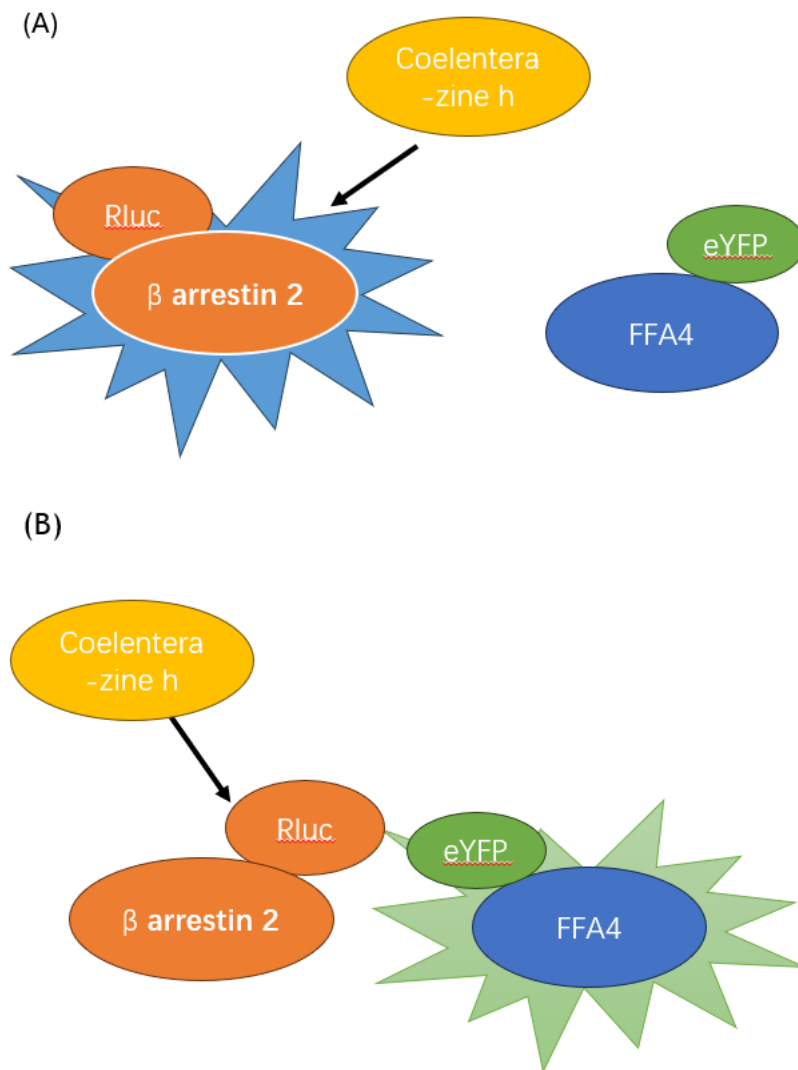


**Figure 2.1 The mechanism of BRET assay**

(A) When the distance between the energy donor Rluc and the energy receptor eYFP is far, Coelenterazine h interacts with Rluc and produce light with a wavelength of 480nm. (B) When the distance between the energy donor Rluc and the energy receptor eYFP is relatively close, Coelenterazine h interacts with Rluc, then the energy will be transferred from Rluc to eYFP, forming its excitation and emitting an emission light with a wavelength of 530nm.

## 2.14 Experimental animals

### 2.14.1 Animal maintenance

The generation and characterization of both transgenic FFA2-DREADD-HA-expressing and CRE-MINUS mouse lines are detailed in (Bolognini et al., 2019). Three types of mice were used: C57BL/6 mice where FFA4 possessed a hemagglutinin (HA) tag (WT-FFA4-HA), C57BL/6 mice where FFA4 has phosphorylation deficient (PD) mutations (PD-FFA4-HA) and C57BL/6 mice where FFA4 receptor did not express (FFA4-KO). PD-FFA4-HA and PD-FFA4-HA mouse

## Chapter 2

were generated by Genoway. FFA4-KO mouse was generated by Invitrogen. Mice were fed ad libitum with a standard mouse chow diet. Maintenance and killing of mice followed principles of good laboratory practice in accordance with UK national laws and regulations. All experiments were conducted under a home office licence held by the authors.

### **2.14.2 Tissue harvest and Treatment**

Mice were sacrificed by cervical dislocation and tissues (lung, Peyer's patches, mesenteric lymph nodes, colon and white adipose tissue) were collected into ice-cold oxygenated (95% O<sub>2</sub> and 5% CO<sub>2</sub>) Krebs-bicarbonate buffer (118.4 mM NaCl, 24.9 mM NaHCO<sub>3</sub>, 1.9 mM CaCl<sub>2</sub>, 1.2 mM MgSO<sub>4</sub>, 1.2 mM KH<sub>2</sub>PO<sub>4</sub>, 11.7 mM glucose, pH 7.4). The lung was treated with TUG-891 (10 µM) for 20 minutes at 37°C. Other tissues (Peyer's patches, mesenteric lymph nodes, colon and white adipose tissue) treated with 100 µM of MOMBA (100 µM) for 20 minutes at 37°C. For antagonist, tissues were pre-treated with CATPB (10 µM) for 30 minutes. Treated tissues were stored at -80°C until use.

### **2.14.3 Tissue homogenisation**

Tissues were transferred to 1 ml of RIPA buffer (50 mM Tris-HCl pH 8, 150 mM NaCl, 0.5% (w/v) sodium-deoxycholate, 1% (v/v) IGEPAL CA-630, 0.1% (v/v) SDS) supplemented with 1 EDTA-free cOmplete™ protease cocktail inhibitor tablet and 1 PhosSTOP™ phosphatases inhibitor per 10 ml buffer). Tissues were homogenized by homogenizer (Polytron PT3100) before centrifugation at 15,000 rpm at 4°C for 15 minutes to pellet cellular debris. All supernatants were collected and protein concentration was measured using Bradford protein assay. Samples were then frozen at -80°C until required. Samples were analysed by West blot assay described in section 2.11.

### **2.14.4 Membrane extract preparation**

Frozen lungs were homogenised by sonication at 3-5 µg amplitude in 500 µl of T/E buffer (10 mM Tris, 1 mM EDTA, pH 8.0) containing proteinase and phosphatase inhibitors. Samples were then centrifuged at 10,000 x g for 10 min at 4°C. Supernatants were mixed with additional 500 µL T/E buffer and centrifuged at 15,000 x g for 1 hour at 4°C. The pellets were then solubilised in

## Chapter 2

400  $\mu\text{L}$  of RIPA buffer including phosphatase and proteinase inhibitors and incubated for at least 2 hours at  $4^\circ\text{C}$  with end-over-end rotation. After centrifugation of samples at  $14,000 \times g$  for 10 min at  $4^\circ\text{C}$ , the supernatants (membrane extracts) were transferred to fresh microcentrifuge tubes and stored at  $-80^\circ\text{C}$  until use. Protein concentrations were determined by using the Micro BCA protein assay reagent kit according to the manufacturer's instructions. Samples were analysed by West blot assay described in section 2.11.

## 2.15 Statistical analysis

All data are presented as mean  $\pm$  standard error (SEM) using Prism 8 software (GraphPad). The models used for fitting the various concentration response curves was nonlinear regression  $\log(\text{inhibitor})$  vs response (three parameters).

**Table 2-1 List of primary antibodies**

	Antibody	Catalogue Number	Dilution	Host
Phospho- FFA4 antibodies	Anti-Thr <sup>347</sup> (pT347)	7TM0127A	1:1000	Rabbit
	Anti-Thr <sup>349</sup> /Ser <sup>350</sup> (pT347/pS350)	7TM0127B	1:1000 (For immunocytochemistry 1:250)	
Phospho- FFA2 antibodies	Anti-Ser <sup>296</sup> /Ser <sup>297</sup> (pS296/pS297)	7TM0226A	1:1000	
	Anti-Thr <sup>296</sup> /Thr <sup>297</sup> (pT306/pT310)	7TM0226B	1:1000 (For immunocytochemistry 1:500)	

## Chapter 2

**Table 2-2 List of secondary antibodies used for western blot**

Antibody	Catalogue Number	Dilution
IRDye® 800CW Donkey anti-Rabbit IgG (H + L)	926-32213	1:10,000
IRDye® 800CW Donkey anti-Goat IgG (H + L)	926-32214	1:10,000
IRDye® 800CW Donkey anti-Mouse IgG (H + L)	926-32212	1:10,000
IRDye® 800CW Goat anti-Rat IgG (H + L)	926-32219	1:10,000 (For lung 1:1000)

**Table 2-3 List of secondary antibodies used for immunocytochemistry**

Antibody	Catalogue Number	Dilution
Goat anti-Rabbit IgG (H+L) Cross-Adsorbed Secondary Antibody, Alexa Fluor™ 594	A-11012	1:400
Goat anti-Rabbit IgG (H+L) Cross-Adsorbed Secondary Antibody, Alexa Fluor™ 488	A-11008	1:400
Goat anti-Mouse IgG (H+L) Cross-Adsorbed Secondary Antibody, Alexa Fluor™ 568	A-11004	1:400

## Chapter 3 Characterisation of FFA4 phospho-site antibodies

### 3.1 Introduction

GPCR phosphorylation is a complex process involving different enzymes and signal transduction (Premont and Gainetdinov, 2007, Tobin, 2008). More and more evidence has proved that ligand, could differentially regulate signalling outcomes in different cells and tissues by promoting different downstream molecular conformations (Bouzo-Lorenzo et al., 2016, Prihandoko et al., 2016, Nobles et al., 2011). This concept is described by the bar-code hypothesis (Tobin, 2008). Although large number of studies have described GPCRs phosphorylation status, it is still hard to integrate the phosphorylate sites (Ferguson, 2001). Mass spectrometry assay is one of the common methods used to determine the precise sites of phosphorylation in receptors. The phospho-site specific antibodies based on mass spectrometry are able to recognise specific phosphorylation sites. Interestingly, some of these sites were shown to be phosphorylated in an agonist dependent manner leading to the idea that antibodies that recognised agonist-dependent phosphorylation could be used as biomarkers for the activation status of the receptor itself. This has been used for the M1-muscarinic receptor where the development a phospho-specific antibody-based biosensor was used as a read-out of M1 muscarinic acetylcholine receptor (M1 mAChR) activation in vitro and in vivo (Butcher et al., 2016). In other studies M3-muscarinic receptor phospho-specific antibodies have been used to observe different phosphorylation status of the receptor in three cell types (Butcher et al., 2011). Thus, the use of phospho-specific antibodies designed on the basis of mass spectrometry data have been used to define the differential phosphorylation status of receptors in different tissues (i.e. a phosphorylation bar-code) and in the case of agonist-dependent phosphorylation as antibody biosensors for receptor activation (Prihandoko et al., 2016). Here the question was - can similar approaches be used in the investigation of FFA4.

Butcher (Butcher et al., 2014) and colleagues performed mass spectrometry to identify specific amino acids that became phosphorylated in response to the agonist TUG-891 and found there are five phosphorylation sites in human FFA4. These sites locate in the intracellular C-terminal tail (Thr<sup>347</sup>, Thr<sup>349</sup>, Ser<sup>350</sup>

### Chapter 3

Ser<sup>357</sup> and Ser<sup>360</sup>). While in mouse FFA4 phosphorylation response to the synthetic agonist TUG-891 occurs at six residues that are located in two clusters, cluster 1 contained phosphorylation sites on residues Thr<sup>347</sup>, Thr<sup>349</sup>, and Ser<sup>350</sup> and cluster 2 contained sites on Ser<sup>357</sup>, Ser<sup>360</sup> and Ser<sup>361</sup> (Prihandoko et al., 2016).

Accordingly, antibodies were produced; two phospho-site specific antibodies based on human phospho-peptides, which are considered as potential probe against phosphorylated FFA4. The aim of this chapter is to fully characterise these phospho-specific antibodies ahead of use in the following chapters.

Thus, the aims of this chapter were to:

- i ) Assess FFA4 expression in Flp-In TReX 293 cells stably transfected in human FFA4 construct.
- ii ) Assess the specificity and sensitivity of phospho-site specific antibodies anti-pThr<sup>347</sup> FFA4 and anti-pThr<sup>349</sup>/Ser<sup>350</sup> at phosphorylated hFFA4.
- iii) Assess whether the phosphorylation of hFFA4 at Thr<sup>347</sup> FFA4 and Thr<sup>349</sup>/Ser<sup>350</sup> is agonist dependent.

## 3.2 Results

### 3.2.1 Characterisation of antibodies raised against pThr<sup>347</sup> FFA4 and pThr<sup>349</sup>/Ser<sup>350</sup> on human FFA4

Phosphospecific antibodies were raised to a phosphorylated peptide containing phosphate on residue Thr<sup>347</sup> (G<sup>343</sup>AILTDTSVK<sup>352</sup>) and a doubly phosphorylated peptide containing phosphates on residues Thr<sup>349</sup> and Ser<sup>350</sup> (I<sup>345</sup>LTDTSVKRND<sup>354</sup>) of FFA4. These phospho-peptides were chosen because there was evidence from mass spectrometry studies that these residues were phosphorylated and because these peptides were predicted to be highly immunogenic. The antibodies generated from the immunization was subjected to affinity purification that resolved phospho-specific antibodies from non-phospho-specific antibodies.

The Flp-In TReX 293 cells were induced to express human FFA4 receptor with eYFP tag by doxycycline. To test the specificity of the antibodies, FFA4



### Chapter 3

receptors were challenged with vehicle or the FFA4 agonist TUG-891. The receptors were immunoprecipitated by GFP trap and samples were analysed using western blot. Cells without doxycycline induction showed no evidence of the expression of FFA4 receptor (Figure 3.1A). In contrast in cells induced with doxycycline hFFA4-eYFP expression was identified with an anti-eYFP antibody. The aggregated protein observed at a molecular mass of 50-75 kDa was considered as human FFA4 tagged eYFP. The aggregated protein observed at 100-150 kDa was considered as dimerised FFA4.

Lysates prepared from Flp-In TReX 293 cells tagged with eYFP were then probed with phospho-site specific antibodies. The results showed that, without exposure to TUG-891 anti-pThr<sup>347</sup> FFA4 failed to identify the receptor construct (Figure 3.1B) whereas anti-eYFP identified a series of polypeptides clustering at 65 kDa and 130 kDa (Figure 3.1A). In contrast, following the addition of TUG-891 resulted the anti-pThr<sup>347</sup> FFA4 (Figure 3.1B) clearly identified polypeptides that corresponded to hFFA4-eYFP (Figure 3.1A).

Similar results were obtained with antibodies Thr<sup>349</sup>/Ser<sup>350</sup> FFA4 (Figure 3.1C). This antibody identified FFA4 receptor construct in lysates from TUG-891 exposed cells, but did not identify FFA4 construct without exposure to TUG-891 (Figure 3.1C). Anti-pThr<sup>347</sup> and anti-pThr<sup>349</sup>/Ser<sup>350</sup> FFA4 both failed to identify FFA4 receptor construct in samples from cells that were not treated with doxycycline (Figure 3.1B, C).

## Chapter 3

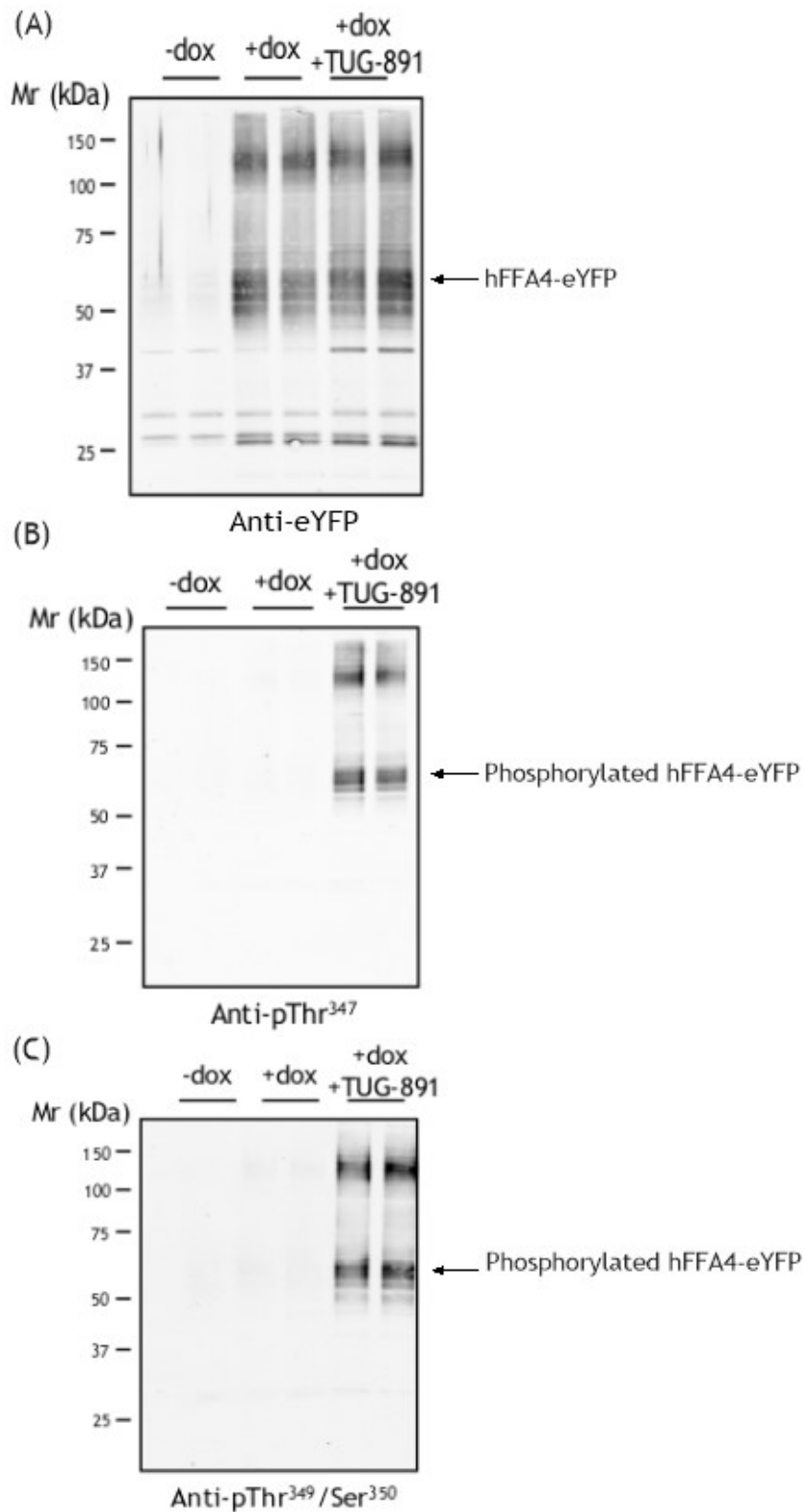


**Figure 3.1 Anti-pThr<sup>347</sup> and anti-pThr<sup>349</sup>/Ser<sup>350</sup> identify FFA4 phosphorylation induced by TUG-891.**

Flp-In TReX 293 cells induced to express human FFA4 receptor with eYFP tag were stimulated with TUG-891 (10 $\mu$ M) or 0.1% DMSO (showed by +dox) as a vehicle control for 5 minutes at 37°C. The receptors were purified by immunoprecipitation using GFP-trap. Proteins were separated by 4-12% SDS-PAGE and analysed by western blot analysis. -Dox, in which cells was not induced by doxycycline, was showed as a negative control. All antibodies were used at 1:1000 dilution. Molecular mass of hFFA4-eYFP is between 50-75 kDa. (A) Representative western blot of anti-GFP showed the expression of hFFA4-eYFP. (B) Representative western blot of anti-pThr<sup>347</sup> identified

## Chapter 3

FFA4 phosphorylation induced by TUG-891. (C) Representative western blot of anti-pThr<sup>349</sup>/Ser<sup>350</sup> identified FFA4 phosphorylation induced by TUG-891 (n=3).

### 3.2.2 Lambda Protein Phosphatase dephosphorylates hFFA4-eYFP cell extracts

Lambda Protein Phosphatase (LPP) is a Mn<sup>2+</sup>-dependent protein phosphatase, which interacts with phosphorylated serine, threonine and tyrosine residues. As it can release phosphate groups from phosphorylated serine, threonine and tyrosine residues, LPP is used to study protein phosphorylation, and to verify the specificity of antibodies against protein phosphorylation sites.

The identification of FFA4-eYFP by anti-pThr<sup>347</sup> FFA4 clearly reflected phosphorylation of the receptor as this was no longer observed after treatment with LPP (Figure 3.2A). The identification of FFA4-eYFP by anti-pThr<sup>349</sup>/Ser<sup>350</sup> FFA4 also influenced by Lambda Protein Phosphatase treatment, though Lambda Protein Phosphatase failed to dephosphorylate completely (Figure 3.2C). Total expression of FFA4 showed slight decrease in samples treated with LPP, but was still recognised by anti-eYFP (Figure 3.2B, D).

## Chapter 3

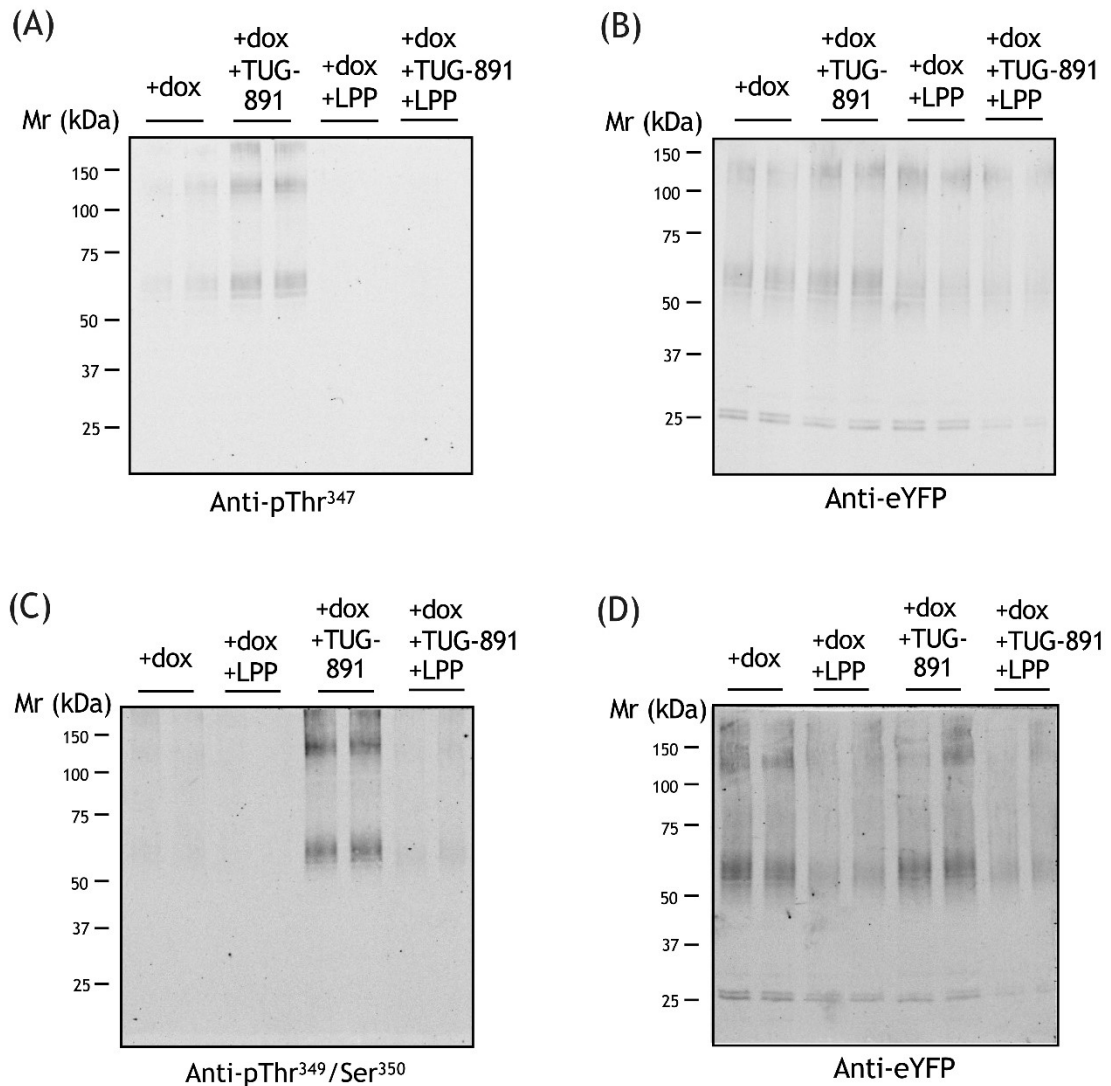


**Figure 3.2 Anti-pThr<sup>347</sup> and anti-pThr<sup>349</sup>/Ser<sup>350</sup> failed to identify FFA4 phosphorylation removed by Lambda Protein Phosphatase (LPP).**

Flp-In TReX 293 cells induced to express human FFA4 receptor with eYFP tag were stimulated with TUG-891 (10 $\mu$ M) or 0.1% DMSO (showed by +dox) as a vehicle control for 5 minutes at 37°C. The receptors were purified by immunoprecipitation using GFP-trap. The samples then were incubated with LPP for 3 hours at 30°C. (A) Anti-pThr<sup>347</sup> FFA4 and (C) anti-pThr<sup>349</sup>/Ser<sup>350</sup> FFA4 identified FFA4 phosphorylation and the phosphorylation was removed by LPP. (B) and (D) showed the expression of hFFA4-eYFP (n=2).

### 3.2.3 Anti-pThr<sup>347</sup> and anti-pThr<sup>349</sup>/Ser<sup>350</sup> identify de-glycosylated FFA4 receptor

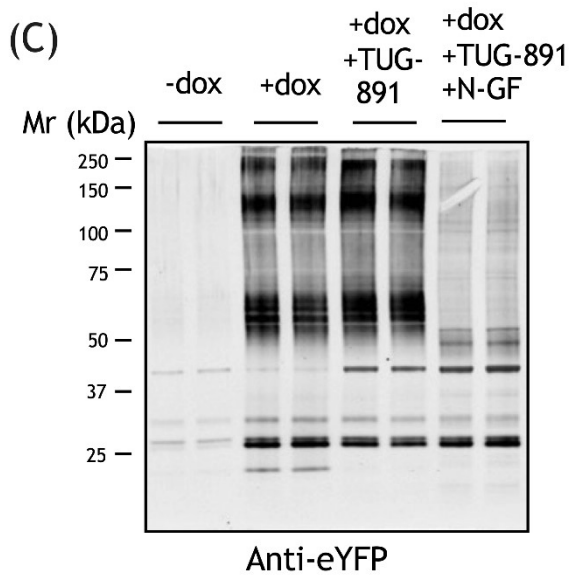
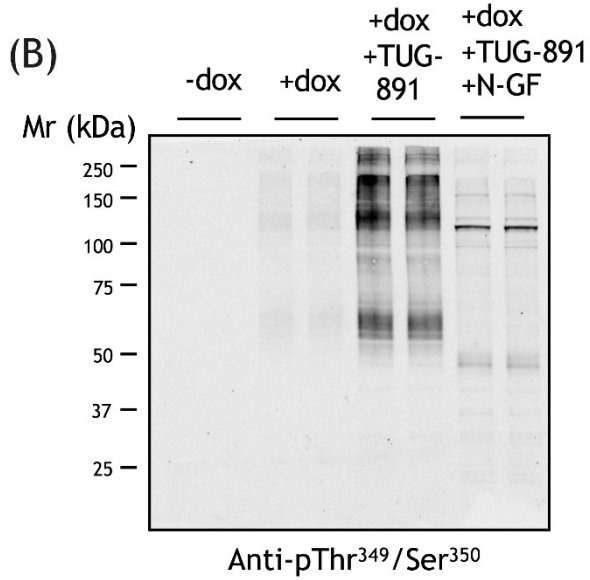
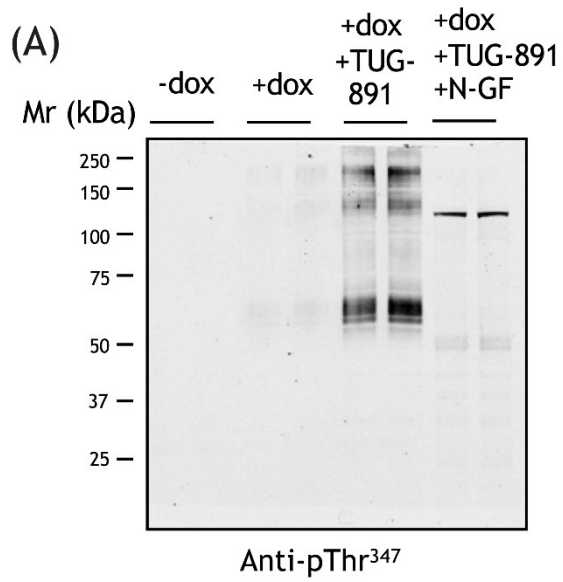
There were a series of bands identified by anti-pThr<sup>347</sup> FFA4 and anti-pThr<sup>349</sup>/Ser<sup>350</sup> FFA4 and anti-eYFP, which were suspected to represent varying levels of receptor glycosylation. FFA4 could be decorated at asparagine linked on N-terminal. To test this notion, N-glycosidase F (showed as N-GF in Figure 3.3) was used to treat samples. N-glycosidase F cleaves asparagine-bound N-glycans. In western blots, the two antibodies still identified the FFA4 receptor construct following exposure to TUG-891, however, samples treated with N-

### Chapter 3

glycosidase F showed single band left at 65 kDa and 130 kDa (Figure 3.3A, B).

The molecular mass also decreased, with the hypothesis that hFFA4 is glycosylated and that glycosylation is lost following hydrolysed by N-glycosidase F (Figure 3.3A, B). One caveat however is that treatment with N-glycosidase F did alter the total amount of hFFA4-eYFP likely due to some protease activity associated with the N-glycosidase F preparation (Figure 3.3C).

## Chapter 3



## Chapter 3

### Figure 3.3 Anti-pThr<sup>347</sup> and anti-pThr<sup>349</sup>/Ser<sup>350</sup> identify FFA4 phosphorylation with the presence of N-glycosidase F (N-GF).

Flp-In TREx 293 cells induced to express human FFA4 receptor with eYFP tag were stimulated with TUG-891 (10 $\mu$ M) or 0.1% DMSO (showed by +dox) as a vehicle control for 5 minutes at 37°C. The cells were lysed and incubated with N-GF for 3 hours at 37 °C. The receptors were purified by immunoprecipitation using GFP-trap. -Dox, in which cells was not induced by doxycycline, was showed as a negative control. (A) Anti-pThr<sup>347</sup> FFA4 and (B) anti-pThr<sup>349</sup>/Ser<sup>350</sup> FFA4 identified FFA4 phosphorylation with or without N-glycosidase F existence. The molecular mass of hFFA4-eYFP showed a slight decrease in samples treated with N-GF. (C) Representative western blot of anti-GFP showed the expression of hFFA4-eYFP (n=2).

## 3.3 Discussion

GPCRs show two types of phosphorylation; constitutive and agonist induced phosphorylation. Constitutive phosphorylation occurs in the absence of agonist stimulation with the kinases responsible and the role in receptor regulation largely unknown. Whereas agonist-induced phosphorylation is largely considered to be mediated by G protein-coupled receptor kinases (GRKs) (Gurevich and Gurevich, 2019). Following GPCR activation, GRKs phosphorylate the intracellular domains of the GPCR and this results in the recruitment of  $\beta$ -arrestin, which mediates desensitisation of GPCR signalling and internalization of GPCRs. This serves to 'turn off' signalling, leading to negative feedback of G protein-dependent GPCR signalling. Moreover, continual agonist stimulation diminishes receptor response, resulting in receptor desensitisation (Delom and Fessart, 2011, Jean-Charles et al., 2017). The desensitised GPCR will be either hydrolysed or recirculated to cell membrane. Previous studies have showed that FFA4 phosphorylation is induced by agonists (Burns et al., 2014, Butcher et al., 2014). Here these results are extended and that the FFA4 agonist TUG-891 induced phosphorylation on specific sites on hFFA4. We have shown that two phospho-antibodies, recognising phosphorylation at Thr<sup>347</sup>, Thr<sup>349</sup> and Ser<sup>350</sup> determine that these sites are phosphorylated in an agonist-dependent manner. The interactions between FFA4, GRKs and  $\beta$ -arrestins is investigated in next chapter.

The antibodies failed to identify phosphorylation in the LPP treatment samples suggesting that they identified specific phosphorylated serine and threonine residues. However, long-time incubation at 30°C in LPP treatment resulting in proteolysis, which decreased the protein expression observed on western blots. The reason that I only repeated these experiments twice in this chapter is that I

### Chapter 3

expected to show LPP remove phosphate group in FFA4, and it is not necessary to quantified. The duplicated loading in this experiment decreased the contingency of the results. In addition, the future plan using phospho-site mutated receptor could give another way to illustrate the antibodies used in this chapter are phospho-site specific.

Glycosylation is one of the most prevalent and complex post-translational modifications (PTMs), which involves a large number of glycosyltransferases, enzymes and transporters. The most common types of glycosylation can be subdivided N-linked glycosylation and O-linked glycosylation. N-linked glycosylation occurs at asparagine (Asn) residues, usually with a consensus sequence asparagine-X-serine/threonine, where X is any amino acid other than proline (Goth et al., 2020). Most mammalian GPCRs are modified with glycosylation at their extracellular N-terminus or on ECLs (Lanctot et al., 2005). N-linked glycosylation is able to influence GPCR cell surface expression, internalization, and GPCR signalling (Kozielowicz et al., 2017, Hauser et al., 2016, Gonzalez de Valdivia et al., 2019). According to the sequence of hFFA4, there is one N-linked glycosylation consensus site (Asn<sup>21</sup>) presenting in the extracellular N-terminal domain. In the immune-blot, samples treated with N-glycosidase F showed a decrease on molecular mass, which suggested N-linked glycosylation on FFA4 was removed. O-linked glycosylation usually occurs at serine or threonine residues without any consensus sequence. There is no evidence showing FFA4 is modified by O-linked glycosylation.

The experiment using N-glycosidase F need to be optimised, because the samples treated with TUG-891 only and treated with TUG-891+ N-glycosidase F were not incubated in completely identical conditions after added N-glycosidase F. Moreover, the protease may be activated when the samples were incubated at 37°C, and to avoid the function of N-glycosidase F was inhibited, the samples did not contain protease inhibitors. These may result in the receptors identified by anti-GFP antibody were at different level. To make the result more convincing the incubation conditions should be completely the same. Adding a control group with protease inhibitors treated is also helpful to measure the influence from protease.



### Chapter 3

GPCRs are used to considered function solely as monomeric receptor, however, evidence for GPCR dimerization and oligomerization has been accumulating that challenges the idea. Dimerization is considered essential for class C GPCR activity (Kniazeff et al., 2011), and class A GPCR are also observed to form oligomers. Early researches have illustrated that oligomers participate in GPCR signalling, ligands binding, and related to cell surface delivery (Ferré et al., 2014). Dimerization of the GPCR regulated by receptor density and multiple dimer conformations co-exist and interconvert. (Calebiro et al., 2013, Dijkman et al., 2018). In our experiments, FFA4 expression was induced by high concentration of doxycycline, which result in overexpression of the receptors. This may be an explain of the unstable expression of proteins which were considered as dimers in immunoblots. The proteins were separated by SDS-page in the experiments. It is mainly used for protein separation and purification, by adding SDS (sodium dodecyl sulfate) to the sample, the protein molecules are encapsulated into spherical shapes, allowing for separation based on molecular size. Theoretically, SDS-page should disintegrate the aggregated proteins. To investigate what the bands are, native page is going to be used to separate the proteins. Native-Page is able to maintain the natural state of proteins without adding any chemical reagents to change their shape or charge, and can therefore be used to observe the natural conformation and interactions of proteins. This technique is suitable for studying the folding state of proteins, interactions between subunits, and interactions between proteins and ligands. If FFA4 receptors display multiple bands in Native-Page, it may indicate that the protein has multiple different conformations or forms complexes with other molecules.

## Chapter 4 Investigation of FFA4 phosphorylation pattern

### 4.1 Introduction

Early all GPCRs exist as phospho-proteins with multiple sites of phosphorylation. Based on the phosphorylation bar-code theory, different patterns of phosphorylation result in distinct consequences in receptor function and signalling (Tobin, 2008). One scenario reported in the literature is that agonist-dependent phosphorylation can be used as a read-out of receptor activation (Butcher et al., 2016). This has been documented for the muscarinic receptor family where agonist-dependent phosphorylation of Ser<sup>228</sup> in the third intracellular loop of the M1-muscarinic receptor has been used as a read out of receptor activation (Butcher et al., 2016). In the case of FFA4, the phosphorylation sites have been investigated and phospho-specific antibodies that recognise phosphorylation at residues in the C-terminal tail have been developed. However detailed examination of FFA4 phosphorylation and the development of antibodies that can act as sensors of receptor activation has not been reported. Here anti-pThr<sup>347</sup> and anti-pThr<sup>349</sup>/Ser<sup>350</sup> FFA4 antibodies are used to study the receptor phosphorylation pattern. FFA4 ligands TUG-891, Agonist 2 and AH-7614 were used to verify how FFA4 ligands affect phosphorylation of FFA4 receptor and whether the phospho-specific antibodies were able to establish the activation status of FFA4.

The aims of this chapter were to:

- i ) Assess the impact of FFA4 ligands on the receptor phosphorylation.
- ii ) Determine the link between phosphorylation and the intracellular location of FFA4 (i.e., internalisation).
- iii) Investigate the role of GRKs in the phosphorylation of FFA4 and in the interaction between  $\beta$ -arrestin-2 and FFA4 receptor.

## Chapter 4

iv) Apply the antibodies to animal tissues and evaluate sensitivity and specificity.

## 4.2 Results

### 4.2.1 Other FFA4 ligands participate in regulation of FFA4 phosphorylation

#### 4.2.1.1 Agonist 2 promotes regulation of FFA4 phosphorylation

To investigate how other FFA4 ligands impact FFA4 phosphorylation, Agonist 2 was used to activate FFA4. A previous study has shown that Agonist 2 is a selective agonist of FFA4 and has an effect on ghrelin secretion in mice (Engelstoft et al., 2013). In pharmacology experiments, 10 $\mu$ M of TUG-891 or Agonist 2 was able to induced maximum phosphorylation of ERK1/2 in mouse FFA4, and this occurred at 5 minutes. In this case, the concentration of agonists and stimulation time would be 10 $\mu$ M and 5 minutes. Recombinant Flp-In TREx 293 cells stably expressing human FFA4 with eYFP tag (hFFA4-eYFP), were serum starved for 1 hour and stimulated with 10  $\mu$ M of Agonist 2 for 5 minutes at 37 $^{\circ}$  C. When treated with Agonist 2, the two phospho-antibodies (anti-pThr<sup>347</sup> and anti-Thr<sup>349</sup>/Ser<sup>350</sup> FFA4) identified phosphorylated FFA4 (Figure 4.1A, B) as a group of polypeptides with apparent  $M_r$  in the region of 60kDa, with a further group of immuno-identified polypeptides migrating with much higher apparent  $M_r$ . These were barely detected by these antibodies without treatment of the cells with Agonist 2. Addition of Agonist 2 resulted in clear identification of each these group of polypeptides by anti-pThr<sup>347</sup> FFA4 (Figure 4.1A, C). Agonist-mediated phosphorylation of very similar sets of polypeptides was also observed at Thr<sup>349</sup>/Ser<sup>350</sup> (Figure 4.1B, C). Anti-eYFP immunoblotting of such samples confirmed similar levels of expression of hFFA4-eYFP in all sample in which expression had been induced (Figure 4.1C)



## Chapter 4

### **Figure 4.1 Anti-pThr<sup>347</sup> and anti-pThr<sup>349</sup>/Ser<sup>350</sup> identify FFA4 phosphorylation induced by Agonist 2.**

Flp-In TReX 293 cells induced to express human FFA4 receptor with eYFP tag were stimulated with Agonist 2 (10 $\mu$ M) or 0.1% DMSO (showed by +dox) as a vehicle control for 5 minutes at 37°C. The receptors were purified by immunoprecipitation using GFP-trap. Proteins were separated by 4-12% SDS-PAGE and analysed by western blot analysis. -Dox, in which cells was not induced by doxycycline, was showed as a negative control. Samples were loaded in duplicate and all antibodies were 1:1000 dilution. Molecular mass of hFFA4-eYFP is between 50-75 kDa. (A) Representative western blot of anti-pThr<sup>347</sup> identified FFA4 phosphorylation induced by Agonist 2. (B) Representative western blot of anti-pThr<sup>349</sup>/Ser<sup>350</sup> identified FFA4 phosphorylation induced by Agonist 2. (C) Representative western blot of anti-eYFP showed the expression of hFFA4-eYFP (n=3).

#### **4.2.1.2 An FFA4 antagonist prevents TUG-891 mediated receptor phosphorylation**

AH-7614 has been described as a FFA4 antagonist (Sparks et al., 2014). Cells were pre-treated with AH-7614 for 30 minutes, followed by 5 minutes TUG-891 treatment. Anti-pThr<sup>347</sup> FFA4 and anti-pThr<sup>349</sup>/Ser<sup>350</sup> antibodies recognized phosphorylation only in the presence of TUG-891, but agonist-mediated phosphorylation was blocked by AH-7614 (Figure 4.2 A, B). Anti-eYFP immunostaining was not affected by AH-7614, which means this this ligand had no influence on receptor expression over this time period (Figure 4.2C).

## Chapter 4

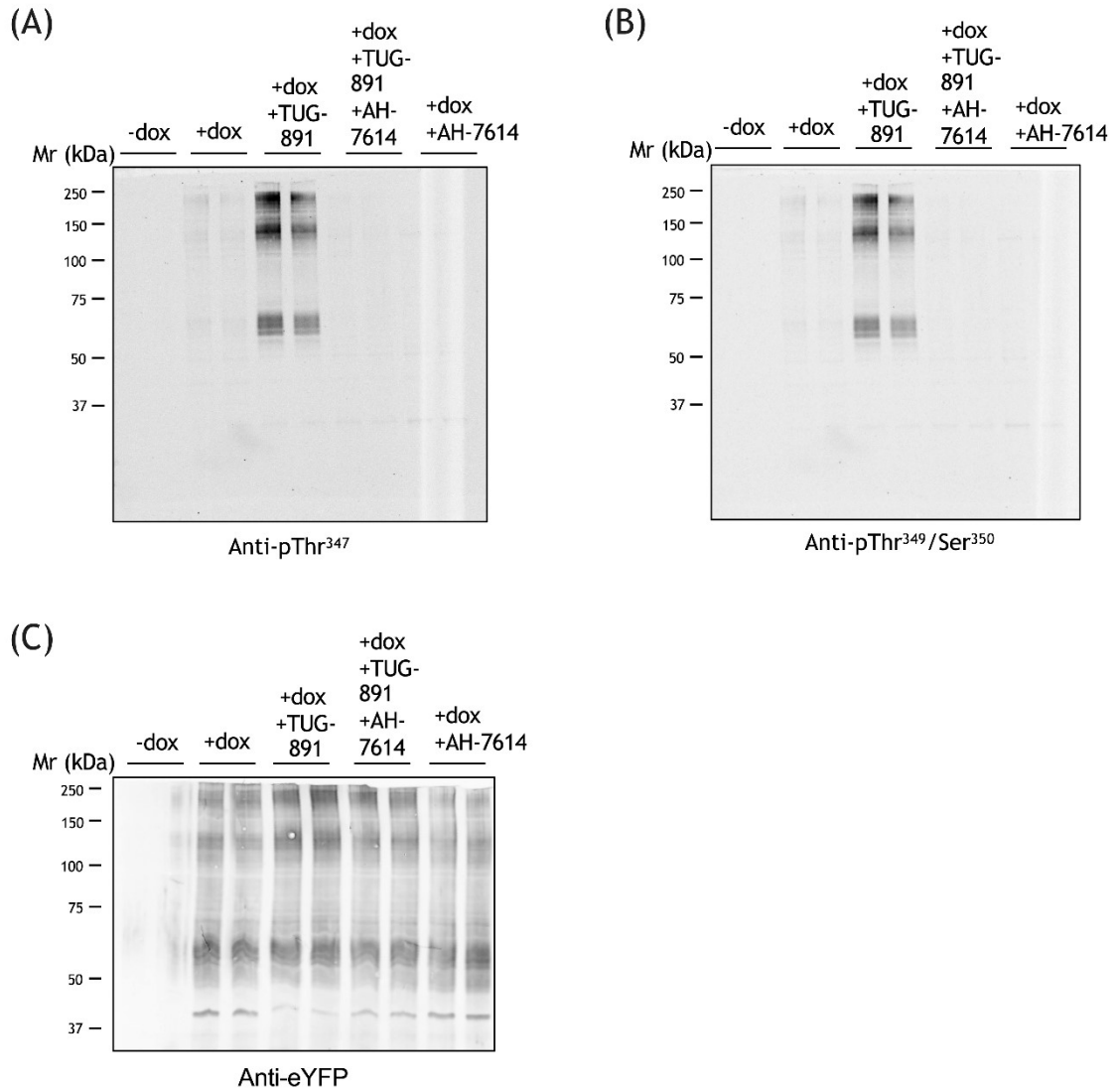


**Figure 4.2 Agonist-induced FFA4 phosphorylation is inhibited by AH-7614.**

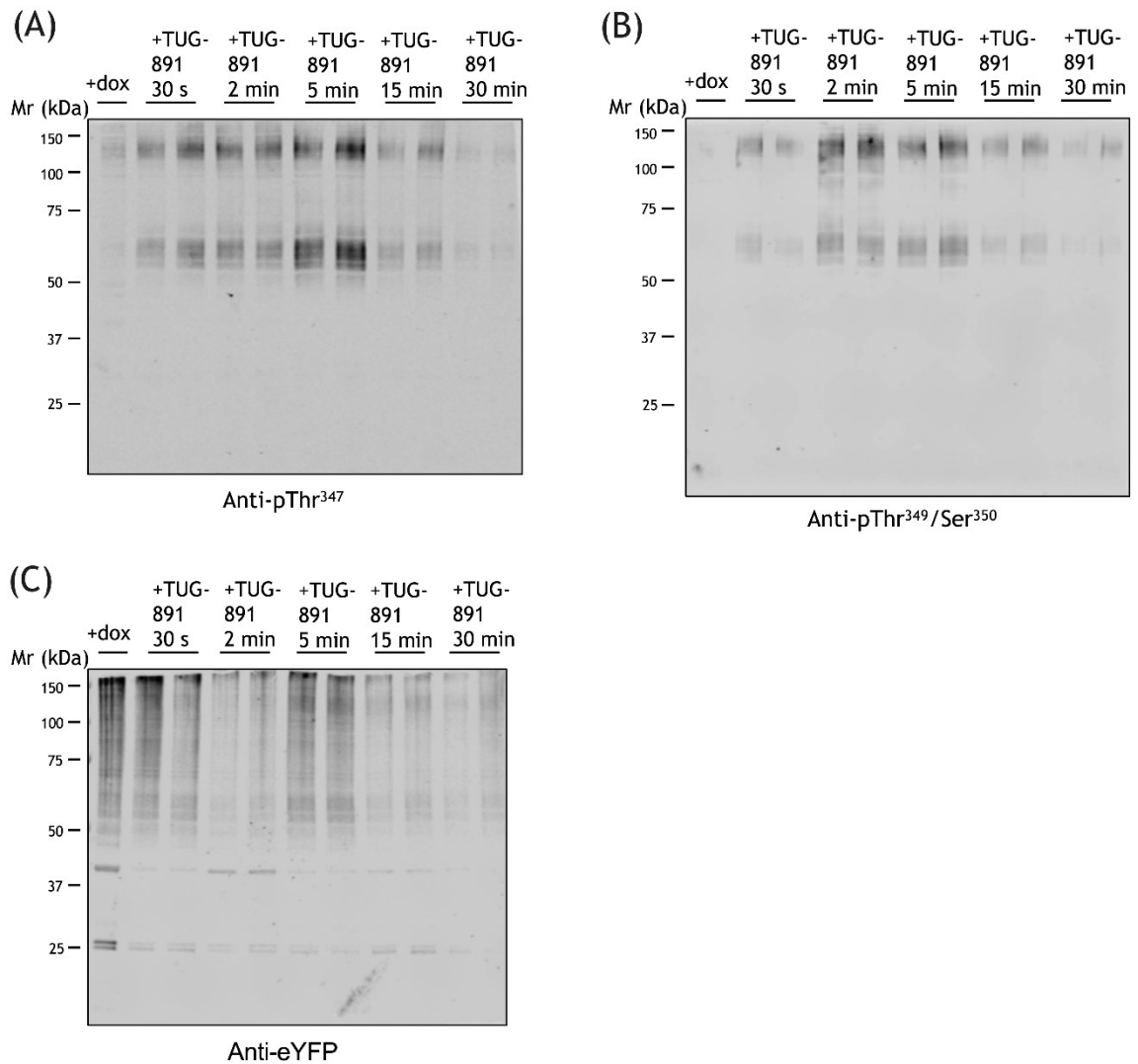
Flp-In TReX 293 cells induced to express human FFA4 receptor with eYFP tag were pre-treated with AH-7614 (10 $\mu$ M) for 30 minutes. Cells were then stimulated with TUG-891 (10 $\mu$ M) or 0.1% DMSO (showed by +dox) as a vehicle control for 5 minutes at 37°C. The receptors were purified by immunoprecipitation using GFP-trap. Samples were separated on 4-12% SDS-PAGE and analysed by western blot analysis. -Dox, in which cells did not express hFFA4-eYFP, was showed as a negative control. Samples were loaded duplicate and all antibodies were 1:1000 dilution. Molecular mass of hFFA4-eYFP is between 50-75 kDa. FFA4 phosphorylation at (A) Thr<sup>347</sup> and (B) Thr<sup>349</sup>/Ser<sup>350</sup> was inhibited after AH-7614 treatment. (C) Representative western blot of anti-eYFP showed the expression of hFFA4-eYFP (n=3).

## Chapter 4

**4.2.2 FFA4 ligands regulate phosphorylation of FFA4 in a time-dependent manner****4.2.2.1 FFA4 becomes phosphorylated in a time-dependent manner**

To investigate the phosphorylation pattern of FFA4 cells were treated with TUG-891 for various times (0.5-30 mins). The identification of phosphorylation with anti-pThr<sup>347</sup> antibodies shown that FFA4 phosphorylation appeared within 30 seconds after cells were given TUG-891, and reached a maximal level at 5 minutes (Figure 4.3A, B, D and E). The phosphorylation levels then reduced within 15-minutes and 30-minutes treatment with TUG-891 (Figure 4.3D). Anti-pThr<sup>349</sup>/Ser<sup>350</sup> showed time course of phosphorylation of FFA4 (Figure 4.3E). Protein recognition by anti-eYFP over this time course is shown in Figure 4.3C. Hence there appeared to be agonist-dependent phosphorylation that reached a maximum at 5 minutes and then reduced over the next 30 minutes.

## Chapter 4

**Figure 4.3 FFA4 becomes phosphorylated in a time-dependent manner.**

Flp-In TReX 293 cells were stimulated with TUG-891 (10 $\mu$ M) or 0.1% DMSO as a vehicle control (+dox) for 30 seconds, 2 minutes, 5 minutes, 15 minutes, 30 minutes at 37°C. The receptors were purified by immunoprecipitation using GFP-trap. Samples were separated on 4-12% SDS-PAGE and analysed by western blot analysis. Samples were loaded duplicate and all antibodies were 1:1000 dilution. Molecular mass of hFFA4-eYFP is between 50-75 kDa. (A) Representative western blot of anti-pThr<sup>347</sup> identified FFA4 phosphorylation. (B) Representative western blot of anti-pThr<sup>349</sup>/Ser<sup>350</sup> identified FFA4 phosphorylation. (C) Representative western blot of anti-eYFP showed the expression level of hFFA4-eYFP. n=3.

**4.2.2.2 AH-7614 inhibits FFA4 phosphorylation in a time-dependent manner**

Phosphorylation is a dynamic and reversible process. To explore how quick the dephosphorylation is, AH-7614 was added to cells after 5 minutes addition of TUG-891. The identification of phosphorylation with anti-pThr<sup>347</sup> antibodies shown that the inhibition of FFA4 phosphorylation within 5 minutes after cells were given AH-7614 (Figure 4.4A). The phosphorylation levels significantly reduced within 5-minutes treatment with AH-7614 (Figure 4.4D). The identification of phosphorylation with anti-pThr<sup>349</sup>/Ser<sup>350</sup> FFA4 antibodies also



## Chapter 4

shown time course of inhibition of AH-7614 (Figure 4.4B). The phosphorylation levels significantly reduced within 5-minutes treatment with AH-7614 (Figure 4.4E). The phosphorylation status of the receptor monitored with both anti-pThr<sup>347</sup> FFA4 and anti-pThr<sup>349</sup>/Ser<sup>350</sup> FFA4 antibodies reduced to near basal levels by 25-minutes AH-7614 treatment, (Figure 4.4A, B). Specific protein hFFA4-eYFP recognition by anti-eYFP over this time course is shown in Figure 4.4C.

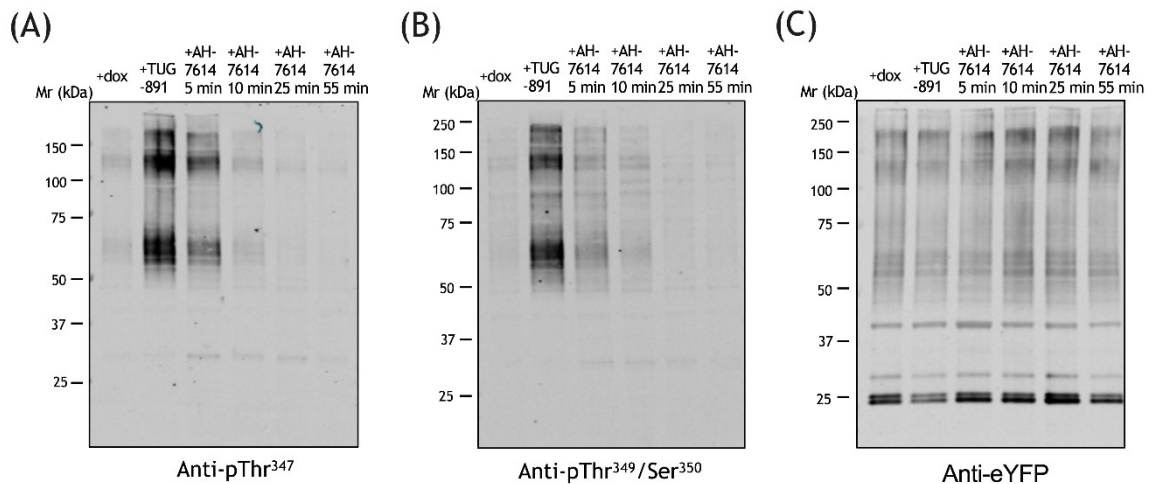


**Figure 4.4 FFA4 antagonist AH-7614 inhibits agonist-induced FFA4 phosphorylation in a time-dependent manner.**

Flp-In TReX 293 cells were stimulated with TUG-891 (10 $\mu$ M) or 0.1% DMSO as a vehicle control (+dox) for 5 minutes. Cells were then treated with AH-7614 (10 $\mu$ M) for 5 minutes, 10 minutes, 25 minutes, 55 minutes, with the presence of TUG-891. The receptors were purified by immunoprecipitation using GFP-trap. Samples were run on 4-12% SDS-PAGE and analysed by western blotting. All antibodies were 1:1000 dilution. Molecular weight of hFFA4-eYFP is between 50-75 kDa. The dephosphorylation level of FFA4, which was caused by AH-7614, was showed by (A) anti-pThr<sup>347</sup> identified FFA4 and (B) anti-pThr<sup>349</sup>/Ser<sup>350</sup> identified FFA4. (C) The expression level of hFFA4-eYFP was showed by anti-eYFP. n=3.

#### 4.2.2.3 Phosphorylation and internalization of FFA4 in Flp-In TReX 293 cells

Previous studies have shown that long-time exposure to TUG-891 results in FFA4 receptor intracellular migration, which is also called internalization (Hudson et al., 2013b). To visualise internalization, immunocytochemistry was utilized in this study. The anti-pThr<sup>349</sup>/Ser<sup>350</sup> antibodies were also capable of identifying TUG-891-activated hFFA4 in immunocytochemical studies. The hFFA4-eYFP cells without doxycycline induction did not express hFFA4-eYFP, which showed only DAPI staining (Figure 4.5-dox). hFFA4-eYFP illuminated the plasma membrane of doxycycline induced hFFA4-eYFP cells (Figure 4.5+dox hFFA4-eYFP). While, anti-pThr<sup>349</sup>/Ser<sup>350</sup> antibody staining showed limited intensity in doxycycline induced

## Chapter 4

hFFA4-eYFP cells. It is difficult to tell whether anti-pThr<sup>349</sup>/Ser<sup>350</sup> antibody staining was constitutive phosphorylation of hFFA4 or the antibody showed an affinity for the un-phosphorylated receptor (Figure 4.5+dox Anti-pThr<sup>349</sup>/Ser<sup>350</sup>). Anti-pThr<sup>349</sup>/Ser<sup>350</sup> antibody staining was more intense in TUG-891 treated cells (Figure 4.5Anti-pThr<sup>349</sup>/Ser<sup>350</sup>). The phosphorylated receptor showed coincidence with hFFA4-eYFP (Figure 4.5 +dox+TUG-891 5minutes hFFA4-eYFP and Anti-pThr<sup>349</sup>/Ser<sup>350</sup>).

## Chapter 4

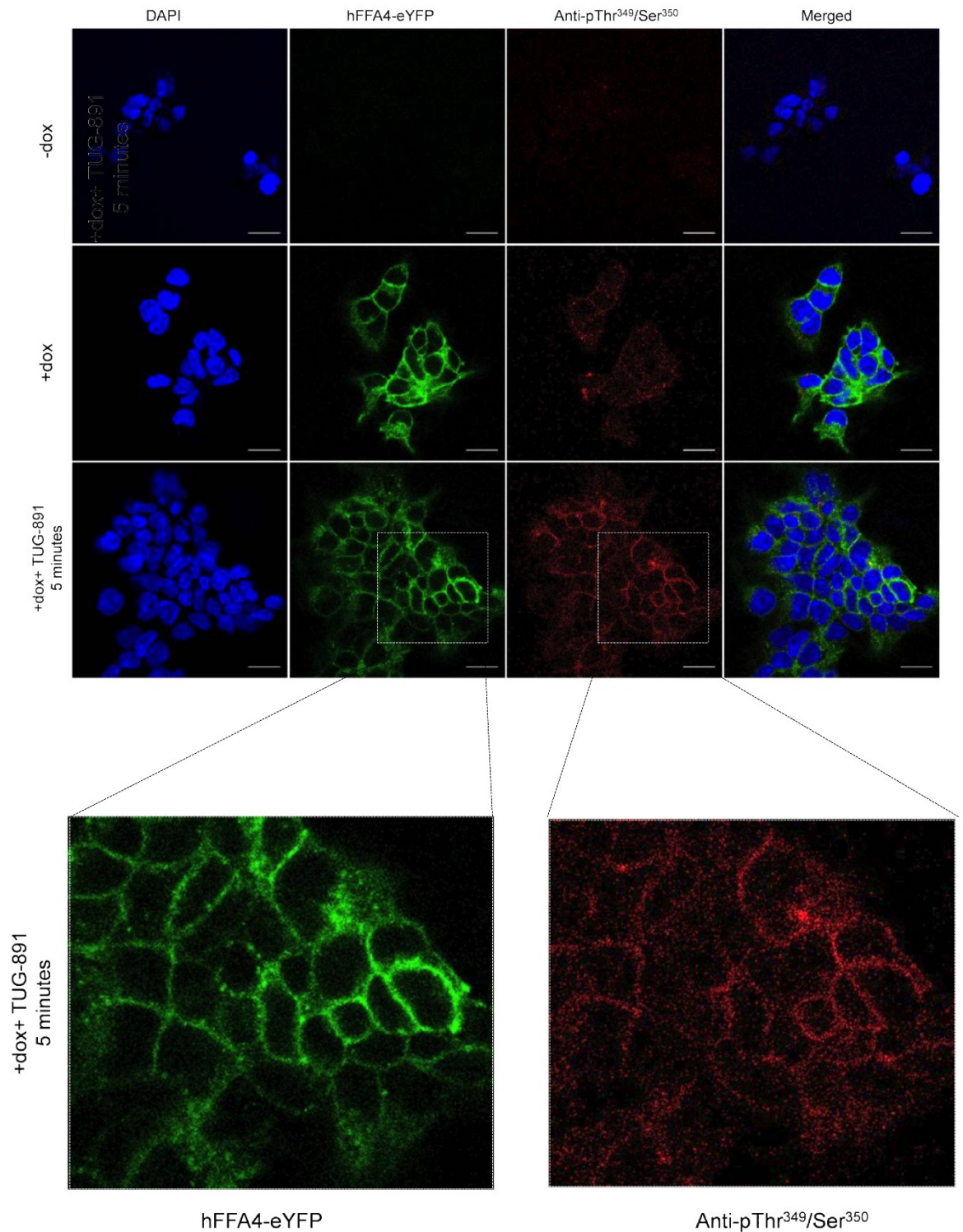


**Figure 4.5 immunocytochemistry of FFA4 phosphorylation induced by TUG-891.**

Flp-In TReX 293 cells expressed hFFA4-eYFP were grown on coverslips, stimulated with TUG-891 (10  $\mu$ M) and fixed at different time points. After fixation, cells were treated anti-pThr<sup>349</sup>/Ser<sup>350</sup> FFA4 (1:250 dilution) antibodies. Mounting medium with DAPI was used to identify cell nuclei. Blue, DAPI; green, eYFP; and red, anti-pThr<sup>349</sup>/Ser<sup>350</sup> FFA4. The merged images illustrate colocalization of eYFP-tagged receptor and the phosphorylation site-specific antibody. The enlarged section of the images (in dotted line) showed the coincidence between phosphorylated receptor and hFFA4-eYFP. Images were taken using a Zeiss LSM 880 confocal equipped with a 63x/1.4 NA Plan Apochromat oil immersion objective. Scale bar = 20  $\mu$ m

#### Chapter 4

In Flp-In 293 cells expressing hFFA4-eYFP, the receptors were located at the cell surface, while FFA4 receptors internalized after exposure to TUG-891 for 15 minutes. And receptor internalization level increased at 30 minutes (Figure 4.6 hFFA4-eYFP). Anti-pThr<sup>349</sup>/Ser<sup>350</sup> FFA4 staining was substantially more intense in cells with five-minute-treated with TUG-891 than it was with later time points. (Figure 4.6 Anti-pThr<sup>349</sup>/Ser<sup>350</sup>).

## Chapter 4

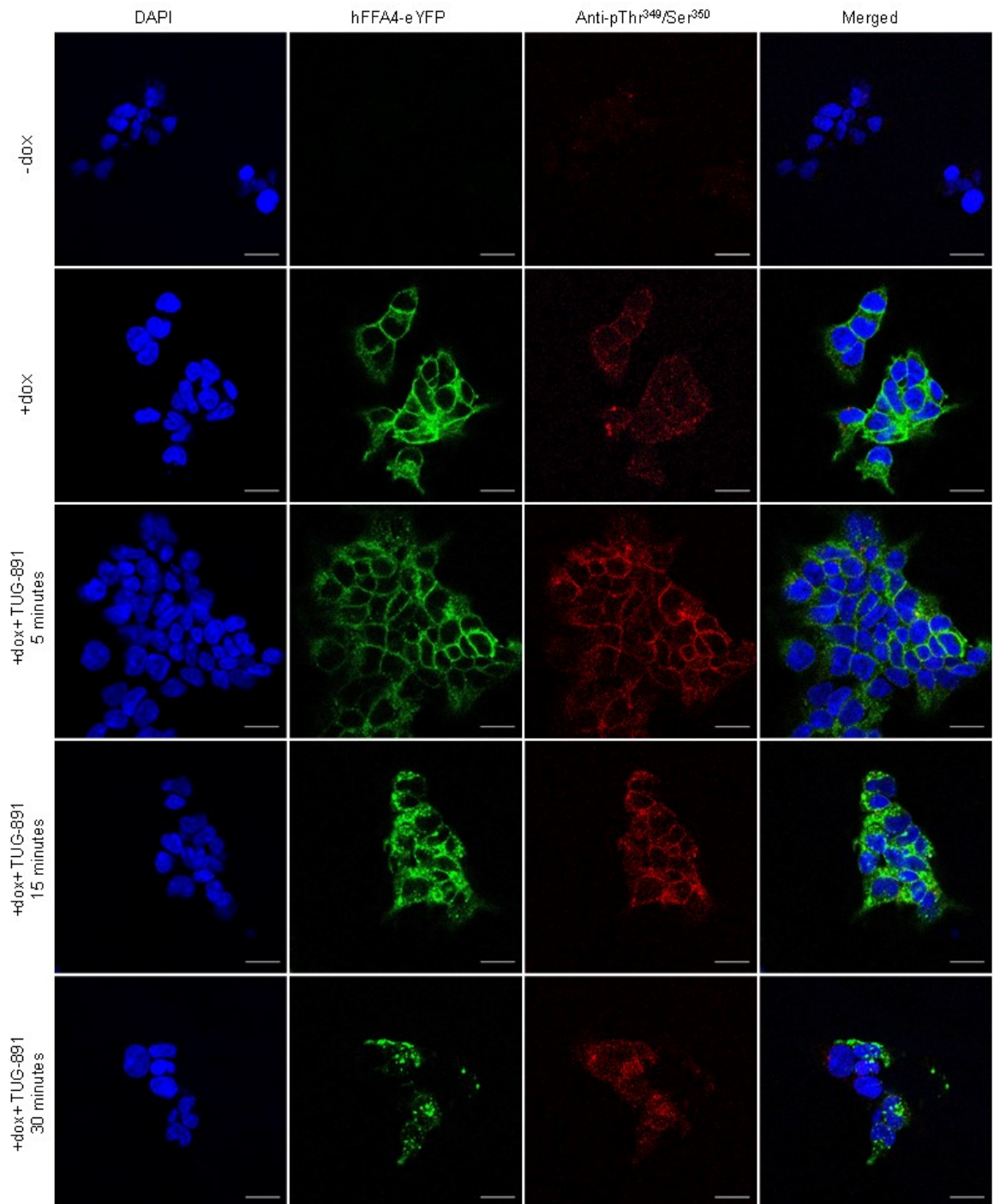


**Figure 4.6 Immunocytochemistry of FFA4 phosphorylation induced by TUG-891 in a time-dependent manner.**

Flp-In TREx 293 cells expressed hFFA4-eYFP were grown on coverslips, stimulated with TUG-891 (10  $\mu$ M) and fixed at different time points. After fixation, cells were treated anti-pThr<sup>349</sup>/Ser<sup>350</sup> FFA4 (1:250 dilution) antibodies. Mounting medium with DAPI was used to identify cell nuclei. Blue, DAPI; green, eYFP; and red, anti-pThr<sup>349</sup>/Ser<sup>350</sup> FFA4. The merged images illustrate colocalization of eYFP-tagged receptor and the phosphorylation site-specific antibody. Images were taken using a Zeiss LSM 880 confocal equipped with a 63x/1.4 NA Plan Apochromat oil immersion objective. Scale bar = 20  $\mu$ m

### 4.2.3 GRKs participate in the regulation of FFA4 phosphorylation

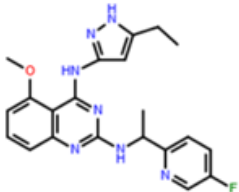
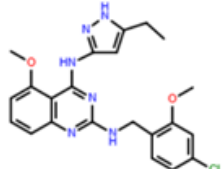
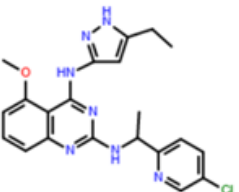
#### 4.2.3.1 GRK inhibitors affect FFA4 phosphorylation

To investigate the involvement of GRKs in the phosphorylation of FFA4 a number of GRK inhibitors were used. Flp-In TReX 293 cells were pre-treated with various GRK inhibitors. These included the GRK6 inhibitors compound 15, compound 18, compound 19 and the GRK2/3 inhibitor compound 101 for 3 hours, followed by TUG-891 treatment (Thal et al., Uehling et al., 2021). western blot analysis of lysates from these treatments with anti-pThr<sup>349</sup>/Ser<sup>350</sup> FFA4 antibodies demonstrated that, compound 19 significantly inhibited TUG-891 mediated FFA4 phosphorylation at these sites. Samples from cells treated with compound 15 also showed less phosphorylation, compared with samples only treated with vehicle. Compound 101 did not result in inhibition of FFA4 phosphorylation (Figure 4.7C). By contrast anti-pThr<sup>347</sup> still identified FFA4 phosphorylation, in the presence of any of the GRK inhibitors (Figure 4.8A, C). Importantly, FFA4-eYFP expression was not affected by the inhibitors, as shown by probing with anti-eYFP (Figure 4.7B, D, Figure 4.8B, D).

## Chapter 4

Table 4-1 IC<sub>50</sub> of GRK5/6 inhibitors

Referenced from (Uehling et al., 2021)

Compound	Chemical structure	Chemical Formula	GRK6 IC <sub>50</sub> (nM)
Compound 15		(S)-N4-(3-Ethyl-1H-pyrazol-5-yl)-N2-(1-(5-fluoropyridin-2-yl)-ethyl)-5-methoxyquinazoline-2,4-diamine	7.2±1.3
Compound 18		N2-(4-Chloro-2-methoxybenzyl)-N4-(5-ethyl-1H-pyrazol-3-yl)-5-methoxyquinazoline-2,4-diamine	8±2
Compound 19		(S)-N2-(1-(5-Chloropyridin-2-yl)ethyl)-N4-(5-ethyl-1H-pyrazol-3-yl)-5-methoxyquinazoline-2,4-diamine	3.5±0.5



## Chapter 4

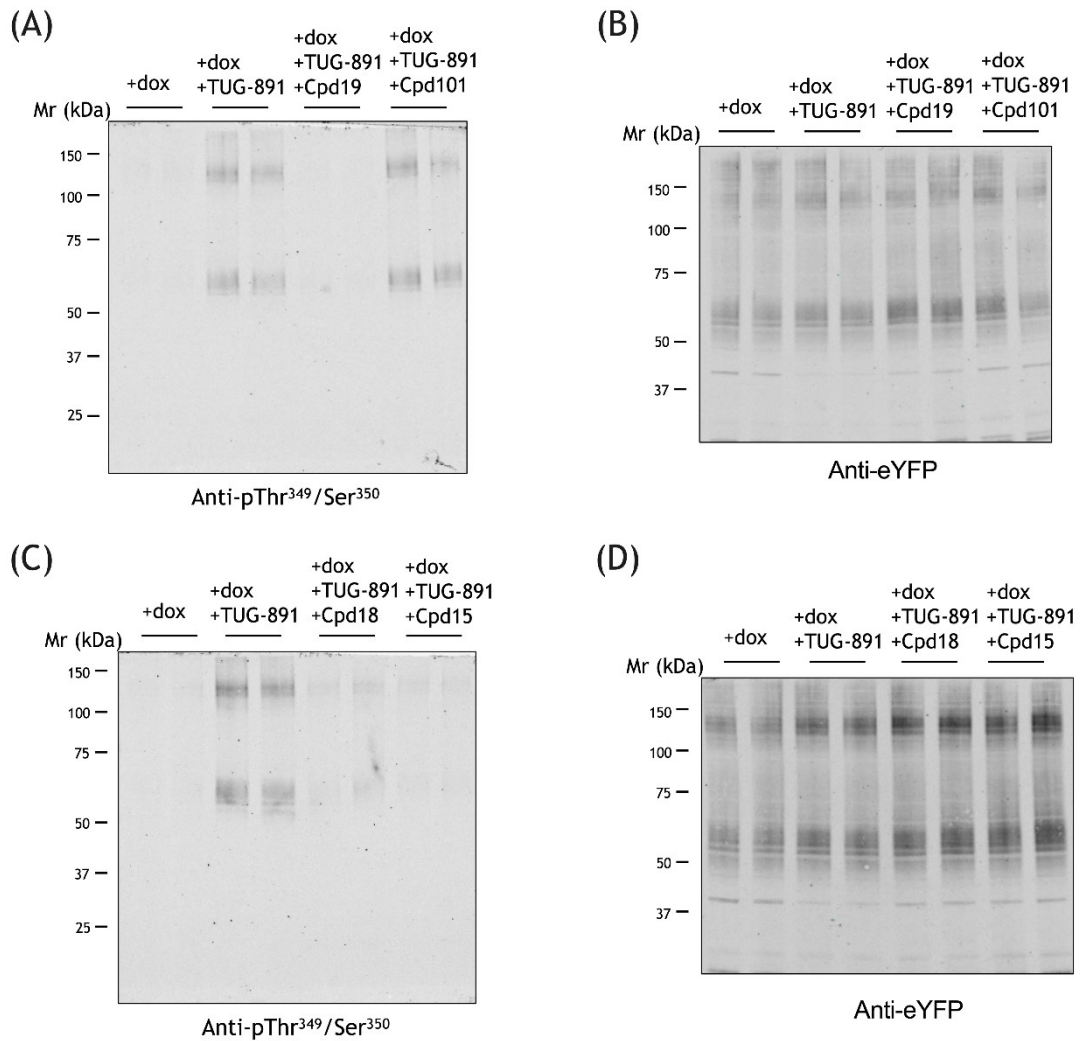


**Figure 4.7 Identification of GRK inhibitors regulation of hFFA4 phosphorylation status using phospho-site specific antibody anti-pThr<sup>349</sup>/Ser<sup>350</sup> FFA4.**

Flp-In TREx 293 cells were pre-treated with 10 $\mu$ M of GRK inhibitors for 3 hours. Cells were then stimulated with TUG-891 (10 $\mu$ M) or 0.1% DMSO as a vehicle control (+dox) for 5 minutes at 37°C. The receptors were purified by immunoprecipitation using GFP-trap. Samples were run on 4-12% SDS-PAGE and analysed by western blotting. (A) Anti-pThr<sup>349</sup>/Ser<sup>350</sup>-identified FFA4 phosphorylation with the presence of GRK inhibitor compound 19 (Cpd 19), and compound 101 (Cpd 101). (C) Anti-pThr<sup>349</sup>/Ser<sup>350</sup> identified FFA4 phosphorylation with the presence of GRK inhibitor compound 18 (Cpd 18), and compound 15 (Cpd 15). (B) and (D) Representative western blot of anti-eYFP showed the expression level of hFFA4-eYFP. All antibodies were 1:1000 dilution. n=3.



## Chapter 4

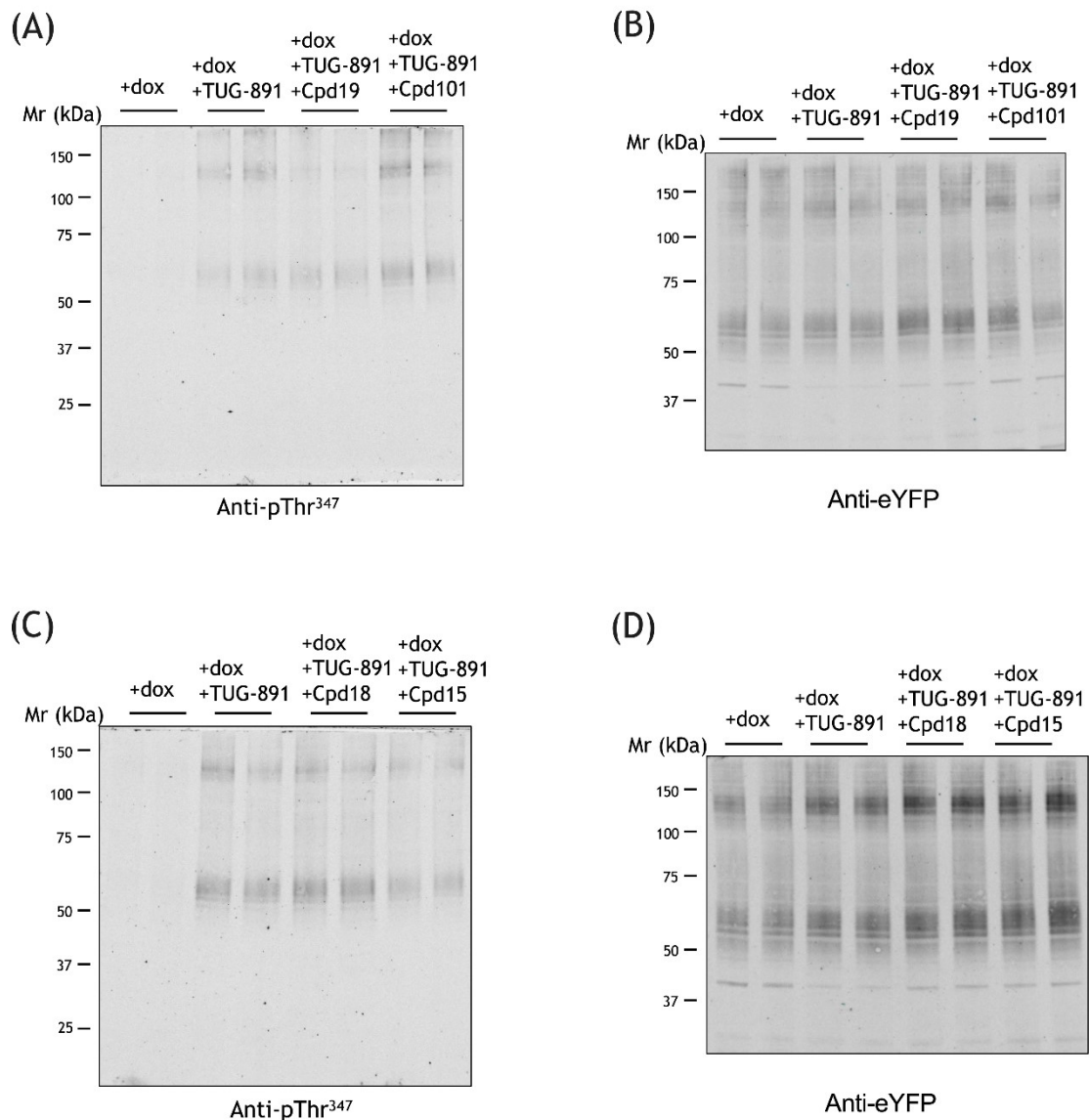


**Figure 4.8 Identification of GRK inhibitors regulation of hFFA4 phosphorylation status using phospho-site specific antibody anti-pThr<sup>347</sup> FFA4.**

Flp-In TReX 293 cells were pre-treated with 10 $\mu$ M of GRK inhibitors for 3 hours. Cells were then stimulated with TUG-891 (10 $\mu$ M) or 0.1% DMSO as a vehicle control (+dox) for 5 minutes at 37°C. The receptors were purified by immunoprecipitation using GFP-trap. Samples were run on 4-12% SDS-PAGE and analysed by western blotting. Samples were loaded duplicate and all antibodies were 1:1000 dilution. (A) Anti-pThr<sup>347</sup> identified FFA4 phosphorylation with the presence of GRK inhibitor compound 19 (Cpd 19), and compound 101 (Cpd 101). (C) Anti-pThr<sup>347</sup> identified FFA4 phosphorylation with the presence of GRK inhibitor compound 18 (Cpd 18), and compound 15 (Cpd 15). (B) and (D) Representative western blot of anti-eYFP showed the expression level of hFFA4-eYFP.

#### 4.2.3.2 Interactions between FFA4 and $\beta$ -arrestin 2 in the presence of GRK inhibitors

The involvement of GRKs in the phosphorylation of hFFA4 was explored in a series of  $\beta$ -arrestin 2 recruitment assay studies performed in HEK293 cells co-expressing hFFA4-eYFP and  $\beta$ -arrestin 2 tagged with Renilla luciferase. Stimulation of HEK293 cells with TUG-891 produced a concentration-dependent

## Chapter 4

(mean  $pEC_{50} = 6.95 \pm 0.13$ ,  $n=3$ ) increase in the  $\beta$ -arrestin 2 recruitment (Figure 4.9A). GRK inhibitors were then used to pre-treat hFFA4-eYFP HEK293 cells for 30 minutes and followed by 5 minutes TUG-891 treatment. All the GRK inhibitors reduced hFFA4 interaction with  $\beta$ -arrestin 2 to some extent in a concentration-dependent manner (Figure 4.9B). Cells treated with compound 15 or compound 101 showed about 25% reduction of the maximum response of TUG-891. Compound 19 showed 40% reduction the concentration tested 10  $\mu$ M (Figure 4.9B).

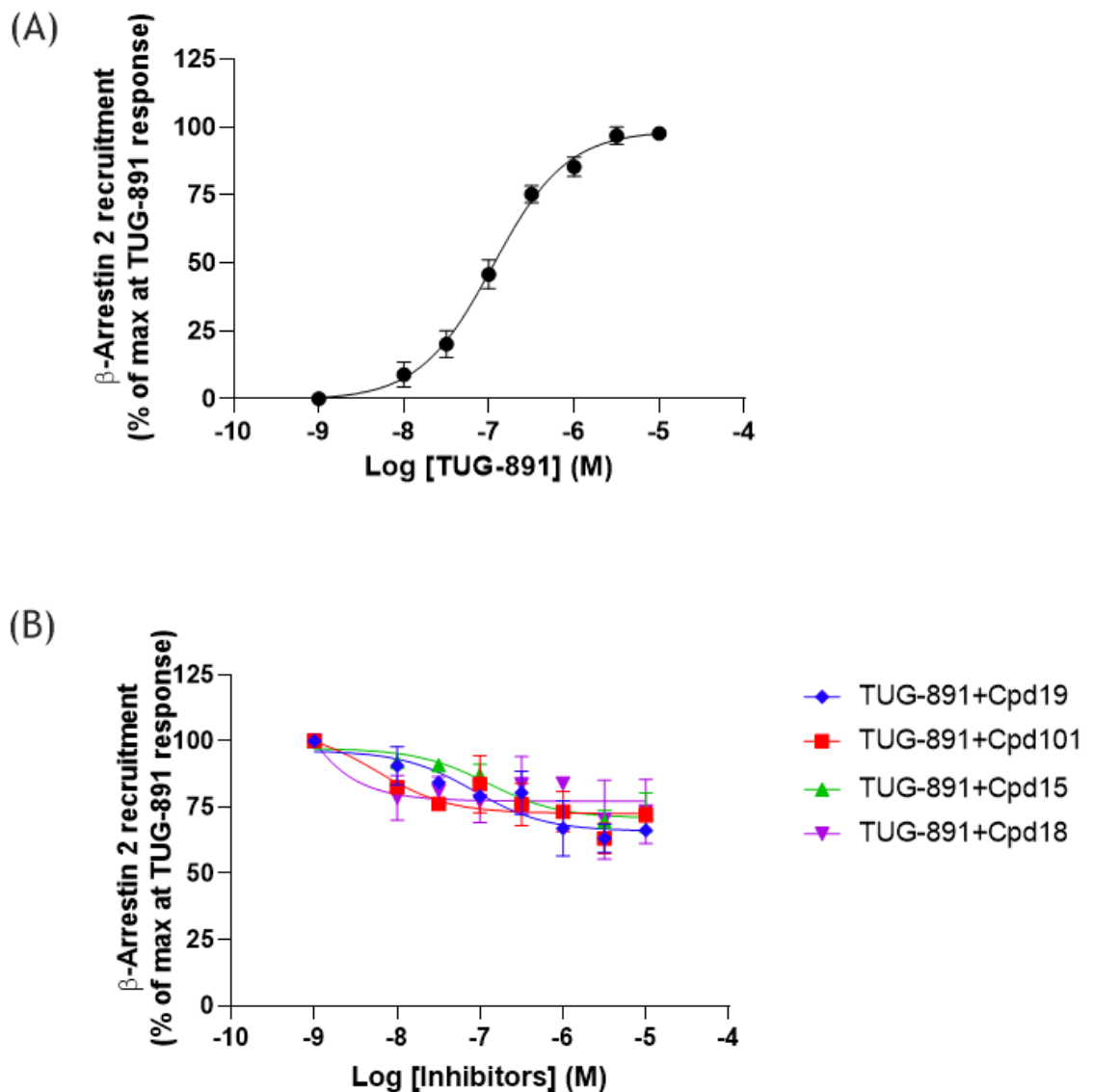


**Figure 4.9  $\beta$ -arrestin 2 recruitment affected by TUG-891 and GRK inhibitors.**

BRET studies were performed in HEK293T cells transfected to coexpress FFA4-eYFP and  $\beta$ -arrestin 2–Renilla luciferase. (A) After addition of the indicated concentrations of TUG-891 for 5 minutes,

## Chapter 4

BRET was recorded (n=3). Data are given as means  $\pm$  S.E.M. of duplicate data points from a single experiment. (B) Cells were pre-treated with the indicated concentrations of compound 19 (Cpd 19), compound 101 (Cpd 101), compound 15 (Cpd 15), compound 18 (Cpd 18) for 30 minutes, followed by 5-minute treatment of TUG-891. Interaction was recorded and data normalized by the maximum response that observed for the TUG-891(10  $\mu$ M) treated receptor (n=2). Data are given as means  $\pm$  S.D. of duplicate data points from a single experiment.

**Table 4-2 IC50 of GRK inhibitors in  $\beta$ -arrestin2 recruitment assay**

GRK inhibitor	Cpd19	Cpd15	Cpd18	Cpd101
IC50 ( $\mu$ M)	$8.519 \times 10^{-8}$	$1.251 \times 10^{-7}$	$1.386 \times 10^{-10}$	$5.749 \times 10^{-9}$

As the inhibition effect on  $\beta$ -arrestin recruitment FFA4 phosphorylation by a single inhibitor was not complete, a combination of compound 19 and compound 101 was used to treat cells. The combination of compound 19 and compound 101 had an additive effect on the interaction of  $\beta$ -arrestin 2, reducing the maximal  $\beta$ -arrestin 2 recruitment assay signals to 25% of that observed for the TUG-891 treated receptor (Figure 4.10).

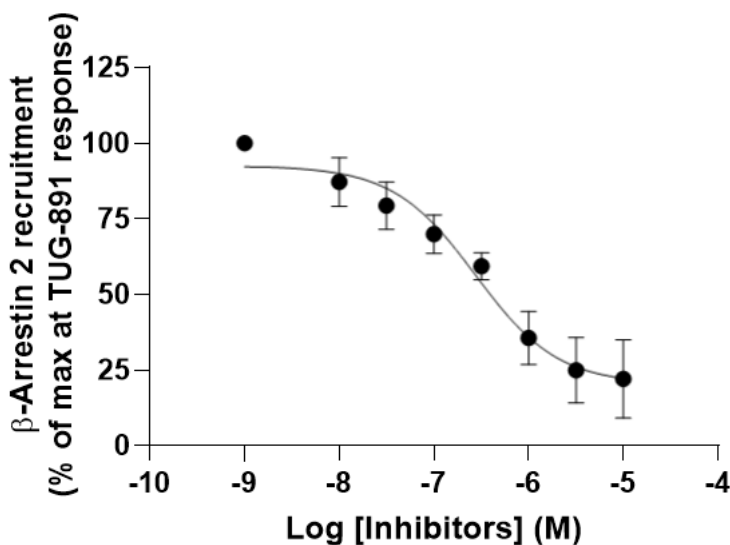


**Figure 4.10  $\beta$ -arrestin 2 recruitment inhibited by a combination of compound 19 and compound 101.**

BRET studies were performed in HEK293T cells transfected to coexpress  $\beta$ -arrestin 2–Renilla luciferase. Cells were pre-treated with the indicated concentrations of a combination of compound 19 (Cpd 19) and compound 101 (Cpd 101), followed by 5-minute treatment of TUG-891. Interaction was recorded and data normalized by the maximum response that observed for the TUG-891 treated receptor. Data are given as means  $\pm$  S.E.M. of triplicate data points from a single experiment, n=3

## Chapter 4

We also investigated compound 19 inhibited  $\beta$ -arrestin 2 recruitment in the presence of 10  $\mu$ M of compound 101. This pairing showed higher potency and efficiency. The compounds reduced 85%  $\beta$ -arrestin 2 recruitment of that observed for the TUG-891 treated receptor (Figure 4.11).

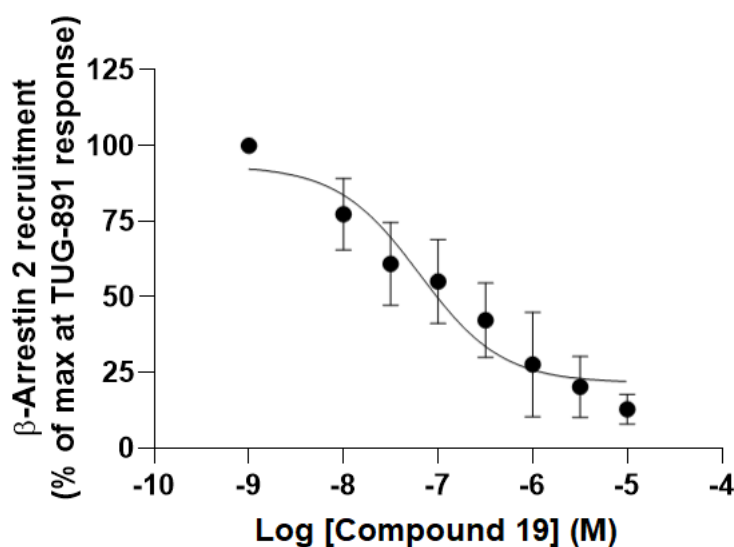


**Figure 4.11  $\beta$ -arrestin 2 recruitment inhibited by a combination of compound 19 and 10  $\mu$ M of compound 101.**

BRET studies were performed in HEK293T cells transfected to coexpress  $\beta$ -arrestin 2–Renilla luciferase. Cells were pre-treated with the indicated concentrations of compound 19 (Cpd 19) and 10  $\mu$ M of compound 101 (Cpd 101), followed by 5-minute treatment of TUG-891. Interaction was recorded and data normalized by the maximum response that observed for the TUG-891 treated receptor. Data are given as means  $\pm$  S.E.M. of duplicate data points from a single experiment,  $n=3$ .

## 4.2.4 Investigation of phosphorylation status of mouse FFA4

### 4.2.4.1 Anti-pThr<sup>349</sup>/Ser<sup>350</sup> identified mFFA4 in CHO cells

To investigate whether the phospho-site specific antibody anti-pThr<sup>349</sup>/Ser<sup>350</sup> FFA4 is able to probe the phosphorylation status of the mouse FFA4 *in vivo*. I firstly established if our phospho-specific antibodies could recognise phosphorylation sites on the mouse FFA4 expressed recombinantly in CHO cells. C-terminally HA-tagged mouse FFA4 receptors expressed in CHO cells were challenged with either vehicle or 10  $\mu$ M TUG-891. The receptors were immunoprecipitated by HA trap and samples were analysed using western blot. Non-transfected CHO cells (CHO NT) cells showed no evidence of the expression

## Chapter 4

of FFA4 receptor (Figure 4.12A). In contrast FFA4-HA expression was identified with an anti-HA antibody in hFFA4-HA and mFFA4-HA cells (Figure 4.12A). Total expression of FFA4 showed slight decrease in samples treated with TUG-891 in CHO mFFA4-HA cells, but was still recognised by anti-HA (Figure 4.12A).

Lysates prepared from CHO cells expressing mFFA4-HA or hFFA4-HA were then probed with phospho-site specific antibody anti-pThr<sup>349</sup>/Ser<sup>350</sup> FFA4. CHO-NT were used as a negative control. The results showed that, without exposure to TUG-891 anti-pThr<sup>349</sup>/Ser<sup>350</sup> FFA4 failed to identify the receptor construct whereas anti-HA identified a series of polypeptides clustering around 40 kDa and 75 kDa (Figure 4.12). In contrast, following the addition of TUG-891 the anti-pThr<sup>349</sup>/Ser<sup>350</sup> FFA4 clearly identified polypeptides that corresponding to hFFA4-eYFP in both CHO mFFA4-HA and CHO hFFA4-HA cell lysates (Figure 4.12B).

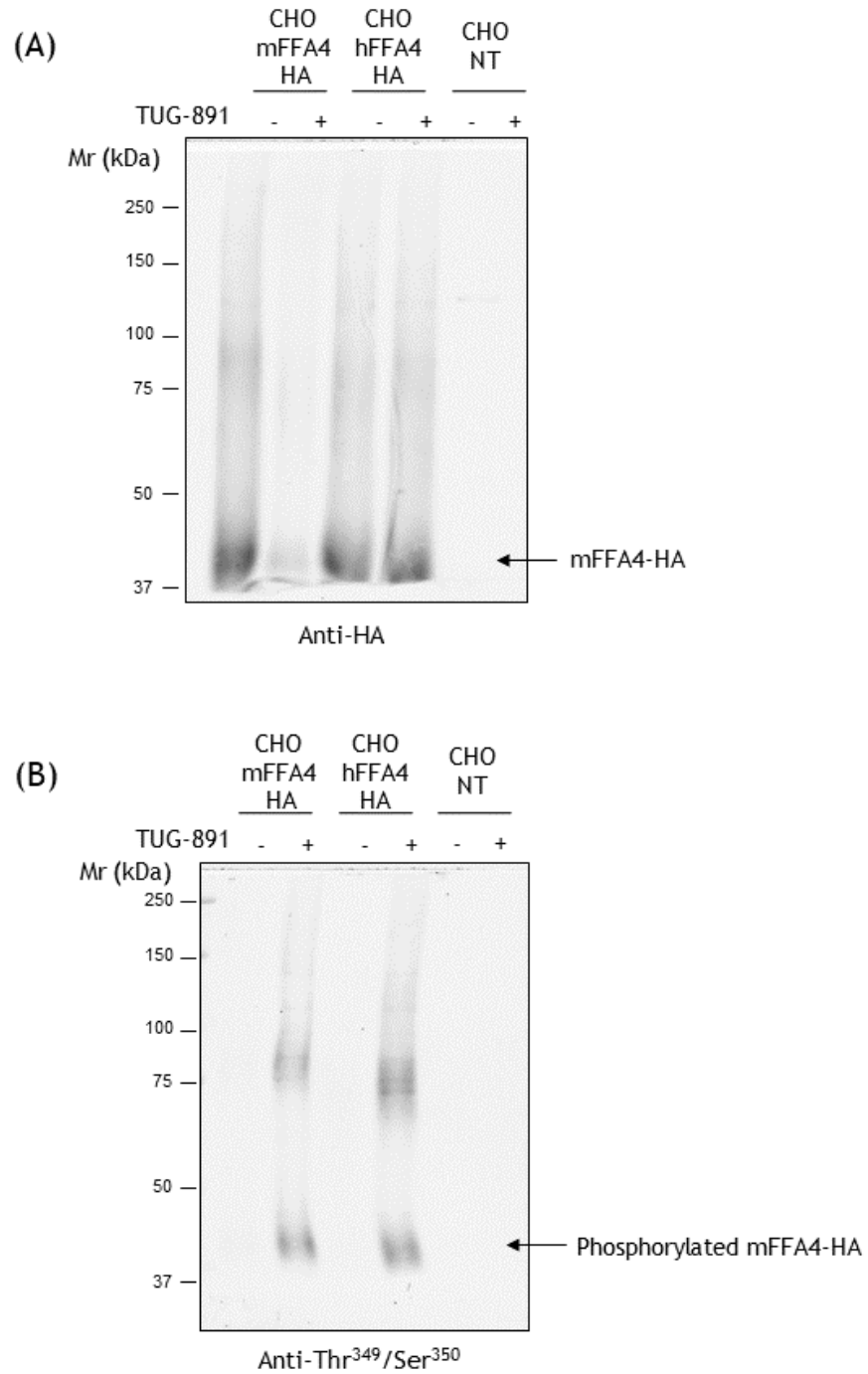


**Figure 4.12 Characterisation of anti-pThr<sup>349</sup>/Ser<sup>350</sup> in CHO cells**

CHO mFFA4-HA, CHO hFFA4-HA, CHO NT cells were stimulated with TUG-891 (10 $\mu$ M) (showed by "+") or 0.1% DMSO (showed by "-") as a vehicle control for 5 minutes at 37°C. The receptors were purified by immunoprecipitation using HA-trap. Proteins were separated by 4-12% SDS-PAGE and analysed by western blot analysis. All antibodies were 1:1000 dilution. Molecular mass of FFA4-HA is between 37-50 kDa. (A) Representative western blot of anti-HA showed the expression of FFA4-

## Chapter 4

HA. (B) Representative western blot of anti-pThr<sup>349</sup>/Ser<sup>350</sup> identified FFA4 phosphorylation induced by TUG-891. (n=3).

### 4.2.4.2 Characterisation of anti-pThr<sup>349</sup>/Ser<sup>350</sup> in lung tissue

To investigate whether anti-pThr<sup>349</sup>/Ser<sup>350</sup> FFA4 was able to identify the phosphorylated form of FFA4 in vivo I investigated the phosphorylation of the receptor in mouse lung. Lung tissues were collected from transgenic mice expressing HA-tagged FFA4-WT receptors and from mice where a phosphorylation-deficient version of FFA4 (FFA4-PD) was knocked into the receptor gene locus. Mice were treated with TUG-891 for 20 minutes at 37°C. FFA4 expression was confirmed in western blots by probing with anti-HA antibodies. These studies identified FFA4-WT and FFA4-PD in lung samples but failed to identify the receptor in FFA4-KO mouse tissue. TUG-891 treatment had no influence on FFA4 expression (Figure 4.13A). However, anti-pThr<sup>349</sup>/Ser<sup>350</sup> antibodies failed to identify the phosphorylation form of the receptor (Figure 4.13B).

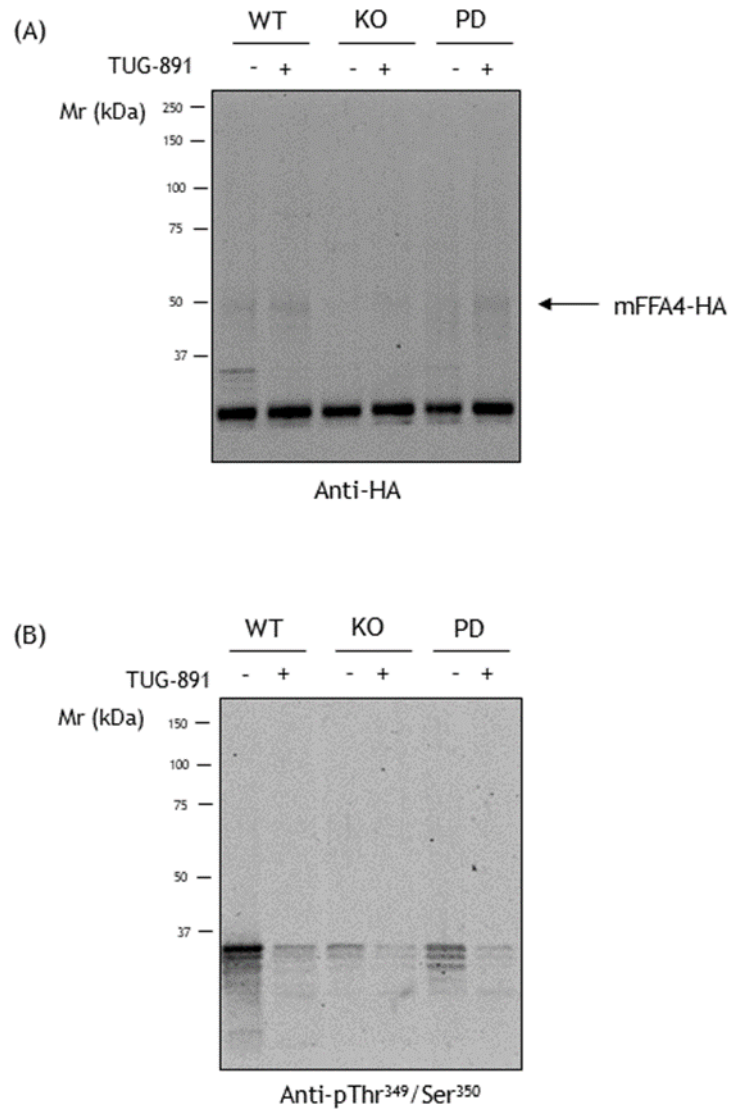


**Figure 4.13 Characterisation of anti-pThr<sup>349</sup>/Ser<sup>350</sup> FFA4 in lung.**

Lung tissues from FFA4-WT-HA, FFA4-KO, FFA4-PD-HA mice were homogenised after treatment with 0.1% DMSO (showed as “-” in figure) or TUG-891 (10 mM, 20 minutes, showed as “+” in figure), and immunoprecipitated with anti-HA affinity matrix overnight. Proteins were separated by 4-12% SDS-PAGE and analysed by western blot analysis. All antibodies were used at 1:1000 dilution. (A) Representative western blot of anti-HA showed the expression of mFFA4-HA (B) Representative western blot of anti-pThr<sup>349</sup>/Ser<sup>350</sup> identified FFA4 phosphorylation induced by TUG-891. (n=2)

#### 4.2.4.3 FFA4 expression in membrane preparations from mouse lung

The western blots in Figure 4.13 showed FFA4 low expression in the lung. Considering FFA4 express on membrane, I then tried to collect membrane proteins instead of total proteins. Membrane proteins were extracted from lung tissues from FFA4-WT, FFA4-KO and FFA4-PD mice with HA tag and separated by 4-12% bio-tris gel (Detailed description was in 2.14.4). Antibody against HA was used to confirmed FFA4 expression. Although the western blot showed anti-HA



## Chapter 4

identified FFA4 in WT and PD mice, the expression of FFA4 was still low (Figure 4.14). Antibody against HA failed to identify in KO mice (Figure 4.14).

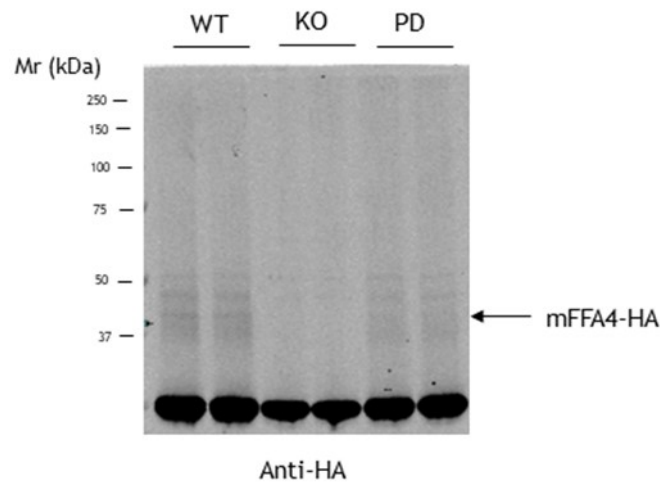


**Figure 4.14 FFA4 expression in membrane protein extract from lung.**

Lung tissues from FFA4-WT-HA, FFA4-KO, FFA4-PD-HA mice were homogenised, and immunoprecipitated with anti-HA affinity matrix for 2 hours at 4 °C. Proteins were separated by 4-12% SDS-PAGE and analysed by western blot analysis. Antibody against HA (1:1000 dilution) was used to assess the expression of mFFA4-HA in lung tissues.

### 4.3 Discussion

In recent years, FFA4 has garnered significant attention as a novel therapeutic target for the treatment of metabolic disease. However, a lack of potent and selective ligands for the receptor has limited its development. Although several ligands have been reported, the most widely used ligand is TUG-891, which is described as a potent and selective FFA4 agonist. In this chapter I extended these studies to include the more recently described Agonist 2. This agonist has previously been used in *in vivo* studies shown to inhibit somatostatin secretion induced by glucose in murine islets (Engelstoft et al., 2013). Furthermore, oral administration of Agonist 2 decreased plasma ghrelin in mice under fasting conditions (Engelstoft et al., 2013). Despite these studies reporting *in vivo* effect of Agonist 2 on metabolic function, there is a lack of information on Agonist 2 pharmacology. Our results have shown that Agonist 2 phosphorylated hFFA4 and showed similar efficacy to TUG-891. However, because the gels with TUG-891

## Chapter 4

samples and Agonist 2 samples were not running parallelly, it is difficult to tell whether Agonist 2 has higher potency than TUG-891.

AH-7614 is a xanthene derivative of a diarylsulfonamide-based FFA4 agonist, however it can block effects of both the polyunsaturated  $\omega$ -6 fatty acid linoleic acid and the synthetic FFA4 agonist GSK137647A. Therefore, AH-7614 was described as the first ligands for the FFA4 receptor (Watterson et al., 2017). AH-7614 inhibited promotion of  $\text{Ca}^{2+}$  mobilization in Flp-In T-REx 293 cells induced to express hFFA4-eYFP and also blocked TUG-891-mediated internalization of FFA4 from the cell surface (Sparks et al., 2014). In my studies AH-7614 inhibited FFA4 receptor phosphorylation consistent with its antagonist properties. Having established that phosphorylation is blocked by AH-7614, it was concluded that the antagonist could be used to determine the rate of dephosphorylation. By adding the antagonist after TUG-891 mediated phosphorylation dephosphorylation of the receptor was monitored. In these experiments the receptor was completely dephosphorylated by 25 minutes.

Dephosphorylation is an important part of the GPCRs activation/deactivation cycle and essential for receptor resensitisation (Kliwer et al., 2017). This process occurs through protein phosphatases. Previous studies have shown that protein phosphatase 1 (PP1) and protein phosphatase 2A (PP2A) act as GPCR phosphatases (Pöll et al., Ishier et al., 2013, Kliwer et al., 2017). Which phosphatases are involved in the dephosphorylation of FFA4 remains to be discovered. However, models have proposed that phosphorylated receptors internalise and that dephosphorylation occurs at intracellular locations such as endosomal vesicles. After dephosphorylation the internalised GPCRs are recycled to the plasma membrane for resensitisation (Kliwer et al., 2017).

Immunocytochemistry images demonstrated that hFFA4 internalized following TUG-891 treatment. But according to previous studies, the extent of internalized receptor increased in a quasi-linear fashion and reached a maximum level within 40 minutes measured by high content imaging assay (Hudson et al., 2013b). This is consistent of our results which showed that the receptor internalization increased over 30 minutes in the presence of TUG-891 was presence.

## Chapter 4

Phosphorylation and internalization are usually a combined process related to receptor desensitization. The eYFP tag illuminated the plasma membrane of hFFA4-eYFP cells, showing the location of the receptor. Antibody anti-pThr<sup>347</sup>/pSer<sup>350</sup> staining was also detected at plasma membrane of cells with 5 minutes TUG-891 treatment, which suggested the phosphorylated receptor located at the membrane. western blots revealed that the peak of TUG 891-mediated phosphorylation of hFFA4 occurs at 5 minutes. Interestingly the phosphorylation status of the receptor decreased from its peak at 5 minutes. This decrease in phosphorylation observed in western blots mirrored receptor internalisation that is evident within 15 minutes of TUG-891 treatment. By 30-minutes treatment with TUG-891, limited receptor was detected at plasma membrane and phosphorylation of the receptor had reduced to near basal levels. These results are consistent with the notion that receptors are phosphorylated at plasma membrane. This drives receptor internalisation into acidic endosomes where the receptor is dephosphorylated (Prihandoko et al., 2016, Kliewer et al., 2017). In the time course experiments, the expression of FFA4 showed by anti-GFP was not equivalent, but we can still determine that the phosphorylation increased between 2 minutes to 5 minutes. Although eYFP tag is considered could be used to measure the expression of FFA4, it is better to show FFA4 expression with FFA4 structural antibody.

To investigate which GRKs are responsible for FFA4 phosphorylation. the selective GRK inhibitors were used in this chapter. Our results also showed that the potent GRK6 inhibitor compound 19 prevented FFA4 phosphorylation on Thr<sup>349</sup>/Ser<sup>350</sup> and also inhibited  $\beta$ -arrestin2 recruitment. The compound 101 failed to inhibit phosphorylation on sites Thr<sup>349</sup>/Ser<sup>350</sup> in immunoblot, which suggest that GRK2/3 did not regulate phosphorylation of FFA4 on these residues. Then I measured  $\beta$ -arrestin2 recruitment and found the single application of GRK6 or GRK2/3 inhibitors hardly to prevented  $\beta$ -arrestin2 recruitment, however the treating the cells with compound 19 and compound 101 together significantly inhibited  $\beta$ -arrestin2 recruitment. This suggested that  $\beta$ -arrestin recruitment to FFA4 is regulated by GRK2/3 and GRK6.

Attempts were made to translate the in vitro findings described above to endogenous FFA4 expressed in lung tissues. Expression of FFA4 in lung tissue was

#### Chapter 4

confirmed in western blots of lung tissue extracts from FFA4-HA and FFA4-PD transgenic mice using an anti-HA antibody. However, the anti-pThr<sup>349</sup>/Ser<sup>350</sup> failed to identify the phospho-sites in FFA4-HA mice. In vitro studies demonstrated phospho-acceptor sites on mFFA4 appeared in two clusters: cluster 1 contains Thr<sup>347</sup>, Thr<sup>349</sup>, and Ser<sup>350</sup>, which are consistent with human FFA4 and cluster 2 Ser<sup>357</sup>, Ser<sup>360</sup> and Ser<sup>361</sup> (Prihandoko et al., 2016). In my study I determined that the anti-Thr<sup>349</sup>/Ser<sup>350</sup> recognised phosphorylation sites in both the mouse and human forms of FFA4. Despite this I was not able to observe anti-Thr<sup>349</sup>/Ser<sup>350</sup> immunoreactivity in western blots from the mouse lung. It is not possible to conclude from my studies whether the lack of observable phosphorylation is due to low levels of receptor expression or genuinely due to a lack of phosphorylation.

## **Chapter 5 Investigation of phosphorylation status of FFA2 *ex vivo***

### **5.1 Introduction**

#### **5.1.1 From FFA4 to FFA2**

One of the core aims for my studies was to test the hypothesis that receptor phospho-specific antibodies could be used to establish the phosphorylation status of GPCRs in native tissues. This I have attempted for FFA4 where in the previous chapters I describe the characterisation of FFA4 phospho-specific antibodies using *in vitro* recombinant systems. Despite these antibodies showing promise *in vitro* it was not possible to detect phosphorylated forms of FFA4 in native tissues (i.e., lung). To address the question of whether receptor-phospho-specific antibodies might be useful reporters of *in vivo* receptor phosphorylation I decided to switch to the investigation of another free fatty acid receptor in this case the short chain fatty acid receptor, FFA2.

Free fatty acid receptors were divided into long chain fatty acid receptors (FFA1 and FFA4), and short chain fatty acid receptor (FFA2 and FFA3). Although FFA4 and FFA2 are activated by different ligands, they have some similar features. Both FFA2 and FFA4 can conduct signals through G $\alpha$ i/o and G $\alpha$ q and participate in metabolic and inflammatory processes. Hence, FFA4 and FFA2 are considered as potential drug targets to type 2 diabetes and anti-inflammatory. Moreover, our lab has phospho-sites specific antibodies raised against peptides from the hFFA2 sequence incorporating Ser<sup>296</sup>/Ser<sup>297</sup> (anti-pSer<sup>296</sup>/Ser<sup>297</sup> hFFA2) and Thr<sup>306</sup>/Thr<sup>310</sup> (anti-pThr<sup>306</sup>/Thr<sup>310</sup> hFFA2) (Figure 5.1). The specificity and sensitivity of antibodies have been tested before (by Domonkos Dedeo from our lab). Therefore, I decided to switch to the investigation of FFA2.

#### **5.1.2 Pharmacological tools to study function of FFA2**

FFA2 is endogenously activated by acetate, propionate, and butyrate. These ligands, however, also activate FFA3, making them undesirable as pharmacological tool compounds (Hudson et al., 2012b). Over the years, various synthetic ligands have been studied for FFA2, which have shown high efficacy and selectivity for the receptor. These ligands include the allosteric agonists 4-

## Chapter 5

CMTB (4-chloro- $\alpha$ -(1-methylethyl)-N-2-thiazolylbenzeneacetamide) and AZ1729 (4-fluoro-N-[3-[2-[(aminoiminomethyl)amino]-4-methyl-5-thiazolyl]phenyl]benzamide) (Smith et al., 2011, Lee et al., 2008, Bolognini et al., 2016a). Both of the ligands bind to allosteric sites of FFA2 and show higher potency than C3 in stimulating Gi signalling (Bolognini et al., 2016a). In addition, FFA2 orthosteric antagonists GLPG0974 (4-butyric acid) and CATPB ((S)-3-[2-(3-chlorophenyl)acetamido]-4-[4-(trifluoromethyl)phenyl] butanoic acid) have also been studied. These two ligands are known to be highly selective for human FFA2 and lack affinity for rodent orthologues (Pizzonero et al., 2014, Hudson et al., 2012b). Given this, I used hFFA2-DREADD mouse model in this chapter. As mentioned in section [错误!未找到引用源。](#), the designed receptor can be activated by MOMBA. The ligands are displayed in Table 5-1.

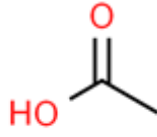
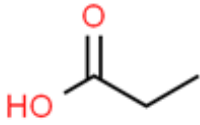
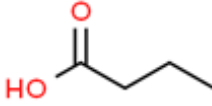
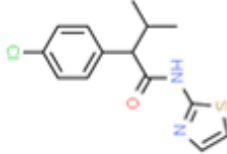
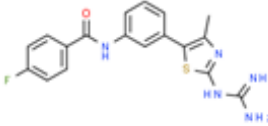
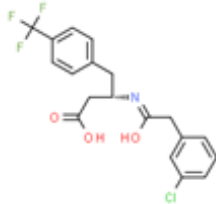
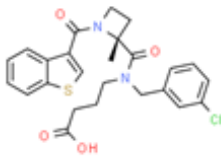
### 5.1.3 Aims

The aims of this chapter were to:

- i ) Assess FFA2 expression in cells and tissues.
- ii ) Assess whether the FFA2-DREADD ligand, MOMBA, is able to active hFFA2-DREADD.
- iii) Assess whether hFFA2-DREADD was phosphorylated at different phospho-sites in different tissues.

## Chapter 5

Table 5-1 Ligands at wild type human FFA2.

	Ligand	Structure	Chemical Formula
	C2		Acetic acid
Orthosteric agonists	C3		Propionic acid
	C4		Butyric acid
Allosteric agonists	4-CMTB		4-chloro- $\alpha$ -(1-methylethyl)- N-2- thiazolylbenzeneacetamide
	AZ1729		4-Fluoro-N-[3-[2- [(aminoimino)methyl]amino]- 4-methyl-5- thiazolyl]phenyl]benzamide
Antagonists	CATPB		3-[2-(3- chlorophenyl)acetamido]-4- [4-(trifluoromethyl)phenyl] butanoic acid
	GLPG0974		4-[(R)-1- (benzo[b]thiophene-3- carbonyl)-2-methyl- azetidine-2-carbonyl]- (3-chloro-benzyl)-amino- butanoic acid

## Chapter 5

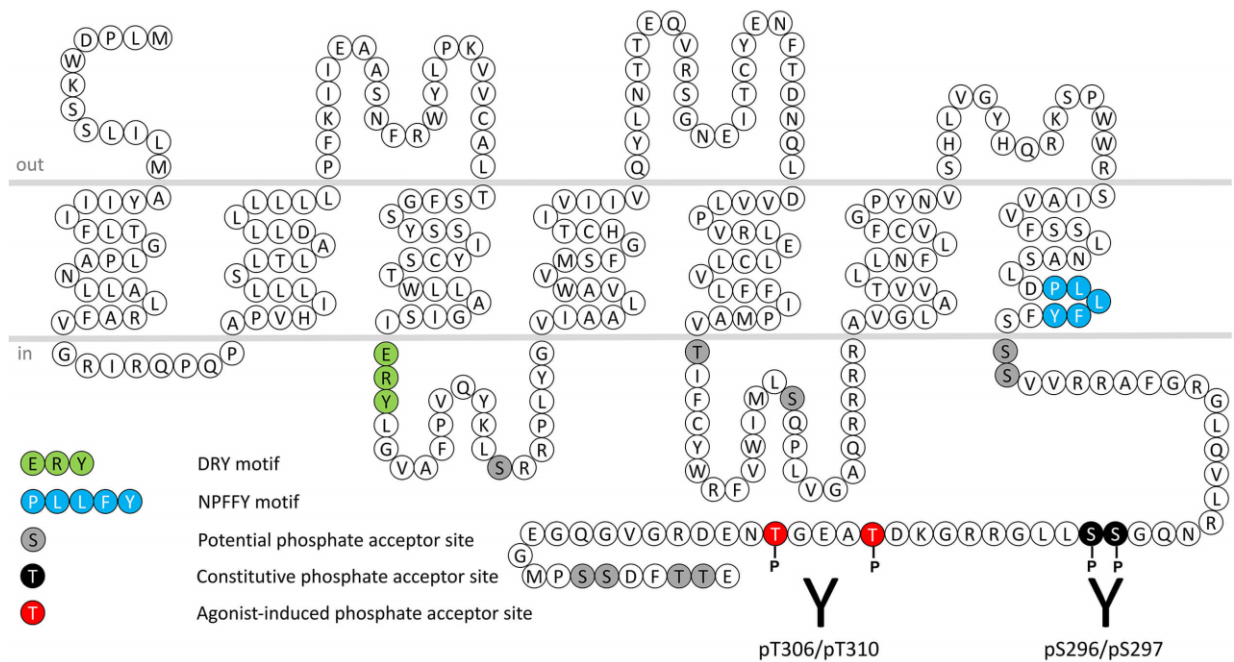


**Figure 5.1 Primary amino acid sequence of human FFA2**

Amino acid residues from the FFA2 are displayed as a snake plot. Constitutive phosphate acceptor sites are marked in black. The agonist-induced phosphate acceptor sites are marked in red. Figure referenced from [Free Fatty Acid Receptor 2 Antibodies | 7TM Antibodies](#)

## 5.2 Results

### 5.2.1 Characterisation of anti-pSer<sup>296</sup>/Ser<sup>297</sup> hFFA2 and anti-pThr<sup>306</sup>/Thr<sup>310</sup> hFFA2

#### 5.2.1.1 Characterisation of anti-pSer<sup>296</sup>/Ser<sup>297</sup> hFFA2 and anti-pThr<sup>306</sup>/Thr<sup>310</sup> hFFA2 in cell lines

To investigate the phosphorylation status of FFA2 and characterise the novel antibodies anti-pSer<sup>296</sup>/Ser<sup>297</sup> and anti-pThr<sup>306</sup>/Thr<sup>310</sup> FFA2, we administered vehicle or several FFA2 agonists to Flp-In TREx 293 cells stably expressing human FFA2-DREADD with an attached eYFP tag (hFFA2-DREADD-eYFP). Samples were immunoprecipitated with GFP trap, resolved by 4-12% SDS-PAGE, and analysed by western blot analysis. An antibody against GFP was also used to assess the expression of hFFA2-DREADD-eYFP. Immunoblots using the antibody against GFP demonstrated the presence FFA2 receptor with a molecular mass at approximately 70-kDa in all samples (Figure 5.2A). Immunoblotting anti-pSer<sup>296</sup>/Ser<sup>297</sup> FFA2 detected phosphorylated form of hFFA2-DREADD-eYFP in the samples treated with 10  $\mu$ M, 50  $\mu$ M and 100  $\mu$ M of MOMBA (Figure 5.2B). However, anti-pThr<sup>306</sup>/Thr<sup>310</sup> hFFA2 only identified phosphorylated in hFFA2-DREADD



## Chapter 5

samples treated with high concentration of MOMBA (50  $\mu\text{M}$  and 100  $\mu\text{M}$ ), but not in sample treated with 10  $\mu\text{M}$  of MOMBA (Figure 5.2C). The results suggested that MOMBA induced phosphorylation of hFFA2-DREADD in a concentration-dependent manner. Detection of these polypeptides also in the vehicle-treated samples might reflect constitutive phosphorylation of hFFA2-DREADD (Figure 5.2B). Immunoblotting with anti-pThr<sup>306</sup>/Thr<sup>310</sup> hFFA2 demonstrated no constitutive phosphorylation on the residues of Thr<sup>306</sup> and Thr<sup>310</sup> (Figure 5.2C).

For other samples treated with FFA2 agonists 4-CMTB and AZ1729, immunoblotting with anti-pSer<sup>296</sup>/Ser<sup>297</sup> hFFA2 identified a lower phosphorylation level produced by 4-CMTB and AZ1729 (Figure 5.2B). Anti-pThr<sup>306</sup>/Thr<sup>310</sup> hFFA2 only detected low level of phosphorylation in sample treated with 4-CMTB (Figure 5.2C). However, when treating cells with a combination of MOMBA and 4-CMTB or AZ1729, either anti-pSer<sup>296</sup>/Ser<sup>297</sup> hFFA2 or anti-pThr<sup>306</sup>/Thr<sup>310</sup> hFFA2 increased phosphorylation level of hFFA2-DREADD than the samples treated with 4-CMTB or AZ1729 (Figure 5.2B, C), which suggested the phosphorylation of hFFA2-DREADD on Ser<sup>296</sup>/Ser<sup>297</sup> and Thr<sup>306</sup>/Thr<sup>310</sup> was increased when 4-CMTB or AZ1729 cooperated with MOMBA.

## Chapter 5

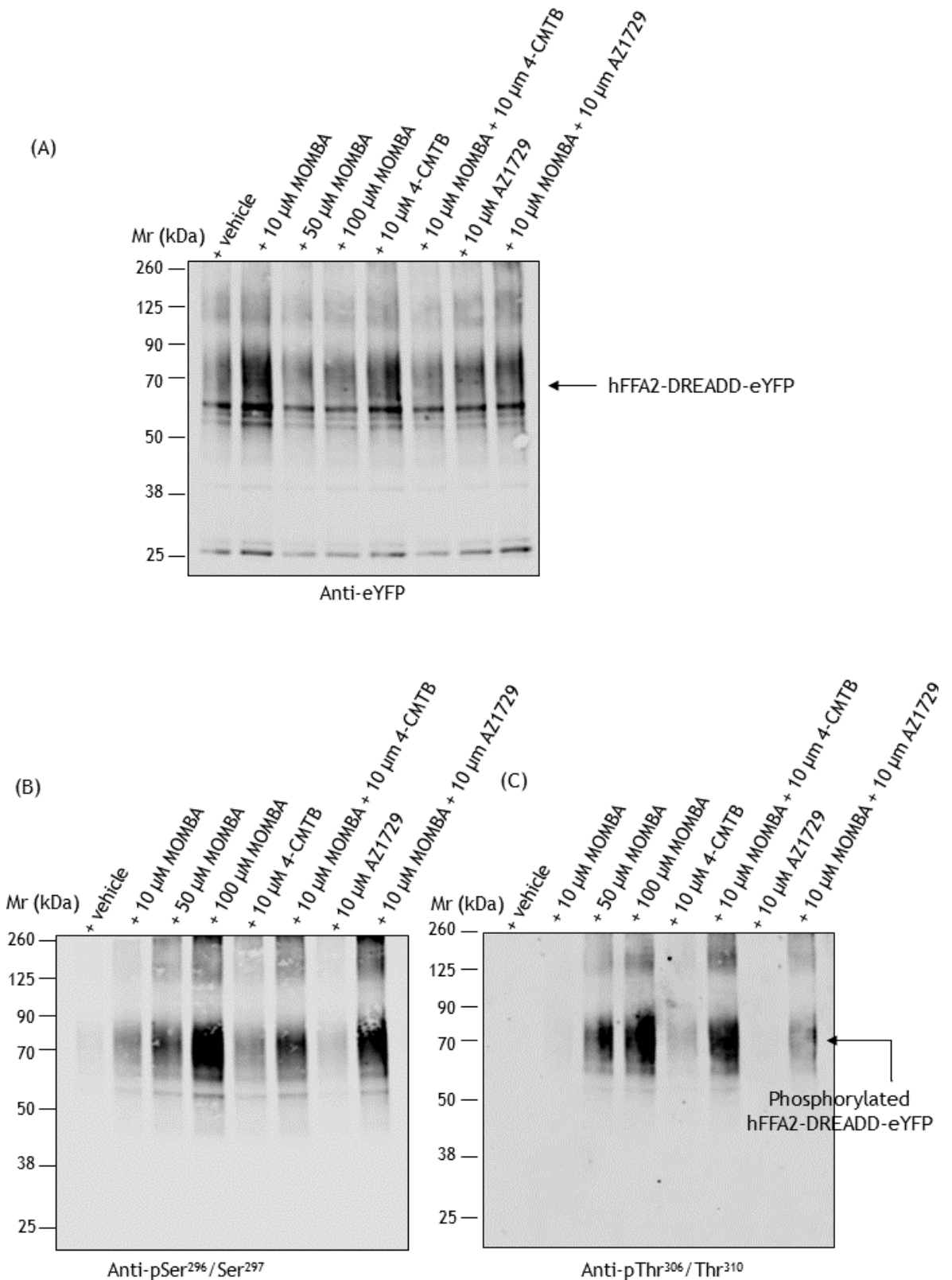


**Figure 5.2 Identification of agonist regulation of hFFA2-DREADD phosphorylation status using phospho-site specific antibodies.**

Flp-In TREx 293 cells induced to express hFFA2-DREADD-eYFP were stimulated with FFA2 activators (10 $\mu$ M) or 0.1% DMSO as a vehicle control for 5 minutes at 37°C. The receptors were purified by immunoprecipitation using GFP-trap. Proteins were separated by 4-12% SDS-PAGE and analysed by western blot analysis. All antibodies were used at 1:1000 dilution. Molecular mass of

## Chapter 5

hFFA2-DREADD-eYFP is approximately 70kDa. (A) Representative western blot of anti-GFP showed the expression of hFFA2-DREADD-eYFP (B) Representative western blot of anti-pSer<sup>296</sup>/Ser<sup>297</sup> hFFA2 identified hFFA2-DREADD-eYFP phosphorylation induced by agonists. (C) Representative western blot of anti-pThr<sup>306</sup>/Thr<sup>310</sup> hFFA2 identified hFFA2-DREADD-eYFP phosphorylation induced by agonists. (n=3)

The antibody anti-pThr<sup>306</sup>/Thr<sup>310</sup> hFFA2 was also capable of identifying MOMBA activated hFFA2-DREADD in immunocytochemical studies. The data is referenced from immunocytochemical studies made by Natasja Barki, because of the insufficient time to finish immunocytochemical in hFFA2-DREADD-eYFP cells. Flp-In TREx 293 cells transiently transfected with human FFA2-DREADD with HA tag was induced by doxycycline. Antibody against HA was used to assess the expression of the receptor. A lack of anti-HA staining of cells without doxycycline treatment showed that there was no hFFA2-DREADD-HA expressed in these cells (Figure 5.3 -dox). The antibody anti-pThr<sup>306</sup>/Thr<sup>310</sup> hFFA2 illuminated agonist-treated cells and merging of images of the antibody staining with those of the location of the HA tag showed strong overlap (Figure 5.3 +dox MOMBA). Anti-pThr<sup>306</sup>/Thr<sup>310</sup> hFFA2 staining was not observed in cells without MOMBA treatment (Figure 5.3 +dox basal), which indicated the specificity of the anti-pThr<sup>306</sup>/Thr<sup>310</sup> hFFA2 recognition of the phosphorylated form of hFFA2-DREADD.

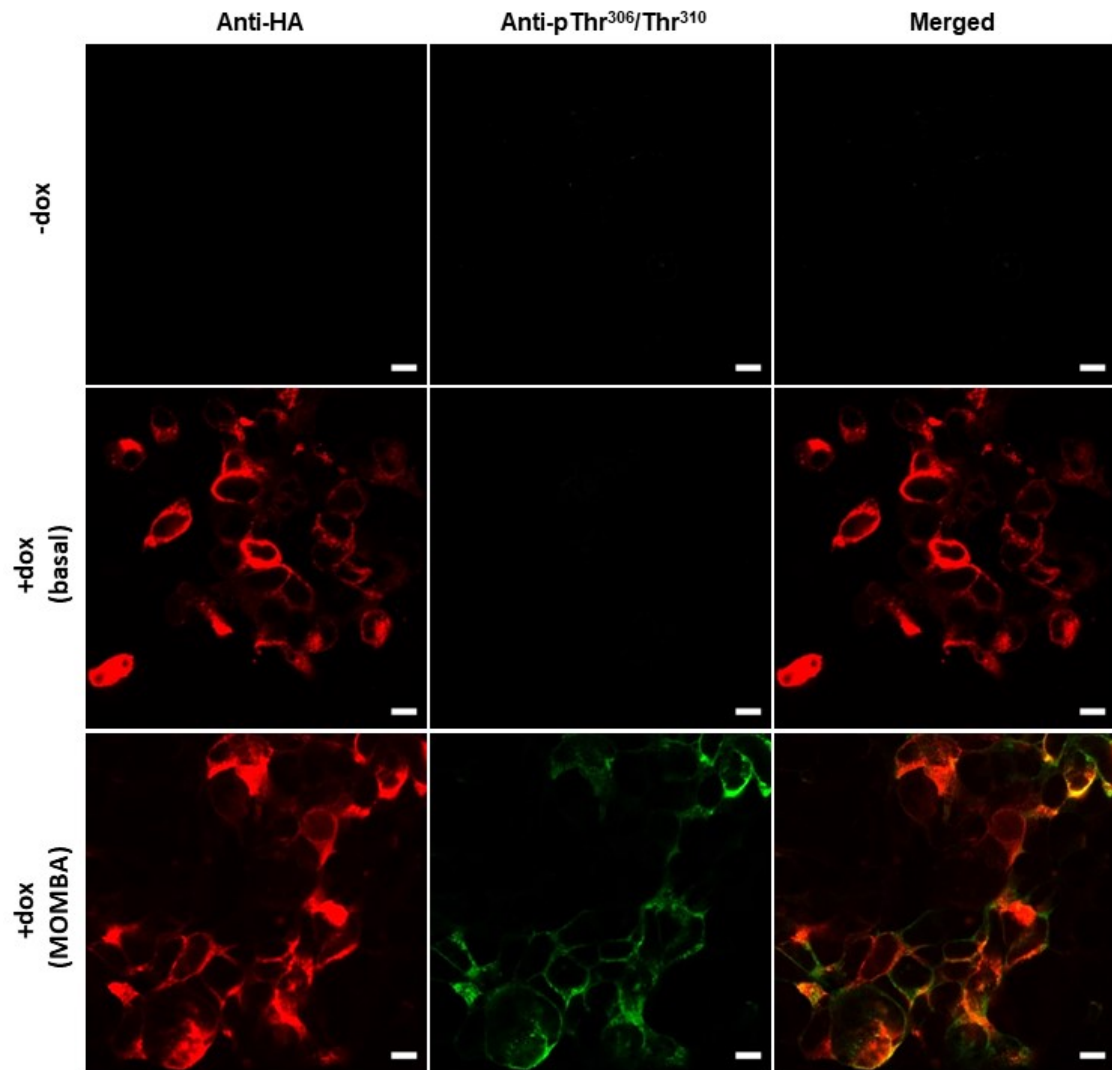


**Figure 5.3 Phosphorylated hFFA2-DREADD is identified in immunocytochemical studies.** Flp-In TREx 293 cells stably expressing human FFA2-DREADD with HA tag were grown on coverslips. Cells were induced with doxycycline (+dox basal and MOMBA) and were treated with MOMBA (100  $\mu$ M, 5 minutes). After fixation, cells were treated with the phospho-specific antibody pThr<sup>306</sup>/Thr<sup>310</sup> hFFA2; green, Anti-pThr<sup>306</sup>/Thr<sup>310</sup> hFFA2; and red, Anti-HA. Scale bar =10  $\mu$ m (Referenced from Natasja Barki's result)

## 5.2.2 Investigation of phosphorylation status of FFA2 *ex vivo*

### 5.2.2.1 Investigation of phosphorylation status of hFFA2-DREADD using anti-pSer<sup>296</sup>/Ser<sup>297</sup> hFFA2 and anti-pThr<sup>306</sup>/Thr<sup>310</sup> hFFA2 in Peyer's patches and mesenteric lymph nodes.

To study the phosphorylation of FFA2 in immune cells, we studied Peyer's patches and mesenteric lymph nodes (MLNs). Large number of immune cells are found in both of these lymphoid organs associated with the gastrointestinal tract. Peyer's patches (PP) are lymphoid follicles scattered throughout the small intestine. The location of peyer's patches is shown as Figure 5.4. They are considered as the immune sensors of the intestine, involved in responses toward

## Chapter 5

gut antigens and bacteria (Jung et al., 2010). By contrast, mesenteric lymph nodes are embedded inside the mesentery between the small and large intestine. They play an important role in inducing tolerance to food proteins and prevent intestinal microbes from penetrating the systemic immune system (Macpherson and Smith, 2006).

To evaluate whether our hFFA2-DREADD-HA mice express the receptor in Peyer's patches and MLNs, an antibody against HA was used. Following lysate preparation and receptor immunoprecipitation with anti-HA affinity matrix beads, the sample was separated and transferred by electrophoresis. The resulting immunoblot was probed using an anti-HA antibody. Cre-Minus mice (Bolognini et al., 2019) were used as negative control, because although the receptor at the same genetic locus, its expression has not been induced and hence they do not express hFFA2-DREADD-HA (Figure 5.5A, B). The expression of hFFA2-DREADD-HA in mice was confirmed by immune blots, which showed the presence of similar levels of receptor protein in all samples from hFFA2-DREADD-HA mice. (Figure 5.5A, B).

The next step was to study the phosphorylation of hFFA2-DREADD-HA *ex vivo*. In order to do this, Peyer's patches and MLNs were treated either with vehicle (0.1% DMSO), MOMBA (100  $\mu$ M) or MOMBA (100  $\mu$ M) + CATPB (10  $\mu$ M). Immunoblot using anti-pSer<sup>296</sup>/Ser<sup>297</sup> hFFA2 showed that it failed to identify the phosphorylation residues on sites Ser<sup>296</sup> and Ser<sup>297</sup>, which suggested these two sites did not become phosphorylated on receptor activation by MOMBA in Peyer's patches (Figure 5.5C). Anti-pThr<sup>306</sup>/Thr<sup>310</sup> hFFA2, however, identified the phosphorylation after addition of MOMBA (Figure 5.5D). But when the tissues were pre-treated with CATPB anti-pThr<sup>306</sup>/Thr<sup>310</sup> hFFA2 also failed to identify the phosphorylation (Figure 5.5D), which suggested CATPB inhibited the activation of the receptor.

## Chapter 5

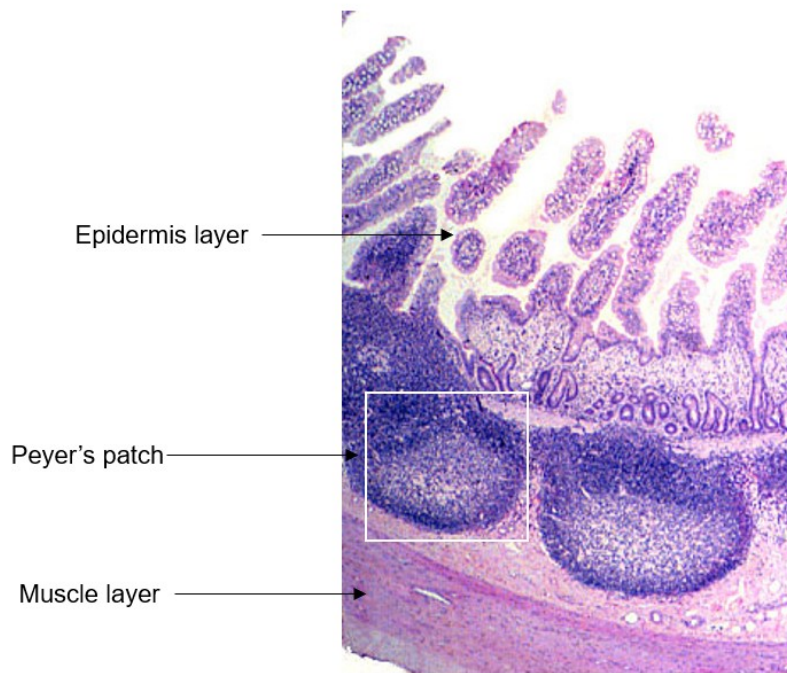


**Figure 5.4 Histology slice of small intestine in cross section**

Arrows show the muscle layer, Peyer's patches (white square) and epidermis layer. (Adopt from <https://www.toppr.com/guides/biology/human-body/peyers-patches/>)

## Chapter 5

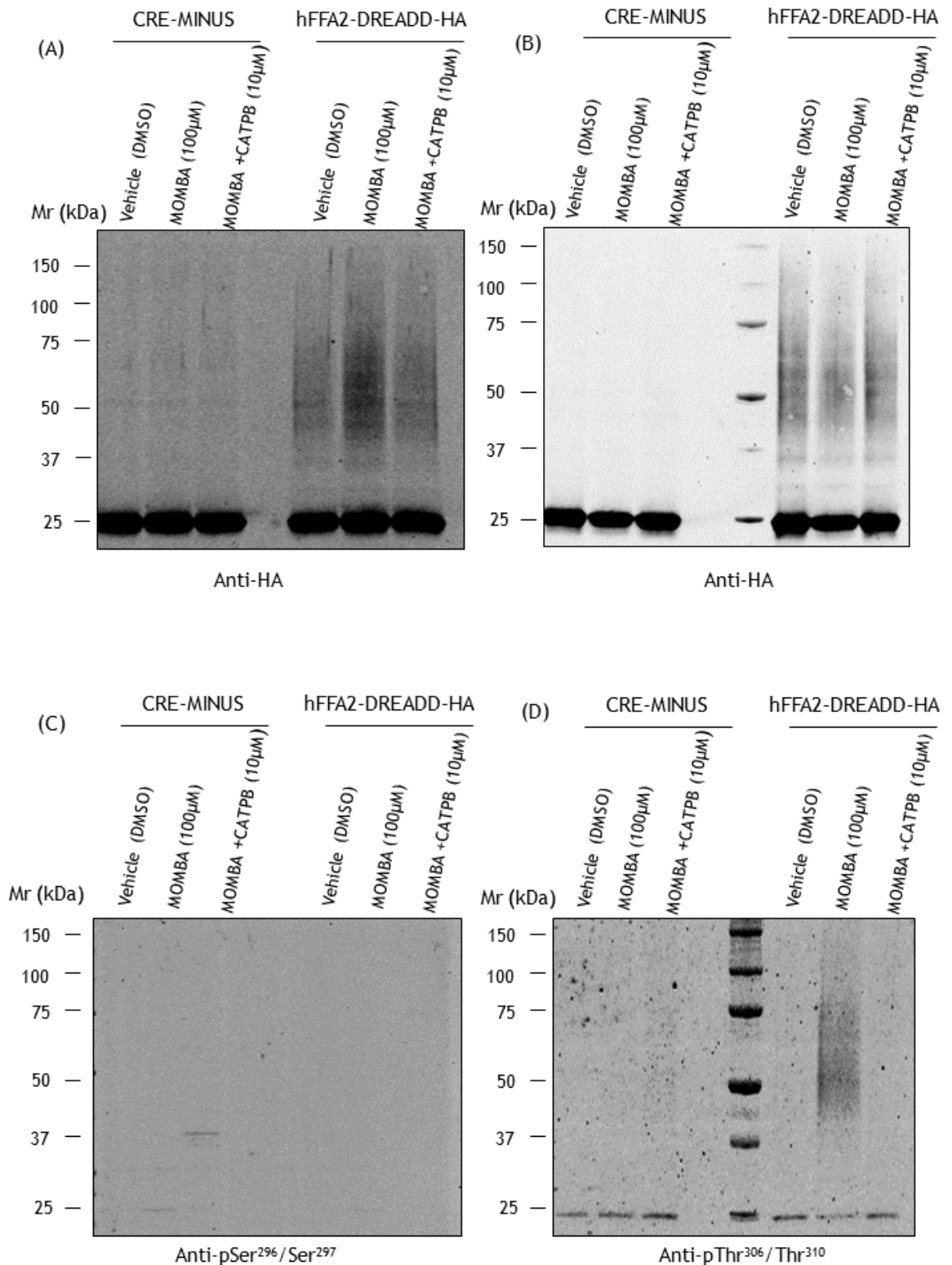


**Figure 5.5 Identification of agonist regulation of hFFA2-DREADD-HA phosphorylation status in Peyer's patches and MLNs using phospho-specific antibodies.**

Peyer's patches from FFA2 Cre-Minus mice and hFFA2-DREADD-HA mice were homogenised after treatment with vehicle (0.1% DMSO), MOMBA (100 μM) or a combination of MOMBA (100 μM) and CATPB (10 μM) for 20 minutes, and immunoprecipitated with anti-HA affinity matrix overnight. Proteins were separated by 4-12% SDS-PAGE and analysed by western blot. All antibodies were

## Chapter 5

used at 1:1000 dilution. (A) and (B) Antibody against HA was used to assess the expression of hFFA2-DREADD-HA in Peyer's patches. (A) and (C) were run parallelly, and (B) and (D) were run parallelly. (n=3) (C) Antibody anti-pSer<sup>296</sup>/Ser<sup>297</sup> was used to assess the phosphorylation status of hFFA2-DREADD-HA. (D) Antibody anti-pThr<sup>306</sup>/Thr<sup>310</sup> was used to assess the phosphorylation status of hFFA2-DREADD-HA.

### 5.2.2.2 Investigation of phosphorylation status of FFA2-DREADD using anti-pSer<sup>296</sup>/Ser<sup>297</sup> FFA2 and anti-pThr<sup>306</sup>/Thr<sup>310</sup> FFA2 in white adipose tissue

Different outcomes were observed in white adipose tissue. Immunoblot using an anti-HA antibody demonstrated the expression of the receptor in hFFA2-DREADD-HA mice (Figure 5.6A). Both anti-pSer<sup>296</sup>/Ser<sup>297</sup> and anti-pThr<sup>306</sup>/Thr<sup>310</sup> hFFA2 identified the phosphorylation in the presence of MOMBA (Figure 5.6B, C), meanwhile, the immunoblot demonstrated that there was also constitutive phosphorylation on residues of anti-pSer<sup>296</sup>/Ser<sup>297</sup> hFFA2 (Figure 5.6B). Anti-pThr<sup>306</sup>/Thr<sup>310</sup> hFFA2 failed to identify constitutive phosphorylation of FFA2 (Figure 5.6C). FFA2 antagonist CATPB also showed the ability to inhibit the activation of the receptor by MOMBA in white adipose tissue (Figure 5.6B). Although samples treated with agonist showed more banding with anti-HA than other two (Figure 5.6A), it was still suspicious that the increase was caused by MOMBA. All antibodies failed to identify the receptor in the tissue from Cre-Minus mice (Figure 5.6A).



## Chapter 5

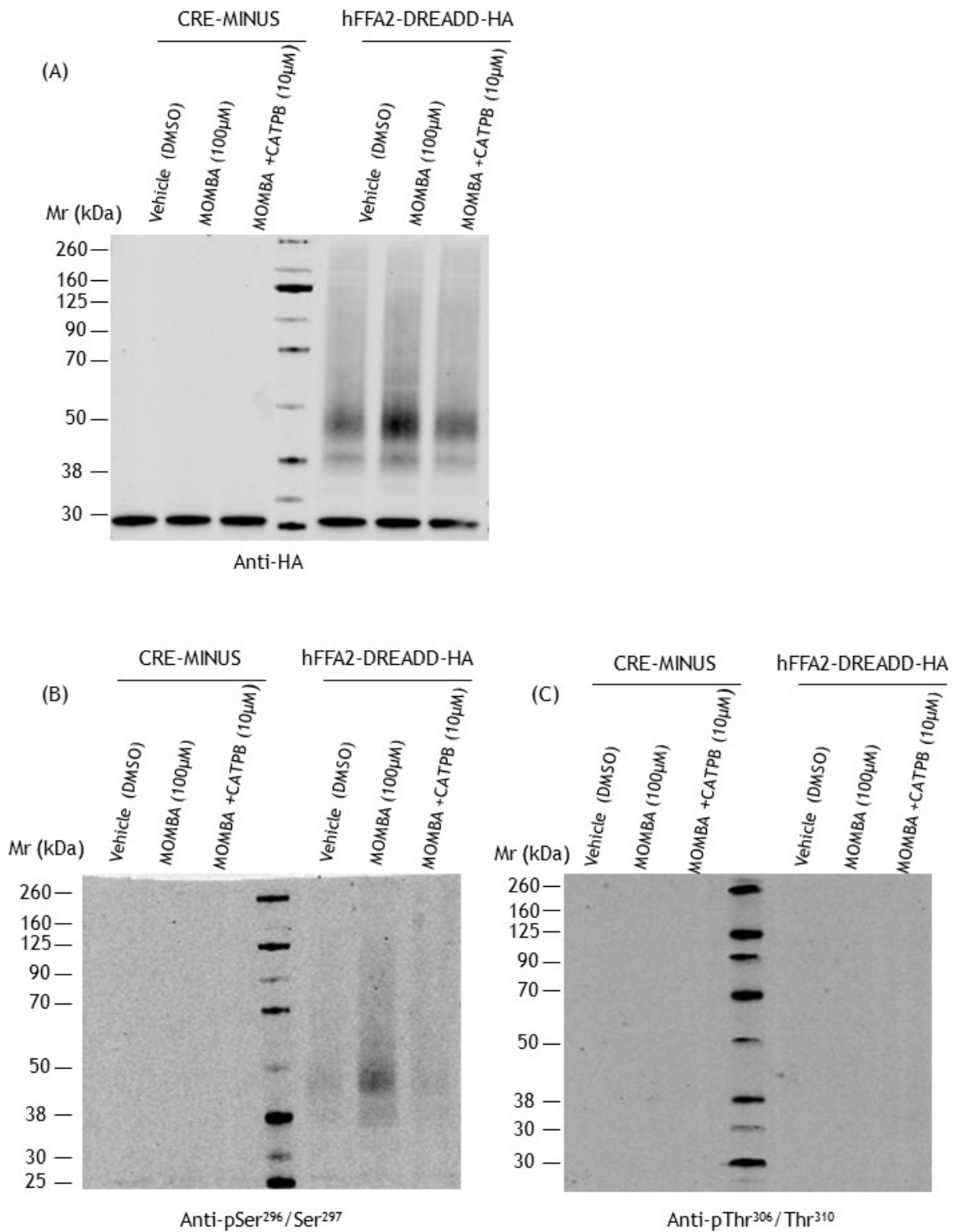


**Figure 5.6 Identification of agonist regulation of hFFA2-DREADD-HA phosphorylation status in white adipose tissue using phospho-specific antibodies.**

White adipose tissue from Cre-Minus mice and hFFA2-DREADD-HA expressing mice were homogenised after treatment with vehicle (0.1% DMSO), MOMBA (100  $\mu$ M) or a combination of MOMBA (100  $\mu$ M) and CATPB (10  $\mu$ M) for 20 minutes, and immunoprecipitated with anti-HA affinity matrix overnight. Proteins were separated by 4-12% SDS-PAGE and analysed by western blot

## Chapter 5

analysis. All antibodies were used at 1:1000 dilution. (A) Antibody against HA was used to assess the expression of hFFA2-DREADD-HA in white adipose tissue. B) Antibody anti-pSer<sup>296</sup>/Ser<sup>297</sup> was used to assess the phosphorylation status of hFFA2-DREADD-HA. (C) Antibody anti-pThr<sup>306</sup>/Thr<sup>310</sup> was used to assess the phosphorylation status of hFFA2-DREADD-HA.

### 5.2.2.3 Investigation of phosphorylation status of FFA2-DREADD-HA using anti-pSer<sup>296</sup>/Ser<sup>297</sup> hFFA2 and anti-pThr<sup>306</sup>/Thr<sup>310</sup> hFFA2 in colonic epithelium

The colonic epithelium was also used to characterise the phosphorylation status of FFA2-DREADD-HA. Immunoblots showed that in the colonic epithelium from hFFA2-DREADD-HA mice, both anti-pSer<sup>296</sup>/Ser<sup>297</sup> and anti-pThr<sup>306</sup>/Thr<sup>310</sup> FFA2 identified phosphorylation of FFA2 induced by MOMBA. However, the phosphorylation level was limited (Figure 5.7B, C). Neither anti-pSer<sup>296</sup>/Ser<sup>297</sup> or anti-pThr<sup>306</sup>/Thr<sup>310</sup> FFA2 were able to identify phosphorylation in the presence of CATPB (Figure 5.7B, C). The constitutive phosphorylation on Ser<sup>296</sup> and Ser<sup>297</sup> sites also identified by anti-pSer<sup>296</sup>/Ser<sup>297h</sup> FFA2 (Figure 5.7B), which was consistent with the result observed in adipose tissue. The expression of hFFA2-DREADD was demonstrated by anti-HA, which was not influenced by the agonist or antagonist. All antibodies failed to identify the receptor in the tissue from Cre-Minus mice (Figure 5.7A).

## Chapter 5

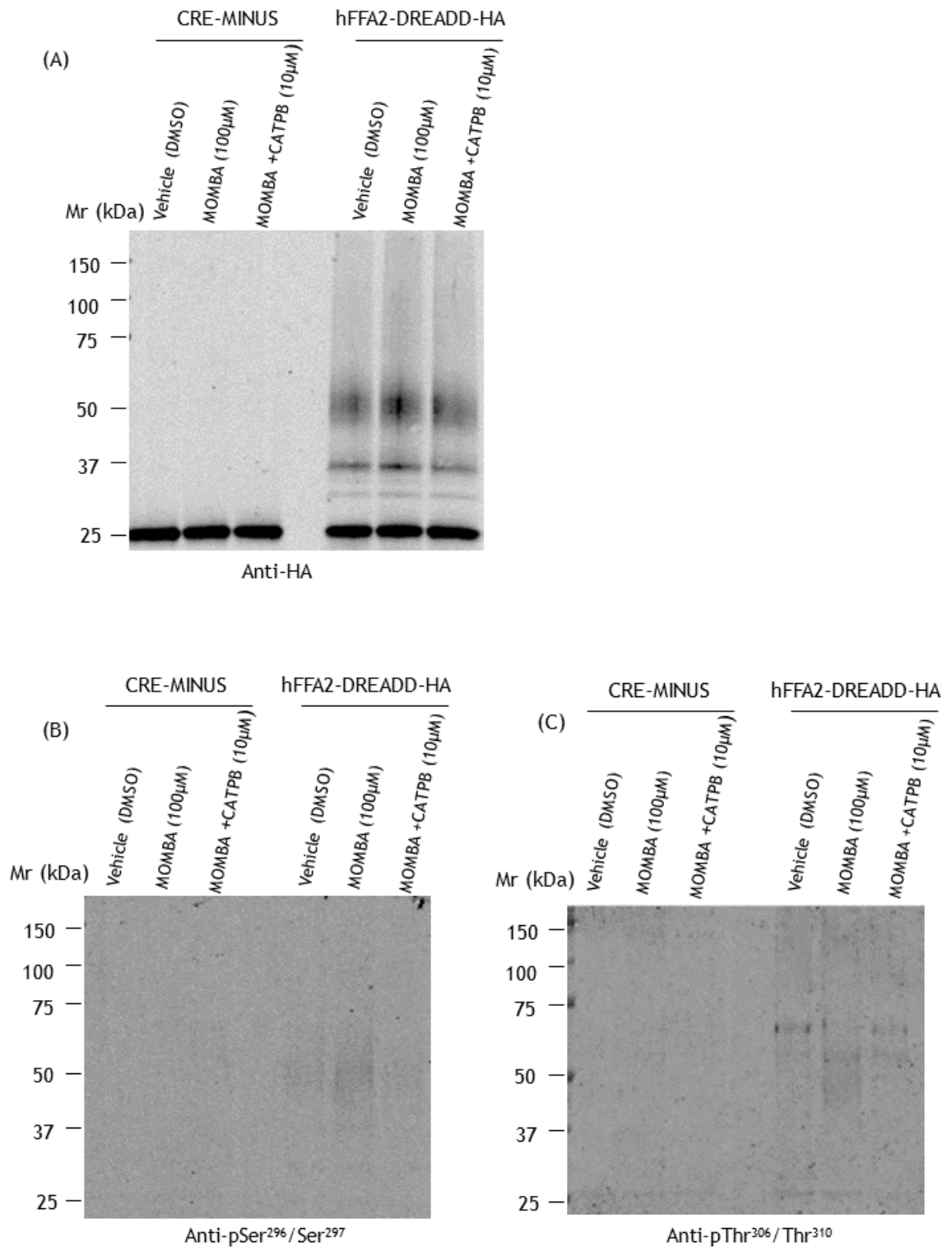


**Figure 5.7 Identification of agonist regulation of hFFA2-DREADD phosphorylation status in colonic epithelium using phospho-specific antibodies.**

The colonic epithelium from Cre-Minus mice and hFFA2-DREADD-HA expressing mice were homogenised after treatment with vehicle (0.1% DMSO), MOMBA (100  $\mu$ M) or a combination of MOMBA (100  $\mu$ M) and CATPB (10  $\mu$ M) for 20 minutes, and immunoprecipitated with anti-HA affinity matrix overnight. Proteins were separated by 4-12% SDS-PAGE and analysed by western blot analysis. All antibodies were used at 1:1000 dilution. (A) Antibody against HA was used to assess the expression of hFFA2-DREADD-HA in colonic epithelium. (B) Antibody anti-pSer<sup>296</sup>/Ser<sup>297</sup> was used to assess the phosphorylation status of hFFA2-DREADD-HA. (C) Antibody anti-pThr<sup>306</sup>/Thr<sup>310</sup> was used to assess the phosphorylation status of hFFA2-DREADD-HA.

### 5.3 Discussion

As GPCRs respond to various stimuli and are involved in many physiological processes they have attracted a lot of interest in drug discovery (Insel et al., 2019). One of the barriers however to the drug-discovery process is to determine the activation status of GPCRs in vivo following agonist/drug stimulation. Whereas techniques such as fluorescent resonance energy transfer (FRET) can be used to monitor receptor conformational changes in response to ligand occupation these approaches are restricted to in vitro systems (Ziegler et al., 2011, Hudson et al., 2012a, Malik et al., 2013, Venkatakrishnan et al., 2013). Our results have successfully detected agonist-mediated phosphorylation of hFFA2-DREADD in tissues opening the prospect that these antibodies could be used to assess the activated state of FFA2 in vivo. In comparable studies. the activation status of the M1 mAChR was monitored with phosphor-specific antibodies that linked receptor activation with receptor-mediated regulation of learning and memory (Butcher et al., 2016). The next step for the studies described here will be to test whether anti-pSer<sup>296</sup>/Ser<sup>297</sup> and anti-pThr<sup>306</sup>/Thr<sup>310</sup> to FFA2 can be used to monitor the activation state (i.e., phosphorylation status) of the receptor in vivo following drug administration. If this were the case, then it might be possible to correlate the activation status of FFA2 with physiological responses, which can be used in the assessment of receptor engagement with synthetic ligands.

A complementary approach to the one described here has emerged from a recent study that combined a DREADD with positron emission tomography (PET) to provide a means for non-invasive confirmation of receptor expression and function (Bonaventura et al., 2019). PET is a molecular imaging modality that enables in vivo exploration of metabolic processes. This technique has been utilized in the assessment of a wide range of physiologic and pathologic conditions (Colom et al., 2019). Bonaventura et al. (2019) have firstly developed a high-affinity <sup>18</sup>F-labeled DREADD PET ligand, and observed strong somatic signalling of receptor expression from the new PET ligand in vivo. This suggests another way to detect activated FFA2 by developing agonist radiotracers for PET. Our results and previous study have shown that MOMBA is a highly selective agonist of hFFA2-DREADD (Barki et al., 2022), which can be used as a material of

## Chapter 5

agonist radiotracer. Additionally, isotope  $^{11}\text{C}$  also widely used in PET ligands (Colom et al., 2019), which is able to replace carbon atoms in MOMBA.

In this chapter the immunoblotting studies performed on lysates of hFFAR2-DREADD- eYFP cells showed that the antibodies Thr<sup>306</sup>/Thr<sup>310</sup> and Ser<sup>296</sup>/Ser<sup>297</sup> were able to identify the phosphorylation of hFFAR2- DREADD- eYFP in a sensitive and agonist activation- dependent manner. I also find that cooperation between MOMBA and 4-CMTB or AZ1792 on hFFA2-DREADD. To show tissue-selective phosphorylation of the tissues (peyer's patches, white adipose tissues, colonic epithelium) from hFFAR2- DREADD mouse. The expression of the receptor was identified by HA tag added to the C- terminus of the receptor. it is observed that the phosphorylation of Ser<sup>296</sup>/Ser<sup>297</sup> increased in white adipose tissues and colonic epithelium with agonist treatment. For residues Thr<sup>306</sup>/Thr<sup>310</sup>, agonist regulated phosphorylation was observed in peyer's patches and colonic epithelium, but not in white adipocytes. Moreover, although the expression level of the receptor was equivalent in three tissues, the phosphorylation of those sites was lower in colonic epithelial than other two tissues. The results present in this chapter have demonstrated that phospho-sites Thr<sup>306</sup>, Thr<sup>310</sup> in hFFA2-DREADD can be phosphorylated in an agonist-dependent manner in both a heterologous cells line. Additionally, phospho-sites Ser<sup>296</sup> and Ser<sup>297</sup> show constitutive phosphorylation without agonist activation, however, evidence from mass spectrometry indicates that this only occurs at Ser<sup>297</sup> (personal communication Dr Louis Dwomoh). However, recent study from (Barki et al., 2023) showed different result from mine. They observed that agonis-enhanced phosphorylation on Thr<sup>306</sup>/Thr<sup>310</sup> and Ser<sup>296</sup>/Ser<sup>297</sup> were both identified by the antibodies. It is likely because that the aliquot of anti- Ser<sup>296</sup>/Ser<sup>297</sup> expired when I used.

Flp-In TReX 293 cells stably expressing human FFA2-DREADD with eYFP tag were used in western blot analysis. In hFFA2-DREADD-eYFP cells, the transfected gene integrated into the genome, therefore, it was replicated and stably expressed. To make the expression and phosphorylation of hFFA2-DREADD visible the same cell type should have used. However, because of the time limited, immunocytochemistry data is referenced from Natasja Barki's result. The cells used in immunohistochemistry were Flp-In TReX 293 cells transiently transfected

## Chapter 5

with human FFA2-DREADD with HA tag. These cells rapidly expressed hFFA2-DREADD in the short term, but would lose the transfected gene in several days with the growth and division of cells. In addition, high copy number transfected genetic material in cells occurs in transient transfection resulting in overexpression of target gene. Given the difference between hFFA2-DREADD-eYFP cells and hFFA2-DREADD-HA cells, immunohistochemistry in hFFA2-DREADD-eYFP cells still need to be finished.

## Chapter 6 Final discussion

GPCRs are substantially involved in human pathophysiology and respond to a wide variety of different stimuli, which makes them the most interesting drug target in a long time. Currently, approximately 174 GPCRs are considered as drug targets, and a total of 481 GPCR drugs have been approved by the FDA (Hauser et al., 2017, Sriram and Insel, 2018) (<https://gpcrdb.org/> accessed on May 15, 2023). Previous studies have suggested that identifying specific GPCR phosphorylation status may be a mechanism to diversify potential signalling outcomes (also known as phosphorylation bar-codes). Therefore, determining the phosphorylation status of GPCRs is crucial for understanding the receptor physiology and signalling properties of GPCRs.

Various tools such as mass spectrometry, Isotopic labeling and western blot analysis have primarily been utilized for the analysis of structural changes that occur with different protein modifications (Delom and Chevet, 2006). Mass spectrometry determines multiple phosphorylation modification sites and levels. Isotope  $^{32}\text{P}$  has been widely used in marking detected protein phosphorylation sites and individual protein phosphorylation. Compared to the methods mentioned previously, western blot has strong specificity and high resolution and its experimental conditions can be achieved easily. The phosphorylated antibodies make it more easily achievable to investigate phosphorylation of the receptors. However, phospho-specific antibodies are difficult to produce and often of poor discriminative quality. Previous studies have generated antibodies predicted to specifically identify phosphorylation of both Thr<sup>347</sup> and Ser<sup>350</sup> of the receptor, or only of Ser<sup>350</sup>, but these antibodies had a limited range of applications (Butcher et al., 2014, Prihandoko et al., 2016). Here, this thesis also characterised novel phospho-specific antibodies agonist FFA4 and FFA2, which have been already developed into commercial antibodies. Our data showed the profile of FFA4 and FFA2 using phospho-specific antibodies. These results illustrated that the novel antisera could be useful tools to profile agonist properties of novel GPCR ligands and identify relevant kinases and phosphatases for GPCR phosphorylation.

Since deorphanisation of FFA4 was revealed in 2005, it has been considered as a potential drug target for metabolic diseases as it is involved in regulation of

## Chapter 6

glucose stimulated insulin release and glucagon secretion (Hirasawa et al., 2005, Suckow et al., 2014, Sundström et al., 2017, Carullo et al., 2021). Moreover, FFA4 participates in pathophysiological regulation of lung function (Prihandoko et al., 2020). In previous studies, the residues Thr<sup>347</sup>, Ser<sup>350</sup> and Ser<sup>357</sup> in the C-terminal tail were likely sites of modification (Burns et al., 2014). These studies were rapidly complemented by Butcher et al. (2014). By using combinations of mass spectrometry, mutagenesis, and the development of phospho-site specific antibodies, they showed that each of Thr<sup>347</sup>, Thr<sup>349</sup>, Ser<sup>350</sup>, Ser<sup>357</sup>, and Ser<sup>360</sup> in the C-terminal tail of human FFA4 became phosphorylated in response to the synthetic FFA4 agonist TUG-891 when the receptor was expressed in either CHO or HEK 293 cells (Butcher et al., 2014). These results are extended that the FFA4 agonist TUG-891 induced phosphorylation on specific sites on hFFA4. Data presented in this thesis have shown that two phospho-antibodies, recognising phosphorylation at Thr<sup>347</sup>, Thr<sup>349</sup> and Ser<sup>350</sup> determine that these sites are phosphorylated in an agonist-dependent manner.

GPCRs are used to considered function solely as monomeric receptor, however, evidence for GPCR dimerization and oligomerization has been accumulating that challenges the idea. Dimerization is considered essential for class C GPCR activity (Kniazeff et al., 2011), and class A GPCR are also observed to form oligomers. Early researches have illustrated that oligomers participate in GPCR signalling, ligands binding, and related to cell surface delivery (Ferré et al., 2014). Dimerization of the GPCR regulated by receptor density and multiple dimer conformations co-exist and interconvert. (Calebiro et al., 2013, Dijkman et al., 2018). In this thesis, unknown proteins were observed on immunoblots. This may be an explain of the unstable expression of proteins which were considered as dimers in immunoblots. Recent study from Liu et al. (2022) demonstrated biased signaling in GPCR can be influenced by receptor oligomerization, and the biased ligand binding and signaling observed from GPCR oligomers has important pharmacological implications. The different physiological functions between oligomers and monomers suggest new clinical drug targets. In this thesis, the results presented here demonstrate that human FFA4 may exist as a higher oligomer based on the presence of high molecular weight forms of the receptor in western blots. As mentioned in section 3.3, Native-Page would be helpful on confirmation of these higher order states.



## Chapter 6

A recent study created a panel of eleven combinatorial HEK293 GRK knockout clones, were able to be analysed the GRK contribution to GPCR phosphorylation, recruitment of  $\beta$ -arrestin1 and 2, as well as receptor internalisation in unprecedented detail. Analysis of  $\beta$ -arrestin1/2 interactions on HEK293 knockout cell clones lacking GRK2/3/5/6 showed that there are two main GRK subsets: GRK2/3-regulated and GRK2/3/5/6-regulated receptor phosphorylation (Drube et al., 2022). The question of which GRKs are responsible for FFA4 phosphorylation was addressed using selective GRK inhibitors. These studies showed that GRK6 mediated homologous phosphorylation of FFA4 receptor. This is consistent with previous studies where DHA-mediated FFA4 phosphorylation was significantly reduced in cells treated with GRK6-targeting siRNA (Burns et al., 2014). Our results also showed that the potent GRK6 inhibitor compound 19 prevented FFA4 phosphorylation on Thr<sup>349</sup>/Ser<sup>350</sup> and also inhibited  $\beta$ -arrestin2 recruitment. Interestingly, Drube et al. (2022) still encountered measurable  $\beta$ -arrestin2 recruitment in the absence of GRKs. This could be explained by the inherent affinity of  $\beta$ -arrestin-2 towards ligand-activated, yet unphosphorylated, GPCRs. These results are consistent with a previous study, which displayed that mutating phosphorylation sites individually had little impact on  $\beta$ -arrestin 2 recruitment whereas mutating all phosphorylation sites significantly reduced arrestin-recruitment (Butcher et al., 2014). This suggests that  $\beta$ -arrestin recruitment to FFA4 is dependent on multiple phosphorylation events a notion supported by studies where combining phosphorylation site mutations, as well as structural mutations, was necessary to almost entirely reduce  $\beta$ -arrestin recruitment (Butcher et al., 2014). In my studies the combination of GRK6 and GRK2/3 inhibitors, similarly almost entirely prevented  $\beta$ -arrestin-2 recruitment. Previous studies have been identified that receptors that are functionally phosphorylated by GRK2, 3, 5, and 6 or GRK2 and 3 (Drube et al., 2022). As our results showed that the single application of potent GRK6 inhibitors or GRK2/3 inhibitor were hardly to prevented FFA4 phosphorylation on Thr<sup>347</sup>, it is worth trying to use both GRK2/3 and 6 inhibitors to treat hFFA4-eYFP cells and analyse the results by western blot.

It is indicated that GRK6 was largely responsible for FFA4 homologous phosphorylation mediated by DHA, by using a knockdown strategy in HEK 293 cells. The DHA-mediated heterologous phosphorylation was indicated to be

## Chapter 6

regulated by PKA (Burns et al., 2014). However, the addition of PKC inhibitor did not decrease the levels of TUG-891-dependent phosphorylation in HEK 293 cells, which suggested that agonist-dependent phosphorylation was not PKC-mediated (Butcher et al., 2014). These results probably reflect that agonist-dependent phosphorylation of FFA4 is mediated by one or more GRKs. Our results showed that GRK6 inhibitor (compound 19) decreased TUG-891-dependent phosphorylation in HEK293 cells which expressed human FFA4 receptor, which suggested that agonist-dependent phosphorylation of FFA4 is mediated by GRK6. In another receptor, FFA1 from LCFA family is observed that agonists promote FFA1 phosphorylation at multiple sites in the C-terminus (Guzman-Silva et al., 2022). FFA1 phosphorylated in response to agonist and PKC activation which is similar to what was observed for FFA4 (Sosa-Alvarado et al., 2015). Although both FFA1 and FFA4 are phosphorylated in response to PKC activation, neither is clearly desensitized (Sánchez-Reyes et al., 2014).

Agonist-activated receptors are rapidly internalised into the intracellular membrane compartments of cells, which plays an important role in the regulation of receptor signalling and desensitisation (Ferguson, 2001). Here, immunocytochemistry was utilized to observe the internalisation of hFFA4-eYFP. The images illustrate colocalization of anti-pThr<sup>349</sup>/Ser<sup>350</sup> FFA4 and eYFP, which demonstrates the distribution of phosphorylated FFA4 in cells. These images display FFA4 internalization with long-time exposure to TUG-891. Similar observations have been made in West blot analysis. Our results have shown that FFA4 is regulated by agonist and antagonist in a time-dependent pattern. However, the kinetics of phospho-specific sites Thr<sup>347</sup> and Thr<sup>349</sup>/Ser<sup>350</sup> are not always identical, which may suggest that phosphorylation on different site can dictate the regulation of FFA4 signalling differentially. This surmise has been proved by a study on CXCR4 which showed that phosphorylation at different phosphor-sites occurs with disparate kinetics using phospho-specific antibodies (Busillo et al., 2010). This was proved by the phosphorylation of hFFA2-DRAEDD *ex vivo*.

Because activated GPCRs undergo active conformation and are involved in intracellular signalling, they have attracted a lot of interest in the drug discovery field (Venkatakrisnan et al., 2013, Insel et al., 2019). However,

## Chapter 6

detecting the activation status of the receptor is still challenging. A previous study has linked the activation status of the M1 mAChR to memory acquisition by measuring the phosphorylation status of the receptor using phospho-site specific antibodies (Butcher et al., 2016). Hence, we determined to test whether the phospho-sites specific antibodies were able to detect phosphorylation *in vivo*. The first step was applying the antibodies in tissues.

To apply the antibodies to animal tissues, we tested the expression in lung tissue, which shows the highest level of FFA4 expression (Moniri, 2016). However, the antibody against HA probed limited expression of FFA4-HA, which was unexpected. Considering our lab has received phospho-specific antibodies against hFFA2, we turned to investigate the phosphorylation status of FFA2. First, we confirmed the expression of hFFA2-DREADD in Flp-in 293 cells, and it was activated by MOMBAs. Based on bar-code theory, the receptor is expected to be differentially phosphorylated in different cell types. This regulatory mechanism has been observed in M3 mAChR (Butcher et al., 2011). To address whether hFFA2 would be phosphorylated in a tissue-specific manner, we successfully used phospho-specific antibodies against Thr<sup>306</sup>/Thr<sup>310</sup> and Ser<sup>296</sup>/Ser<sup>297</sup> and found that phosphorylation of hFFA2 occurs at these sites in disparate tissues. In colonic epithelium, it is observed in immunoblots that agonist-enhanced phosphorylation on Thr<sup>306</sup>/Thr<sup>310</sup> and Ser<sup>296</sup>/Ser<sup>297</sup> were both identified by antibodies. In immune cells in gut Peyer's patches and in white adipose tissue, agonist-enhanced phosphorylation on Thr<sup>306</sup>/Thr<sup>310</sup> and Ser<sup>296</sup>/Ser<sup>297</sup> was identified by anti-Thr<sup>306</sup>/Thr<sup>310</sup> and anti-Ser<sup>296</sup>/Ser<sup>297</sup> respectively. An obvious conjecture about this phenomenon is that the mediators in each tissue are distinct. For example, the expression patterns and levels of GRKs vary between different cell types. If the phosphorylation sites in hFFA2 are regulated by distinct GRKs, then I will observe distinct phosphorylation profiles. As bar-code theory has been proved *in vivo*, a future interest is to investigate this theory *in vivo*. To achieve this, the hFFA4-DREADD mice will be given MOMBAs in drinking water and the tissues of interest will be collected. Then the tissues will be homogenized and analyzed by western blot using phospho-site-specific antibodies.

It is speculated that FFA4 exhibits similar behaviour, because of the high level of homology among FFA receptors (Tikhonova and Poerio, 2015). The results

## Chapter 6

provide evidences for a bar-code pattern of receptor phosphorylation, but it remains far from deciphering the code. To investigate the bar-code pattern of receptor phosphorylation, the first problem to be solved is to optimise the technique of determine the expression of FFA4 in tissues. This thesis using anti-HA antibody to measure the expression of FFA4 in lung tissues, but immunoblots showed limited receptor expression. In this case, choosing other tissues which express FFA4 is necessary. Our lab has already tried to measure FFA4 expression in adipose tissues, and found that the antibodies are able to identified FFA4 in immunoblots (Data is unpublished). Additionally, figure out which GRKs participate in regulating FFA4 phosphorylation is helpful to understand FFA4 phosphorylation in distinct cell types. This thesis used selective GRKs inhibitors to eliminate the effect from GRK2/3 or GRK6. Another way to do this is to transfect each individual GRK constructs into GRK knock out cells. In this case, the transfected cells only express a single GRK subtype, which is better to observe the regulation of FFA4 phosphorylation by GRKs.

## References

- ALVAREZ-CURTO, E., INOUE, A., JENKINS, L., RAIHAN, S. Z., PRIHANDOKO, R., TOBIN, A. B. & MILLIGAN, G. 2016. Targeted Elimination of G Proteins and Arrestins Defines Their Specific Contributions to Both Intensity and Duration of G Protein-coupled Receptor Signaling. *J Biol Chem*, 291, 27147-27159.
- ARDITO, F., GIULIANI, M., PERRONE, D., TROIANO, G. & LO MUZIO, L. 2017. The crucial role of protein phosphorylation in cell signaling and its use as targeted therapy (Review). *Int J Mol Med*, 40, 271-280.
- ARORA, T., RUDENKO, O., EGEROD, K. L., HUSTED, A. S., KOVATCHEVA-DATCHARY, P., AKRAMI, R., KRISTENSEN, M., SCHWARTZ, T. W. & BÄCKHED, F. 2019. Microbial fermentation of flaxseed fibers modulates the transcriptome of GPR41-expressing enteroendocrine cells and protects mice against diet-induced obesity. *Am J Physiol Endocrinol Metab*, 316, E453-e463.
- ARSHAVSKY, V. Y., LAMB, T. D. & PUGH, E. N. 2002. G Proteins and Phototransduction. *Annual Review of Physiology*, 64, 153-187.
- BARKI, N., BOLOGNINI, D., BÖRJESSON, U., JENKINS, L., RIDDELL, J., HUGHES, D. I., ULVEN, T., HUDSON, B. D., ULVEN, E. R., DEKKER, N., TOBIN, A. B. & MILLIGAN, G. 2022. Chemogenetics defines a short-chain fatty acid receptor gut-brain axis. *eLife*, 11, e73777.
- BARKI, N., JENKINS, L., MARSANGO, S., DEDEO, D., BOLOGNINI, D., DWOMOH, L., ABDELMALIK, A. M., NILSEN, M., STOFFELS, M., NAGEL, F., SCHULZ, S., TOBIN, A. B. & MILLIGAN, G. 2023. Phosphorylation bar-coding of Free Fatty Acid receptor 2 is generated in a tissue-specific manner. eLife Sciences Publications, Ltd.
- BELLAHCENE, M., O'DOWD, J. F., WARGENT, E. T., ZAIBI, M. S., HISLOP, D. C., NGALA, R. A., SMITH, D. M., CAWTHORNE, M. A., STOCKER, C. J. & ARCH, J. R. 2013. Male mice that lack the G-protein-coupled receptor GPR41 have low energy expenditure and increased body fat content. *Br J Nutr*, 109, 1755-64.
- BOLOGNINI, D., BARKI, N., BUTCHER, A. J., HUDSON, B. D., SERGEEV, E., MOLLOY, C., MOSS, C. E., BRADLEY, S. J., LE GOUILL, C., BOUVIER, M., TOBIN, A. B. & MILLIGAN, G. 2019. Chemogenetics defines receptor-mediated functions of short chain free fatty acids. *Nature Chemical Biology*, 15, 489-498.
- BOLOGNINI, D., MOSS, C. E., NILSSON, K., PETERSSON, A. U., DONNELLY, I., SERGEEV, E., KÖNIG, G. M., KOSTENIS, E., KUROWSKA-STOLARSKA, M.,

- MILLER, A., DEKKER, N., TOBIN, A. B. & MILLIGAN, G. 2016a. A Novel Allosteric Activator of Free Fatty Acid 2 Receptor Displays Unique Gi-functional Bias. *J Biol Chem*, 291, 18915-31.
- BOLOGNINI, D., TOBIN, A. B., MILLIGAN, G. & MOSS, C. E. 2016b. The Pharmacology and Function of Receptors for Short-Chain Fatty Acids. *Mol Pharmacol*, 89, 388-98.
- BONAVENTURA, J., ELDRIDGE, M. A. G., HU, F., GOMEZ, J. L., SANCHEZ-SOTO, M., ABRAMYAN, A. M., LAM, S., BOEHM, M. A., RUIZ, C., FARRELL, M. R., MORENO, A., GALAL FARESS, I. M., ANDERSEN, N., LIN, J. Y., MOADDEL, R., MORRIS, P. J., SHI, L., SIBLEY, D. R., MAHLER, S. V., NABAVI, S., POMPER, M. G., BONCI, A., HORTI, A. G., RICHMOND, B. J. & MICHAELIDES, M. 2019. High-potency ligands for DREADD imaging and activation in rodents and monkeys. *Nature Communications*, 10, 4627.
- BOUZO-LORENZO, M., SANTO-ZAS, I., LODEIRO, M., NOGUEIRAS, R., CASANUEVA, F. F., CASTRO, M., PAZOS, Y., TOBIN, A. B., BUTCHER, A. J. & CAMIÑA, J. P. 2016. Distinct phosphorylation sites on the ghrelin receptor, GHSR1a, establish a code that determines the functions of  $\beta$ -arrestins. *Sci Rep*, 6, 22495.
- BRISCOE, C. P., PEAT, A. J., MCKEOWN, S. C., CORBETT, D. F., GOETZ, A. S., LITTLETON, T. R., MCCOY, D. C., KENAKIN, T. P., ANDREWS, J. L., AMMALA, C., FORNWALD, J. A., IGNAR, D. M. & JENKINSON, S. 2006. Pharmacological regulation of insulin secretion in MIN6 cells through the fatty acid receptor GPR40: identification of agonist and antagonist small molecules. *Br J Pharmacol*, 148, 619-28.
- BRISCOE, C. P., TADAYYON, M., ANDREWS, J. L., BENSON, W. G., CHAMBERS, J. K., EILERT, M. M., ELLIS, C., ELSHOURBAGY, N. A., GOETZ, A. S., MINNICK, D. T., MURDOCK, P. R., SAULS, H. R., JR., SHABON, U., SPINAGE, L. D., STRUM, J. C., SZEKERES, P. G., TAN, K. B., WAY, J. M., IGNAR, D. M., WILSON, S. & MUIR, A. I. 2003. The orphan G protein-coupled receptor GPR40 is activated by medium and long chain fatty acids. *J Biol Chem*, 278, 11303-11.
- BROWN, A. J., GOLDSWORTHY, S. M., BARNES, A. A., EILERT, M. M., TCHEANG, L., DANIELS, D., MUIR, A. I., WIGGLESWORTH, M. J., KINGHORN, I., FRASER, N. J., PIKE, N. B., STRUM, J. C., STEPLEWSKI, K. M., MURDOCK, P. R., HOLDER, J. C., MARSHALL, F. H., SZEKERES, P. G., WILSON, S., IGNAR, D. M., FOORD, S. M., WISE, A. & DOWELL, S. J. 2003. The Orphan G protein-coupled

- receptors GPR41 and GPR43 are activated by propionate and other short chain carboxylic acids. *J Biol Chem*, 278, 11312-9.
- BROWN, S. P., DRANSFIELD, P. J., VIMOLRATANA, M., JIAO, X., ZHU, L., PATTAROPONG, V., SUN, Y., LIU, J., LUO, J., ZHANG, J., WONG, S., ZHUANG, R., GUO, Q., LI, F., MEDINA, J. C., SWAMINATH, G., LIN, D. C. H. & HOUZE, J. B. 2012. Discovery of AM-1638: A Potent and Orally Bioavailable GPR40/FFA1 Full Agonist. *ACS Medicinal Chemistry Letters*, 3, 726-730.
- BURNS, R. N. & MONIRI, N. H. 2010. Agonism with the omega-3 fatty acids alpha-linolenic acid and docosahexaenoic acid mediates phosphorylation of both the short and long isoforms of the human GPR120 receptor. *Biochem Biophys Res Commun*, 396, 1030-5.
- BURNS, R. N., SINGH, M., SENATOROV, I. S. & MONIRI, N. H. 2014. Mechanisms of homologous and heterologous phosphorylation of FFA receptor 4 (GPR120): GRK6 and PKC mediate phosphorylation of Thr<sup>347</sup>, Ser<sup>350</sup>, and Ser<sup>357</sup> in the C-terminal tail. *Biochemical pharmacology*, 87, 650-659.
- BUSILLO, J. M., ARMANDO, S., SENGUPTA, R., MEUCCI, O., BOUVIER, M. & BENOVIC, J. L. 2010. Site-specific phosphorylation of CXCR4 is dynamically regulated by multiple kinases and results in differential modulation of CXCR4 signaling. *J Biol Chem*, 285, 7805-17.
- BUTCHER, A. J., BRADLEY, S. J., PRIHANDOKO, R., BROOKE, S. M., MOGG, A., BOURGOGNON, J. M., MACEDO-HATCH, T., EDWARDS, J. M., BOTTRILL, A. R., CHALLISS, R. A., BROAD, L. M., FELDER, C. C. & TOBIN, A. B. 2016. An Antibody Biosensor Establishes the Activation of the M1 Muscarinic Acetylcholine Receptor during Learning and Memory. *J Biol Chem*, 291, 8862-75.
- BUTCHER, A. J., HUDSON, B. D., SHIMPUKADE, B., ALVAREZ-CURTO, E., PRIHANDOKO, R., ULVEN, T., MILLIGAN, G. & TOBIN, A. B. 2014. Concomitant action of structural elements and receptor phosphorylation determines arrestin-3 interaction with the free fatty acid receptor FFA4. *J Biol Chem*, 289, 18451-65.
- BUTCHER, A. J., PRIHANDOKO, R., KONG, K. C., MCWILLIAMS, P., EDWARDS, J. M., BOTTRILL, A., MISTRY, S. & TOBIN, A. B. 2011. Differential G-protein-coupled receptor phosphorylation provides evidence for a signaling bar code. *J Biol Chem*, 286, 11506-18.
- CALEBIRO, D., RIEKEN, F., WAGNER, J., SUNGKAWORN, T., ZABEL, U., BORZI, A.,

- COCUCCI, E., ZÜRN, A. & LOHSE, M. J. 2013. Single-molecule analysis of fluorescently labeled G-protein-coupled receptors reveals complexes with distinct dynamics and organization. *Proc Natl Acad Sci U S A*, 110, 743-8.
- CARULLO, G., MAZZOTTA, S., VEGA-HOLM, M., IGLESIAS-GUERRA, F., VEGA-PEREZ, J. M., AIELLO, F. & BRIZZI, A. 2021. GPR120/FFAR4 Pharmacology: Focus on Agonists in Type 2 Diabetes Mellitus Drug Discovery. *J Med Chem*, 64, 4312-4332.
- CHAMBERS, E. S., VIARDOT, A., PSICHAS, A., MORRISON, D. J., MURPHY, K. G., ZACVARGHESE, S. E., MACDOUGALL, K., PRESTON, T., TEDFORD, C., FINLAYSON, G. S., BLUNDELL, J. E., BELL, J. D., THOMAS, E. L., MT-ISA, S., ASHBY, D., GIBSON, G. R., KOLIDA, S., DHILLO, W. S., BLOOM, S. R., MORLEY, W., CLEGG, S. & FROST, G. 2015. Effects of targeted delivery of propionate to the human colon on appetite regulation, body weight maintenance and adiposity in overweight adults. *Gut*, 64, 1744-54.
- COLOM, M., VIDAL, B. & ZIMMER, L. 2019. Is There a Role for GPCR Agonist Radiotracers in PET Neuroimaging? *Front Mol Neurosci*, 12, 255.
- DANN, C. E., HSIEH, J. C., RATTNER, A., SHARMA, D., NATHANS, J. & LEAHY, D. J. 2001. Insights into Wnt binding and signalling from the structures of two Frizzled cysteine-rich domains. *Nature*, 412, 86-90.
- DELOM, F. & CHEVET, E. 2006. Phosphoprotein analysis: from proteins to proteomes. *Proteome Science*, 4, 15.
- DELOM, F. & FESSART, D. 2011. Role of Phosphorylation in the Control of Clathrin-Mediated Internalization of GPCR. *International Journal of Cell Biology*, 2011, 246954.
- DIJKMAN, P. M., CASTELL, O. K., GODDARD, A. D., MUNOZ-GARCIA, J. C., DE GRAAF, C., WALLACE, M. I. & WATTS, A. 2018. Dynamic tuneable G protein-coupled receptor monomer-dimer populations. *Nature Communications*, 9, 1710.
- DINGUS, J., WELLS, C. A., CAMPBELL, L., CLEATOR, J. H., ROBINSON, K. & HILDEBRANDT, J. D. 2005. G Protein By Dimer Formation: GB and Gy Differentially Determine Efficiency of in Vitro Dimer Formation. *Biochemistry*, 44, 11882-11890.
- DRAGANO, N. R. V., SOLON, C., RAMALHO, A. F., DE MOURA, R. F., RAZOLLI, D. S., CHRISTIANSEN, E., AZEVEDO, C., ULVEN, T. & VELLOSO, L. A. 2017. Polyunsaturated fatty acid receptors, GPR40 and GPR120, are expressed in the hypothalamus and control energy homeostasis and inflammation.



*Journal of Neuroinflammation*, 14.

- DRUBE, J., HAIDER, R. S., MATTHEES, E. S. F., REICHEL, M., ZEINER, J., FRITZWANKER, S., ZIEGLER, C., BARZ, S., KLEMENT, L., FILOR, J., WEITZEL, V., KLIEWER, A., MIESS-TANNEBERG, E., KOSTENIS, E., SCHULZ, S. & HOFFMANN, C. 2022. GPCR kinase knockout cells reveal the impact of individual GRKs on arrestin binding and GPCR regulation. *Nature Communications*, 13, 540.
- EDFALK, S., STENEBERG, P. & EDLUND, H. 2008. Gpr40 is expressed in enteroendocrine cells and mediates free fatty acid stimulation of incretin secretion. *Diabetes*, 57, 2280-7.
- EICHEL, K., JULLIÉ, D. & VON ZASTROW, M. 2016.  $\beta$ -Arrestin drives MAP kinase signalling from clathrin-coated structures after GPCR dissociation. *Nature Cell Biology*, 18, 303-310.
- ENGELSTOFT, M. S., PARK, W. M., SAKATA, I., KRISTENSEN, L. V., HUSTED, A. S., OSBORNE-LAWRENCE, S., PIPER, P. K., WALKER, A. K., PEDERSEN, M. H., NØHR, M. K., PAN, J., SINZ, C. J., CARRINGTON, P. E., AKIYAMA, T. E., JONES, R. M., TANG, C., AHMED, K., OFFERMANN, S., EGEROD, K. L., ZIGMAN, J. M. & SCHWARTZ, T. W. 2013. Seven transmembrane G protein-coupled receptor repertoire of gastric ghrelin cells. *Mol Metab*, 2, 376-92.
- FERGUSON, S. S. 2001. Evolving concepts in G protein-coupled receptor endocytosis: the role in receptor desensitization and signaling. *Pharmacol Rev*, 53, 1-24.
- FERRÉ, S., CASADÓ, V., DEVI, L. A., FILIZOLA, M., JOCKERS, R., LOHSE, M. J., MILLIGAN, G., PIN, J. P. & GUITART, X. 2014. G protein-coupled receptor oligomerization revisited: functional and pharmacological perspectives. *Pharmacol Rev*, 66, 413-34.
- FONT-BURGADA, J., SUN, B. & KARIN, M. 2016. Obesity and Cancer: The Oil that Feeds the Flame. *Cell Metabolism*, 23, 48-62.
- FREDRIKSSON, R., LAGERSTRÖM, M. C., LUNDIN, L.-G. & SCHIÖTH, H. B. 2003. The G-Protein-Coupled Receptors in the Human Genome Form Five Main Families. Phylogenetic Analysis, Paralogon Groups, and Fingerprints. *Molecular Pharmacology*, 63, 1256.
- GARRIDO, D. M., CORBETT, D. F., DWORNIK, K. A., GOETZ, A. S., LITTLETON, T. R., MCKEOWN, S. C., MILLS, W. Y., SMALLEY, T. L., JR., BRISCOE, C. P. & PEAT, A. J. 2006. Synthesis and activity of small molecule GPR40 agonists. *Bioorg*

*Med Chem Lett*, 16, 1840-5.

- GETHER, U. 2000. Uncovering Molecular Mechanisms Involved in Activation of G Protein-Coupled Receptors. *Endocrine Reviews*, 21, 90-113.
- GILON, P. & HENQUIN, J. C. 2001. Mechanisms and physiological significance of the cholinergic control of pancreatic beta-cell function. *Endocr Rev*, 22, 565-604.
- GONZALEZ DE VALDIVIA, E., SANDÉN, C., KAHN, R., OLDE, B. & LEEB-LUNDBERG, L. M. F. 2019. Human G protein-coupled receptor 30 is N-glycosylated and N-terminal domain asparagine 44 is required for receptor structure and activity. *Biosci Rep*, 39.
- GOTH, C. K., PETÄJÄ-REPO, U. E. & ROSENKILDE, M. M. 2020. G Protein-Coupled Receptors in the Sweet Spot: Glycosylation and other Post-translational Modifications. *ACS Pharmacol Transl Sci*, 3, 237-245.
- GRAVES, J. D. & KREBS, E. G. 1999. Protein Phosphorylation and Signal Transduction. *Pharmacology & Therapeutics*, 82, 111-121.
- GUREVICH, E. V., TESMER, J. J., MUSHEGIAN, A. & GUREVICH, V. V. 2012. G protein-coupled receptor kinases: more than just kinases and not only for GPCRs. *Pharmacol Ther*, 133, 40-69.
- GUREVICH, V. V. & GUREVICH, E. V. 2006. The structural basis of arrestin-mediated regulation of G-protein-coupled receptors. *Pharmacology & Therapeutics*, 110, 465-502.
- GUREVICH, V. V. & GUREVICH, E. V. 2019. GPCR Signaling Regulation: The Role of GRKs and Arrestins. *Front Pharmacol*, 10, 125.
- GUZMAN-SILVA, A., MARTINEZ-MORALES, J. C., MEDINA, L. D. C., ROMERO-AVILA, M. T., VILLEGAS-COMONFORT, S., SOLIS, K. H. & GARCIA-SAINZ, J. A. 2022. Mutation of putative phosphorylation sites in the free fatty acid receptor 1: Effects on signaling, receptor phosphorylation, and internalization. *Mol Cell Endocrinol*, 545, 111573.
- HAMPEL, H., BLENNOW, K., SHAW, L. M., HOESSLER, Y. C., ZETTERBERG, H. & TROJANOWSKI, J. Q. 2010. Total and phosphorylated tau protein as biological markers of Alzheimer's disease. *Experimental Gerontology*, 45, 30-40.
- HAUGE, M., VESTMAR, M. A., HUSTED, A. S., EKBERG, J. P., WRIGHT, M. J., DI SALVO, J., WEINGLASS, A. B., ENGELSTOFT, M. S., MADSEN, A. N., LÜCKMANN, M., MILLER, M. W., TRUJILLO, M. E., FRIMURER, T. M., HOLST, B., HOWARD,

- A. D. & SCHWARTZ, T. W. 2015. GPR40 (FFAR1) - Combined Gs and Gq signaling in vitro is associated with robust incretin secretagogue action ex vivo and in vivo. *Molecular Metabolism*, 4, 3-14.
- HAUSER, A. S., ATTWOOD, M. M., RASK-ANDERSEN, M., SCHLÖTH, H. B. & GLORIAM, D. E. 2017. Trends in GPCR drug discovery: new agents, targets and indications. *Nat Rev Drug Discov*, 16, 829-842.
- HAUSER, M. A., KINDINGER, I., LAUFER, J. M., SPÄTE, A. K., BUCHER, D., VANES, S. L., KRUEGER, W. A., WITTMANN, V. & LEGLER, D. F. 2016. Distinct CCR7 glycosylation pattern shapes receptor signaling and endocytosis to modulate chemotactic responses. *J Leukoc Biol*, 99, 993-1007.
- HIDALGO, M. A., CARRETTA, M. D. & BURGOS, R. A. 2021. Long Chain Fatty Acids as Modulators of Immune Cells Function: Contribution of FFA1 and FFA4 Receptors. *Front Physiol*, 12, 668330.
- HIRASAWA, A., TSUMAYA, K., AWAJI, T., KATSUMA, S., ADACHI, T., YAMADA, M., SUGIMOTO, Y., MIYAZAKI, S. & TSUJIMOTO, G. 2005. Free fatty acids regulate gut incretin glucagon-like peptide-1 secretion through GPR120. *Nat Med*, 11, 90-4.
- HOLLENSTEIN, K., DE GRAAF, C., BORTOLATO, A., WANG, M.-W., MARSHALL, F. H. & STEVENS, R. C. 2014. Insights into the structure of class B GPCRs. *Trends in Pharmacological Sciences*, 35, 12-22.
- HONG, Y. H., NISHIMURA, Y., HISHIKAWA, D., TSUZUKI, H., MIYAHARA, H., GOTOH, C., CHOI, K. C., FENG, D. D., CHEN, C., LEE, H. G., KATOH, K., ROH, S. G. & SASAKI, S. 2005. Acetate and propionate short chain fatty acids stimulate adipogenesis via GPCR43. *Endocrinology*, 146, 5092-9.
- HOPKINS, M. M., ZHANG, Z., LIU, Z. & MEIER, K. E. 2016. Eicosopentanoic Acid and Other Free Fatty Acid Receptor Agonists Inhibit Lysophosphatidic Acid- and Epidermal Growth Factor-Induced Proliferation of Human Breast Cancer Cells. *J Clin Med*, 5.
- HOUTHUIJZEN, J. M. 2016. For Better or Worse: FFAR1 and FFAR4 Signaling in Cancer and Diabetes. *Mol Pharmacol*, 90, 738-743.
- HOUTHUIJZEN, J. M., OOSTEROM, I., HUDSON, B. D., HIRASAWA, A., DAENEN, L. G. M., MCLEAN, C. M., HANSEN, S. V. F., VAN JAARSVELD, M. T. M., PEEPER, D. S., JAFARI SADATMAND, S., ROODHART, J. M. L., VAN DE LEST, C. H. A., ULVEN, T., ISHIHARA, K., MILLIGAN, G. & VOEST, E. E. 2017. Fatty acid 16:4(n-3) stimulates a GPR120-induced signaling cascade in splenic

- macrophages to promote chemotherapy resistance. *Faseb j*, 31, 2195-2209.
- HOUZE, J. B., ZHU, L., SUN, Y., AKERMAN, M., QIU, W., ZHANG, A. J., SHARMA, R., SCHMITT, M., WANG, Y., LIU, J., LIU, J., MEDINA, J. C., REAGAN, J. D., LUO, J., TONN, G., ZHANG, J., LU, J. Y.-L., CHEN, M., LOPEZ, E., NGUYEN, K., YANG, L., TANG, L., TIAN, H., SHUTTLEWORTH, S. J. & LIN, D. C. H. 2012. AMG 837: A potent, orally bioavailable GPR40 agonist. *Bioorganic & Medicinal Chemistry Letters*, 22, 1267-1270.
- HU, H., HE, L. Y., GONG, Z., LI, N., LU, Y. N., ZHAI, Q. W., LIU, H., JIANG, H. L., ZHU, W. L. & WANG, H. Y. 2009. A novel class of antagonists for the FFAs receptor GPR40. *Biochemical and Biophysical Research Communications*, 390, 557-563.
- HUDSON, B. D., CHRISTIANSEN, E., TIKHONOVA, I. G., GRUNDMANN, M., KOSTENIS, E., ADAMS, D. R., ULVEN, T. & MILLIGAN, G. 2012a. Chemically engineering ligand selectivity at the free fatty acid receptor 2 based on pharmacological variation between species orthologs. *Faseb j*, 26, 4951-65.
- HUDSON, B. D., DUE-HANSEN ME FAU - CHRISTIANSEN, E., CHRISTIANSEN E FAU - HANSEN, A. M., HANSEN AM FAU - MACKENZIE, A. E., MACKENZIE AE FAU - MURDOCH, H., MURDOCH H FAU - PANDEY, S. K., PANDEY SK FAU - WARD, R. J., WARD RJ FAU - MARQUEZ, R., MARQUEZ R FAU - TIKHONOVA, I. G., TIKHONOVA IG FAU - ULVEN, T., ULVEN T FAU - MILLIGAN, G. & MILLIGAN, G. 2013a. Defining the molecular basis for the first potent and selective orthosteric agonists of the FFA2 free fatty acid receptor.
- HUDSON, B. D., SHIMPUKADE, B., MACKENZIE, A. E., BUTCHER, A. J., PEDIANI, J. D., CHRISTIANSEN, E., HEATHCOTE, H., TOBIN, A. B., ULVEN, T. & MILLIGAN, G. 2013b. The pharmacology of TUG-891, a potent and selective agonist of the free fatty acid receptor 4 (FFA4/GPR120), demonstrates both potential opportunity and possible challenges to therapeutic agonism. *Mol Pharmacol*, 84, 710-25.
- HUDSON, B. D., SHIMPUKADE, B., MILLIGAN, G. & ULVEN, T. 2014. The molecular basis of ligand interaction at free fatty acid receptor 4 (FFA4/GPR120). *J Biol Chem*, 289, 20345-58.
- HUDSON, B. D., TIKHONOVA, I. G., PANDEY, S. K., ULVEN, T. & MILLIGAN, G. 2012b. Extracellular ionic locks determine variation in constitutive activity and ligand potency between species orthologs of the free fatty acid receptors FFA2 and FFA3. *J Biol Chem*, 287, 41195-209.

- INSEL, P. A., SRIRAM, K., GORR, M. W., WILEY, S. Z., MICHKOV, A., SALMERÓN, C. & CHINN, A. M. 2019. GPCRomics: An Approach to Discover GPCR Drug Targets. *Trends Pharmacol Sci*, 40, 378-387.
- ISHIER, R., SAMARJIT, B. & MITRADAS, M. P. 2013. Functional Selectivity in Serotonin Receptor 2A (5-HT<sub>2A</sub>) Endocytosis, Recycling, and Phosphorylation. *Molecular Pharmacology*, 83, 42.
- ITOH, Y., KAWAMATA, Y., HARADA, M., KOBAYASHI, M., FUJII, R., FUKUSUMI, S., OGI, K., HOSOYA, M., TANAKA, Y., UEJIMA, H., TANAKA, H., MARUYAMA, M., SATOH, R., OKUBO, S., KIZAWA, H., KOMATSU, H., MATSUMURA, F., NOGUCHI, Y., SHINOHARA, T., HINUMA, S., FUJISAWA, Y. & FUJINO, M. 2003. Free fatty acids regulate insulin secretion from pancreatic beta cells through GPR40. *Nature*, 422, 173-6.
- JEAN-CHARLES, P. Y., KAUR, S. & SHENOY, S. K. 2017. G Protein-Coupled Receptor Signaling Through beta-Arrestin-Dependent Mechanisms. *J Cardiovasc Pharmacol*, 70, 142-158.
- JUNG, C., HUGOT, J. P. & BARREAU, F. 2010. Peyer's Patches: The Immune Sensors of the Intestine. *Int J Inflam*, 2010, 823710.
- KAHN, S. E., COOPER, M. E. & DEL PRATO, S. 2014. Pathophysiology and treatment of type 2 diabetes: perspectives on the past, present, and future. *The Lancet*, 383, 1068-1083.
- KAKU, K., ENYA, K., NAKAYA, R., OHIRA, T. & MATSUNO, R. 2015. Efficacy and safety of fasiglifam (TAK-875), a G protein-coupled receptor 40 agonist, in Japanese patients with type 2 diabetes inadequately controlled by diet and exercise: a randomized, double-blind, placebo-controlled, phase III trial. *Diabetes, Obesity and Metabolism*, 17, 675-681.
- KANG, S., HUANG, J., LEE, B.-K., JUNG, Y.-S., IM, E., KOH, J.-M. & IM, D.-S. 2018. Omega-3 polyunsaturated fatty acids protect human hepatoma cells from developing steatosis through FFA4 (GPR120). *Biochimica et Biophysica Acta (BBA) - Molecular and Cell Biology of Lipids*, 1863, 105-116.
- KATRITCH, V., CHEREZOV, V. & STEVENS, R. C. 2013. Structure-function of the G protein-coupled receptor superfamily. *Annu Rev Pharmacol Toxicol*, 53, 531-56.
- KATSUMA, S., HATAE, N., YANO, T., RUIKE, Y., KIMURA, M., HIRASAWA, A. & TSUJIMOTO, G. 2005. Free fatty acids inhibit serum deprivation-induced apoptosis through GPR120 in a murine enteroendocrine cell line STC-1. *J*

*Biol Chem*, 280, 19507-15.

- KEBEDE, M., ALQUIER, T., LATOUR, M. G., SEMACHE, M., TREMBLAY, C. & POITOUT, V. 2008. The fatty acid receptor GPR40 plays a role in insulin secretion in vivo after high-fat feeding. *Diabetes*, 57, 2432-7.
- KIMURA, I., OZAWA, K., INOUE, D., IMAMURA, T., KIMURA, K., MAEDA, T., TERASAWA, K., KASHIHARA, D., HIRANO, K., TANI, T., TAKAHASHI, T., MIYAUCHI, S., SHIOI, G., INOUE, H. & TSUJIMOTO, G. 2013. The gut microbiota suppresses insulin-mediated fat accumulation via the short-chain fatty acid receptor GPR43. *Nat Commun*, 4, 1829.
- KLIEWER, A., REINSCHEID, R. K. & SCHULZ, S. 2017. Emerging Paradigms of G Protein-Coupled Receptor Dephosphorylation. *Trends in Pharmacological Sciences*, 38, 621-636.
- KNIAZEFF, J., PRÉZEAU, L., RONDARD, P., PIN, J. P. & GOUDET, C. 2011. Dimers and beyond: The functional puzzles of class C GPCRs. *Pharmacol Ther*, 130, 9-25.
- KOMOLOV, K. E. & BENOVIC, J. L. 2018. G protein-coupled receptor kinases: Past, present and future. *Cell Signal*, 41, 17-24.
- KOTARSKY, K., NILSSON, N. E., FLODGREN, E., OWMAN, C. & OLDE, B. 2003a. A human cell surface receptor activated by free fatty acids and thiazolidinedione drugs. *Biochem Biophys Res Commun*, 301, 406-10.
- KOTARSKY, K., NILSSON, N. E., OLDE, B. & OWMAN, C. 2003b. Progress in Methodology Improved Reporter Gene Assays Used to Identify Ligands Acting on Orphan Seven-Transmembrane Receptors. *Pharmacology & Toxicology*, 93, 249-258.
- KOZIELEWICZ, P., ALOMAR, H., YUSOF, S., GRAFTON, G., COOPER, A. J., CURNOW, S. J., IRONSIDE, J. W., PALL, H. & BARNES, N. M. 2017. N-glycosylation and expression in human tissues of the orphan GPR61 receptor. *FEBS Open Bio*, 7, 1982-1993.
- LAGERSTRÖM, M. C. & SCHIÖTH, H. B. 2008. Structural diversity of G protein-coupled receptors and significance for drug discovery. *Nature Reviews Drug Discovery*, 7, 339-357.
- LAMBRIGHT, D. G., SONDEK, J., BOHM, A., SKIBA, N. P., HAMM, H. E. & SIGLER, P. B. 1996. The 2.0 Å crystal structure of a heterotrimeric G protein. *Nature*, 379, 311-319.
- LAN, H., HOOS, L. M., LIU, L., TETZLOFF, G., HU, W., ABBONDANZO, S. J.,

- VASSILEVA, G., GUSTAFSON, E. L., HEDRICK, J. A. & DAVIS, H. R. 2008. Lack of FFAR1/GPR40 does not protect mice from high-fat diet-induced metabolic disease. *Diabetes*, 57, 2999-3006.
- LANCTOT, P. M., LECLERC, P. C., CLÉMENT, M., AUGER-MESSIER, M., ESCHER, E., LEDUC, R. & GUILLEMETTE, G. 2005. Importance of N-glycosylation positioning for cell-surface expression, targeting, affinity and quality control of the human AT1 receptor. *Biochem J*, 390, 367-76.
- LATOURE, M. G., ALQUIER, T., OSEID, E., TREMBLAY, C., JETTON, T. L., LUO, J., LIN, D. C. & POITOUT, V. 2007. GPR40 is necessary but not sufficient for fatty acid stimulation of insulin secretion in vivo. *Diabetes*, 56, 1087-94.
- LE POUL, E., LOISON, C., STRUYF, S., SPRINGAEL, J. Y., LANNOY, V., DECOBECQ, M. E., BREZILLON, S., DUPRIEZ, V., VASSART, G., VAN DAMME, J., PARMENTIER, M. & DETHEUX, M. 2003. Functional characterization of human receptors for short chain fatty acids and their role in polymorphonuclear cell activation. *J Biol Chem*, 278, 25481-9.
- LEE, K. P., PARK, S. J., KANG, S., KOH, J. M., SATO, K., CHUNG, H. Y., OKAJIMA, F. & IM, D. S. 2017. omega-3 Polyunsaturated fatty acids accelerate airway repair by activating FFA4 in club cells. *Am J Physiol Lung Cell Mol Physiol*, 312, L835-L844.
- LEE, T., SCHWANDNER R FAU - SWAMINATH, G., SWAMINATH G FAU - WEISZMANN, J., WEISZMANN J FAU - CARDOZO, M., CARDOZO M FAU - GREENBERG, J., GREENBERG J FAU - JAECKEL, P., JAECKEL P FAU - GE, H., GE H FAU - WANG, Y., WANG Y FAU - JIAO, X., JIAO X FAU - LIU, J., LIU J FAU - KAYSER, F., KAYSER F FAU - TIAN, H., TIAN H FAU - LI, Y. & LI, Y. 2008. Identification and functional characterization of allosteric agonists for the G protein-coupled receptor FFA2.
- LEFKOWITZ, R. J. 2004. Historical review: a brief history and personal retrospective of seven-transmembrane receptors. *Trends Pharmacol Sci*, 25, 413-22.
- LEFKOWITZ, R. J. & SHENOY, S. K. 2005. Transduction of receptor signals by beta-arrestins. *Science*, 308, 512-7.
- LIAPAKIS, G., CORDOMÍ, A. & PARDO, L. 2012. The G-protein coupled receptor family: actors with many faces. *Curr Pharm Des*, 18, 175-85.
- LIU, A. P., LU, X., SEI, Y., ZHAO, X., PECHHOLD, S., CARRERO, R. J., RAYBOULD, H. E. & WANK, S. 2011. The G-protein-coupled receptor GPR40 directly

- mediates long-chain fatty acid-induced secretion of cholecystokinin. *Gastroenterology*, 140, 903-12.
- LIU, J., TANG, H., XU, C., ZHOU, S., ZHU, X., LI, Y., PRÉZEAU, L., XU, T., PIN, J.-P., RONDARD, P., JI, W. & LIU, J. 2022. Biased signaling due to oligomerization of the G protein-coupled platelet-activating factor receptor. *Nature Communications*, 13, 6365.
- LIU, Z., HOPKINS, M. M., ZHANG, Z., QUISENBERRY, C. B., FIX, L. C., GALVAN, B. M. & MEIER, K. E. 2015. Omega-3 fatty acids and other FFA4 agonists inhibit growth factor signaling in human prostate cancer cells. *J Pharmacol Exp Ther*, 352, 380-94.
- LODOWSKI, D. T., TESMER, V. M., BENOVIC, J. L. & TESMER, J. J. 2006. The structure of G protein-coupled receptor kinase (GRK)-6 defines a second lineage of GRKs. *J Biol Chem*, 281, 16785-93.
- LUTTRELL, L. M. & GESTY-PALMER, D. 2010. Beyond Desensitization: Physiological Relevance of Arrestin-Dependent Signaling. *Pharmacological Reviews*, 62, 305.
- LUTTRELL, L. M. & LEFKOWITZ, R. J. 2002. The role of  $\beta$ -arrestins in the termination and transduction of G-protein-coupled receptor signals. *Journal of Cell Science*, 115, 455-465.
- MACPHERSON, A. J. & SMITH, K. 2006. Mesenteric lymph nodes at the center of immune anatomy. *J Exp Med*, 203, 497-500.
- MALIK, R. U., RITT, M., DEVREE, B. T., NEUBIG, R. R., SUNAHARA, R. K. & SIVARAMAKRISHNAN, S. 2013. Detection of G protein-selective G protein-coupled receptor (GPCR) conformations in live cells. *J Biol Chem*, 288, 17167-78.
- MANOSALVA, C., MENA, J., VELASQUEZ, Z., COLENZO, C. K., BRAUCHI, S., BURGOS, R. A. & HIDALGO, M. A. 2015. Cloning, Identification and Functional Characterization of Bovine Free Fatty Acid Receptor-1 (FFAR1/GPR40) in Neutrophils. *PLOS ONE*, 10, e0119715.
- MASLOWSKI, K. M., VIEIRA, A. T., NG, A., KRANICH, J., SIERRA, F., YU, D., SCHILTER, H. C., ROLPH, M. S., MACKAY, F., ARTIS, D., XAVIER, R. J., TEIXEIRA, M. M. & MACKAY, C. R. 2009. Regulation of inflammatory responses by gut microbiota and chemoattractant receptor GPR43. *Nature*, 461, 1282-6.
- MCKEOWN, S. C., CORBETT, D. F., GOETZ, A. S., LITTLETON, T. R., BIGHAM, E., BRISCOE, C. P., PEAT, A. J., WATSON, S. P. & HICKEY, D. M. 2007. Solid phase



- synthesis and SAR of small molecule agonists for the GPR40 receptor. *Bioorg Med Chem Lett*, 17, 1584-9.
- MENA, S. J., MANOSALVA, C., CARRETTA, M. D., TEUBER, S., OLMO, I., BURGOS, R. A. & HIDALGO, M. A. 2016. Differential free fatty acid receptor-1 (FFAR1/GPR40) signalling is associated with gene expression or gelatinase granule release in bovine neutrophils. *Innate Immunity*, 22, 479-489.
- MENON, V., LINCOFF, A. M., NICHOLLS, S. J., JASPER, S., WOLSKI, K., MCGUIRE, D. K., MEHTA, C. R., ROSENSTOCK, J., LOPEZ, C., MARCINAK, J., CAO, C., NISSEN, S. E. & FOR THE, G. I. 2018. Fasiglifam-Induced Liver Injury in Patients With Type 2 Diabetes: Results of a Randomized Controlled Cardiovascular Outcomes Safety Trial. *Diabetes Care*, 41, 2603-2609.
- MILLIGAN, G., ALVAREZ-CURTO, E., HUDSON, B. D., PRIHANDOKO, R. & TOBIN, A. B. 2017. FFA4/GPR120: Pharmacology and Therapeutic Opportunities. *Trends Pharmacol Sci*, 38, 809-821.
- MILLIGAN, G., BARKI, N. & TOBIN, A. B. 2021. Chemogenetic Approaches to Explore the Functions of Free Fatty Acid Receptor 2. *Trends in Pharmacological Sciences*, 42, 191-202.
- MISHRA, S. P., KARUNAKAR, P., TARAPHDER, S. & YADAV, H. 2020. Free Fatty Acid Receptors 2 and 3 as Microbial Metabolite Sensors to Shape Host Health: Pharmacophysiological View. *Biomedicines*, 8.
- MIYAUCHI, S., HIRASAWA, A., IGA, T., LIU, N., ITSUBO, C., SADAKANE, K., HARA, T. & TSUJIMOTO, G. 2009. Distribution and regulation of protein expression of the free fatty acid receptor GPR120. *Naunyn Schmiedebergs Arch Pharmacol*, 379, 427-34.
- MONIRI, N. H. 2016. Free-fatty acid receptor-4 (GPR120): Cellular and molecular function and its role in metabolic disorders. *Biochem Pharmacol*, 110-111, 1-15.
- MOORE, K., ZHANG, Q., MURGOLO, N., HOSTED, T. & DUFFY, R. 2009. Cloning, expression, and pharmacological characterization of the GPR120 free fatty acid receptor from cynomolgus monkey: comparison with human GPR120 splice variants. *Comp Biochem Physiol B Biochem Mol Biol*, 154, 419-26.
- NAMOUR, F., GALIEN, R., VAN KAEM, T., VAN DER AA, A., VANHOUTTE, F., BEETENS, J. & VAN'T KLOOSTER, G. 2016. Safety, pharmacokinetics and pharmacodynamics of GLPG0974, a potent and selective FFA2 antagonist, in healthy male subjects. *Br J Clin Pharmacol*, 82, 139-48.

- NEGORO, N., SASAKI, S., MIKAMI, S., ITO, M., TSUJIHATA, Y., ITO, R., SUZUKI, M., TAKEUCHI, K., SUZUKI, N., MIYAZAKI, J., SANTOU, T., ODANI, T., KANZAKI, N., FUNAMI, M., MOROHASHI, A., NONAKA, M., MATSUNAGA, S., YASUMA, T. & MOMOSE, Y. 2012. Optimization of (2,3-dihydro-1-benzofuran-3-yl)acetic acids: discovery of a non-free fatty acid-like, highly bioavailable G protein-coupled receptor 40/free fatty acid receptor 1 agonist as a glucose-dependent insulinotropic agent. *J Med Chem*, 55, 3960-74.
- NIKAIDO, Y., KOYAMA, Y., YOSHIKAWA, Y., FURUYA, T. & TAKEDA, S. 2015. Mutation analysis and molecular modeling for the investigation of ligand-binding modes of GPR84. *The Journal of Biochemistry*, 157, 311-320.
- NILSSON, N. E., KOTARSKY, K., OWMAN, C. & OLDE, B. 2003. Identification of a free fatty acid receptor, FFA2R, expressed on leukocytes and activated by short-chain fatty acids. *Biochemical and Biophysical Research Communications*, 303, 1047-1052.
- NOBLES, K. N., XIAO, K., AHN, S., SHUKLA, A. K., LAM, C. M., RAJAGOPAL, S., STRACHAN, R. T., HUANG, T. Y., BRESSLER, E. A., HARA, M. R., SHENOY, S. K., GYGI, S. P. & LEFKOWITZ, R. J. 2011. Distinct phosphorylation sites on the  $\beta(2)$ -adrenergic receptor establish a barcode that encodes differential functions of  $\beta$ -arrestin. *Sci Signal*, 4, ra51.
- OH, D. Y., TALUKDAR, S., BAE, E. J., IMAMURA, T., MORINAGA, H., FAN, W., LI, P., LU, W. J., WATKINS, S. M. & OLEFSKY, J. M. 2010. GPR120 is an omega-3 fatty acid receptor mediating potent anti-inflammatory and insulin-sensitizing effects. *Cell*, 142, 687-698.
- OH, D. Y., WALENTA, E., AKIYAMA, T. E., LAGAKOS, W. S., LACKEY, D., PESSENTHEINER, A. R., SASIK, R., HAH, N., CHI, T. J., COX, J. M., POWELS, M. A., DI SALVO, J., SINZ, C., WATKINS, S. M., ARMANDO, A. M., CHUNG, H., EVANS, R. M., QUEHENBERGER, O., MCNELIS, J., BOGNER-STRAUSS, J. G. & OLEFSKY, J. M. 2014. A Gpr120-selective agonist improves insulin resistance and chronic inflammation in obese mice. *Nature Medicine*, 20, 942-947.
- OHIRA, H., FUJIOKA, Y., KATAGIRI, C., MAMOTO, R., AOYAMA-ISHIKAWA, M., AMAKO, K., IZUMI, Y., NISHIUMI, S., YOSHIDA, M., USAMI, M. & IKEDA, M. 2013. Butyrate attenuates inflammation and lipolysis generated by the interaction of adipocytes and macrophages. *J Atheroscler Thromb*, 20, 425-42.
- PARK, B. O., KIM, S. H., KONG, G. Y., KIM, D. H., KWON, M. S., LEE, S. U., KIM, M.

- O., CHO, S., LEE, S., LEE, H. J., HAN, S. B., KWAK, Y. S., LEE, S. B. & KIM, S. 2016. Selective novel inverse agonists for human GPR43 augment GLP-1 secretion. *Eur J Pharmacol*, 771, 1-9.
- PASCHOAL, V. A., WALENTA, E., TALUKDAR, S., PESSENTHEINER, A. R., OSBORN, O., HAH, N., CHI, T. J., TYE, G. L., ARMANDO, A. M., EVANS, R. M., CHI, N. W., QUEHENBERGER, O., OLEFSKY, J. M. & OH, D. Y. 2020. Positive Reinforcing Mechanisms between GPR120 and PPAR $\gamma$  Modulate Insulin Sensitivity. *Cell Metab*, 31, 1173-1188.e5.
- PICASCIA, A., CAPOBIANCO, L., IACOVELLI, L. & DE BLASI, A. 2004. 21 - Analysis of Differential Modulatory Activities of GRK2 and GRK4 on G $\alpha$ q-Coupled Receptor Signaling. In: SIDEROVSKI, D. P. (ed.) *Methods in Enzymology*. Academic Press.
- PIZZONERO, M., DUPONT, S., BABEL, M., BEAUMONT, S., BIENVENU, N., BLANQUÉ, R., CHEREL, L., CHRISTOPHE, T., CRESCENZI, B., DE LEMOS, E., DELERIVE, P., DEPREZ, P., DE VOS, S., DJATA, F., FLETCHER, S., KOPIEJEWSKI, S., L'EBRALY, C., LEFRANÇOIS, J. M., LAVAZAIS, S., MANIOC, M., NELLES, L., OSTE, L., POLANCEC, D., QUÉNÉHEN, V., SOULAS, F., TRIBALLEAU, N., VAN DER AAR, E. M., VANDEGHINSTE, N., WAKSELMAN, E., BRYNS, R. & SANIERE, L. 2014. Discovery and optimization of an azetidone chemical series as a free fatty acid receptor 2 (FFA2) antagonist: from hit to clinic. *J Med Chem*, 57, 10044-57.
- PÖLL, F., DOLL C FAU - SCHULZ, S. & SCHULZ, S. Rapid dephosphorylation of G protein-coupled receptors by protein phosphatase 1 $\beta$  is required for termination of  $\beta$ -arrestin-dependent signaling.
- PREMONT, R. T. & GAINETDINOV, R. R. 2007. Physiological roles of G protein-coupled receptor kinases and arrestins. *Annu Rev Physiol*, 69, 511-34.
- PRIHANDOKO, R., ALVAREZ-CURTO, E., HUDSON, B. D., BUTCHER, A. J., ULVEN, T., MILLER, A. M., TOBIN, A. B. & MILLIGAN, G. 2016. Distinct Phosphorylation Clusters Determine the Signaling Outcome of Free Fatty Acid Receptor 4/G Protein-Coupled Receptor 120. *Molecular Pharmacology*, 89, 505.
- PRIHANDOKO, R., KAUR, D., WIEGMAN, C. H., ALVAREZ-CURTO, E., DONOVAN, C., CHACHI, L., ULVEN, T., TYAS, M. R., EUSTON, E., DONG, Z., ALHARBI, A. G. M., KIM, R. Y., LOWE, J. G., HANSBRO, P. M., CHUNG, K. F., BRIGHTLING, C. E., MILLIGAN, G. & TOBIN, A. B. 2020. Pathophysiological regulation of lung function by the free fatty acid receptor FFA4. *Sci Transl Med*, 12.

- RHEE, S. G. 2001. Regulation of Phosphoinositide-Specific Phospholipase C. *Annual Review of Biochemistry*, 70, 281-312.
- RIBAS, C., PENELA, P., MURGA, C., SALCEDO, A., GARCÍA-HOZ, C., JURADO-PUEYO, M., AYMERICH, I. & MAYOR, F. 2007. The G protein-coupled receptor kinase (GRK) interactome: Role of GRKs in GPCR regulation and signaling. *Biochimica et Biophysica Acta (BBA) - Biomembranes*, 1768, 913-922.
- ROSENBAUM, D. M., RASMUSSEN, S. G. & KOBILKA, B. K. 2009. The structure and function of G-protein-coupled receptors. *Nature*, 459, 356-63.
- ROY, C. C., KIEN, C. L., BOUTHILLIER, L. & LEVY, E. 2006. Short-chain fatty acids: ready for prime time? *Nutr Clin Pract*, 21, 351-66.
- SALEHI, A., FLODGREN, E., NILSSON, N. E., JIMENEZ-FELTSTROM, J., MIYAZAKI, J., OWMAN, C. & OLDE, B. 2005. Free fatty acid receptor 1 (FFA(1)R/GPR40) and its involvement in fatty-acid-stimulated insulin secretion. *Cell Tissue Res*, 322, 207-15.
- SAMUEL, B. S., SHAITO, A., MOTOIKE, T., REY, F. E., BACKHED, F., MANCHESTER, J. K., HAMMER, R. E., WILLIAMS, S. C., CROWLEY, J., YANAGISAWA, M. & GORDON, J. I. 2008. Effects of the gut microbiota on host adiposity are modulated by the short-chain fatty-acid binding G protein-coupled receptor, Gpr41. *Proc Natl Acad Sci U S A*, 105, 16767-72.
- SANCHEZ-REYES, O. B., COOKE, A. L. G., TRANTER, D. B., RASHID, D., EILERS, M., REEVES, P. J. & SMITH, S. O. 2017. G Protein-Coupled Receptors Contain Two Conserved Packing Clusters. *Biophys J*, 112, 2315-2326.
- SÁNCHEZ-REYES, O. B., ROMERO-ÁVILA, M. T., CASTILLO-BADILLO, J. A., TAKEI, Y., HIRASAWA, A., TSUJIMOTO, G., VILLALOBOS-MOLINA, R. & GARCÍA-SÁINZ, J. A. 2014. Free fatty acids and protein kinase C activation induce GPR120 (free fatty acid receptor 4) phosphorylation. *European Journal of Pharmacology*, 723, 368-374.
- SAWZDARGO, M., GEORGE, S. R., NGUYEN, T., XU, S., KOLAKOWSKI, L. F. & O'DOWD, B. F. 1997. A Cluster of Four Novel Human G Protein-Coupled Receptor Genes Occurring in Close Proximity to CD22 Gene on Chromosome 19q13.1. *Biochemical and Biophysical Research Communications*, 239, 543-547.
- SCHMIDT, J., SMITH, N. J., CHRISTIANSEN, E., TIKHONOVA, I. G., GRUNDMANN, M., HUDSON, B. D., WARD, R. J., DREWKE, C., MILLIGAN, G., KOSTENIS, E. & ULVEN, T. 2011. Selective orthosteric free fatty acid receptor 2 (FFA2) agonists: identification of the structural and chemical requirements for

- selective activation of FFA2 versus FFA3. *J Biol Chem*, 286, 10628-40.
- SEIBOLD, A., WILLIAMS, B., HUANG, Z. F., FRIEDMAN, J., MOORE, R. H., KNOLL, B. J. & CLARK, R. B. 2000. Localization of the sites mediating desensitization of the beta(2)-adrenergic receptor by the GRK pathway. *Mol Pharmacol*, 58, 1162-73.
- SHENOY, S. K., BARAK, L. S., XIAO, K., AHN, S., BERTHOUBE, M., SHUKLA, A. K., LUTTRELL, L. M. & LEFKOWITZ, R. J. 2007. Ubiquitination of beta-arrestin links seven-transmembrane receptor endocytosis and ERK activation. *J Biol Chem*, 282, 29549-62.
- SHENOY, S. K. & LEFKOWITZ, R. J. 2011.  $\beta$ -arrestin-mediated receptor trafficking and signal transduction. *Trends in Pharmacological Sciences*, 32, 521-533.
- SHIMIZU, H., MASUJIMA, Y., USHIRODA, C., MIZUSHIMA, R., TAIRA, S., OHUEKITANO, R. & KIMURA, I. 2019. Dietary short-chain fatty acid intake improves the hepatic metabolic condition via FFAR3. *Scientific Reports*, 9.
- SHIMPUKADE, B., HUDSON, B. D., HOVGAARD, C. K., MILLIGAN, G. & ULVEN, T. 2012. Discovery of a potent and selective GPR120 agonist. *J Med Chem*, 55, 4511-5.
- SIMON, M. I., STRATHMANN, M. P. & GAUTAM, N. 1991. Diversity of G Proteins in Signal Transduction. *Science*, 252, 802-808.
- SMITH, N. J., WARD, R. J., STODDART, L. A., HUDSON, B. D., KOSTENIS, E., ULVEN, T., MORRIS, J. C., TRANKLE, C., TIKHONOVA, I. G., ADAMS, D. R. & MILLIGAN, G. 2011. Extracellular loop 2 of the free fatty acid receptor 2 mediates allosterism of a phenylacetamide ago-allosteric modulator. *Mol Pharmacol*, 80, 163-73.
- SON, S.-E., PARK, S.-J., KOH, J.-M. & IM, D.-S. 2020. Free fatty acid receptor 4 (FFA4) activation ameliorates 2,4-dinitrochlorobenzene-induced atopic dermatitis by increasing regulatory T cells in mice. *Acta Pharmacologica Sinica*, 41, 1337-1347.
- SOSA-ALVARADO, C., HERNÁNDEZ-MÉNDEZ, A., ROMERO-ÁVILA, M. T., SÁNCHEZ-REYES, O. B., TAKEI, Y., TSUJIMOTO, G., HIRASAWA, A. & GARCÍA-SÁINZ, J. A. 2015. Agonists and protein kinase C-activation induce phosphorylation and internalization of FFA1 receptors. *European Journal of Pharmacology*, 768, 108-115.
- SPARKS, S. M., CHEN, G., COLLINS, J. L., DANGER, D., DOCK, S. T., JAYAWICKREME, C., JENKINSON, S., LAUDEMAN, C., LEESNITZER, M. A., LIANG, X., MALONEY,

- P., MCCOY, D. C., MONCOL, D., RASH, V., RIMELE, T., VULIMIRI, P., WAY, J. M. & ROSS, S. 2014. Identification of diarylsulfonamides as agonists of the free fatty acid receptor 4 (FFA4/GPR120). *Bioorg Med Chem Lett*, 24, 3100-3.
- SRIRAM, K. & INSEL, P. A. 2018. G Protein-Coupled Receptors as Targets for Approved Drugs: How Many Targets and How Many Drugs? *Mol Pharmacol*, 93, 251-258.
- SRIVASTAVA, A., YANO, J., HIROZANE, Y., KEFALA, G., GRUSWITZ, F., SNELL, G., LANE, W., IVETAC, A., AERTGEERTS, K., NGUYEN, J., JENNINGS, A. & OKADA, K. 2014. High-resolution structure of the human GPR40 receptor bound to allosteric agonist TAK-875. *Nature*, 513, 124-7.
- STENEBERG, P., RUBINS, N., BARTOOV-SHIFMAN, R., WALKER, M. D. & EDLUND, H. 2005. The FFA receptor GPR40 links hyperinsulinemia, hepatic steatosis, and impaired glucose homeostasis in mouse. *Cell Metab*, 1, 245-58.
- STERNE-MARR, R., BAILLARGEON, A. I., MICHALSKI, K. R. & TESMER, J. J. 2013. Expression, purification, and analysis of G-protein-coupled receptor kinases. *Methods Enzymol*, 521, 347-66.
- STERNE-MARR, R., DHAMI, G. K., TESMER, J. J. G. & FERGUSON, S. S. G. 2004. 20 - Characterization of GRK2 RH Domain-Dependent Regulation of GPCR Coupling to Heterotrimeric G Proteins. In: SIDEROVSKI, D. P. (ed.) *Methods in Enzymology*. Academic Press.
- STODDART, L. A., SMITH, N. J., JENKINS, L., BROWN, A. J. & MILLIGAN, G. 2008a. Conserved polar residues in transmembrane domains V, VI, and VII of free fatty acid receptor 2 and free fatty acid receptor 3 are required for the binding and function of short chain fatty acids. *J Biol Chem*, 283, 32913-24.
- STODDART, L. A., SMITH, N. J. & MILLIGAN, G. 2008b. International Union of Pharmacology. LXXI. Free Fatty Acid Receptors FFA1, -2, and -3: Pharmacology and Pathophysiological Functions. *Pharmacological Reviews*, 60, 405.
- STONE, V. M., DHAYAL, S., BROCKLEHURST, K. J., LENAGHAN, C., SÖRHEDE WINZELL, M., HAMMAR, M., XU, X., SMITH, D. M. & MORGAN, N. G. 2014. GPR120 (FFAR4) is preferentially expressed in pancreatic delta cells and regulates somatostatin secretion from murine islets of Langerhans. *Diabetologia*, 57, 1182-1191.
- STRAUSBERG, R. L., FEINGOLD, E. A., GROUSE, L. H., DERGE, J. G., KLAUSNER, R.

- D., COLLINS, F. S., WAGNER, L., SHENMEN, C. M., SCHULER, G. D., ALTSCHUL, S. F., ZEEBERG, B., BUETOW, K. H., SCHAEFER, C. F., BHAT, N. K., HOPKINS, R. F., JORDAN, H., MOORE, T., MAX, S. I., WANG, J., HSIEH, F., DIATCHENKO, L., MARUSINA, K., FARMER, A. A., RUBIN, G. M., HONG, L., STAPLETON, M., SOARES, M. B., BONALDO, M. F., CASAVANT, T. L., SCHEETZ, T. E., BROWNSTEIN, M. J., USDIN, T. B., TOSHIYUKI, S., CARNINCI, P., PRANGE, C., RAHA, S. S., LOQUELLANO, N. A., PETERS, G. J., ABRAMSON, R. D., MULLAHY, S. J., BOSAK, S. A., MCEWAN, P. J., MCKERNAN, K. J., MALEK, J. A., GUNARATNE, P. H., RICHARDS, S., WORLEY, K. C., HALE, S., GARCIA, A. M., GAY, L. J., HULYK, S. W., VILLALON, D. K., MUZNY, D. M., SODERGREN, E. J., LU, X., GIBBS, R. A., FAHEY, J., HELTON, E., KETTEMAN, M., MADAN, A., RODRIGUES, S., SANCHEZ, A., WHITING, M., MADAN, A., YOUNG, A. C., SHEVCHENKO, Y., BOUFFARD, G. G., BLAKESLEY, R. W., TOUCHMAN, J. W., GREEN, E. D., DICKSON, M. C., RODRIGUEZ, A. C., GRIMWOOD, J., SCHMUTZ, J., MYERS, R. M., BUTTERFIELD, Y. S., KRZYWINSKI, M. I., SKALSKA, U., SMAILUS, D. E., SCHNERCH, A., SCHEIN, J. E., JONES, S. J. & MARRA, M. A. 2002. Generation and initial analysis of more than 15,000 full-length human and mouse cDNA sequences. *Proc Natl Acad Sci U S A*, 99, 16899-903.
- SUCKOW, A. T., POLIDORI, D., YAN, W., CHON, S., MA, J. Y., LEONARD, J. & BRISCOE, C. P. 2014. Alteration of the glucagon axis in GPR120 (FFAR4) knockout mice: a role for GPR120 in glucagon secretion. *J Biol Chem*, 289, 15751-63.
- SUM, C. S., TIKHONOVA, I. G., COSTANZI, S. & GERSHENGORN, M. C. 2009. Two arginine-glutamate ionic locks near the extracellular surface of FFAR1 gate receptor activation. *J Biol Chem*, 284, 3529-36.
- SUM, C. S., TIKHONOVA, I. G., NEUMANN, S., ENGEL, S., RAAKA, B. M., COSTANZI, S. & GERSHENGORN, M. C. 2007. Identification of residues important for agonist recognition and activation in GPR40. *J Biol Chem*, 282, 29248-55.
- SUN, P., WANG, T., ZHOU, Y., LIU, H., JIANG, H., ZHU, W. & WANG, H. 2013. DC260126: A Small-Molecule Antagonist of GPR40 that Protects against Pancreatic  $\beta$ -Cells Dysfunction in db/db Mice. *PLOS ONE*, 8, e66744.
- SUNDSTRÖM, L., MYHRE, S., SUNDQVIST, M., AHNMARK, A., MCCOULL, W., RAUBO, P., GROOMBRIDGE, S. D., POLLA, M., NYSTRÖM, A. C., KRISTENSSON, L., NÅGÅRD, M. & WINZELL, M. S. 2017. The acute glucose lowering effect of specific GPR120 activation in mice is mainly driven by glucagon-like peptide 1. *PLoS One*, 12, e0189060.

- SUZUKI, T., IGARI, S.-I., HIRASAWA, A., HATA, M., ISHIGURO, M., FUJIEDA, H., ITOH, Y., HIRANO, T., NAKAGAWA, H., OGURA, M., MAKISHIMA, M., TSUJIMOTO, G. & MIYATA, N. 2008. Identification of G protein-coupled receptor 120-selective agonists derived from PPAR $\gamma$  agonists. *Journal of Medicinal Chemistry*, 51, 7640-7644.
- SYKARAS, A. G., DEMENIS, C., CASE, R. M., MCLAUGHLIN, J. T. & SMITH, C. P. 2012. Duodenal enteroendocrine I-cells contain mRNA transcripts encoding key endocannabinoid and fatty acid receptors. *PLoS One*, 7, e42373.
- TANAKA, T., YANO, T., ADACHI, T., KOSHIMIZU, T.-A., HIRASAWA, A. & TSUJIMOTO, G. 2008. Cloning and characterization of the rat free fatty acid receptor GPR120: in vivo effect of the natural ligand on GLP-1 secretion and proliferation of pancreatic  $\beta$  cells. *Naunyn-Schmiedeberg's Archives of Pharmacology*, 377, 515-522.
- TEDELIND, S., WESTBERG, F., KJERRULF, M. & VIDAL, A. 2007. Anti-inflammatory properties of the short-chain fatty acids acetate and propionate: a study with relevance to inflammatory bowel disease. *World J Gastroenterol*, 13, 2826-32.
- THAL, D. M., YEOW RY FAU - SCHOENAU, C., SCHOENAU C FAU - HUBER, J., HUBER J FAU - TESMER, J. J. G. & TESMER, J. J. Molecular mechanism of selectivity among G protein-coupled receptor kinase 2 inhibitors.
- TIKHONOVA, I. G. 2017. Application of GPCR Structures for Modelling of Free Fatty Acid Receptors. *Handb Exp Pharmacol*, 236, 57-77.
- TIKHONOVA, I. G. & POERIO, E. 2015. Free fatty acid receptors: structural models and elucidation of ligand binding interactions. *BMC Struct Biol*, 15, 16.
- TIKHONOVA, I. G., SUM, C. S., NEUMANN, S., THOMAS, C. J., RAAKA, B. M., COSTANZI, S. & GERSHENGORN, M. C. 2007. Bidirectional, Iterative Approach to the Structural Delineation of the Functional "Chemoprint" in GPR40 for Agonist Recognition. *Journal of Medicinal Chemistry*, 50, 2981-2989.
- TOBIN, A. B. 2008. G-protein-coupled receptor phosphorylation: where, when and by whom. *Br J Pharmacol*, 153 Suppl 1, S167-76.
- TOHGO, A., CHOY, E. W., GESTY-PALMER, D., PIERCE, K. L., LAPORTE, S., OAKLEY, R. H., CARON, M. G., LEFKOWITZ, R. J. & LUTTRELL, L. M. 2003. The stability of the G protein-coupled receptor-beta-arrestin interaction determines the mechanism and functional consequence of ERK activation.



*J Biol Chem*, 278, 6258-67.

- TOLHURST, G., HEFFRON, H., LAM, Y. S., PARKER, H. E., HABIB, A. M., DIAKOIANNAKI, E., CAMERON, J., GROSSE, J., REIMANN, F. & GRIBBLE, F. M. 2012. Short-chain fatty acids stimulate glucagon-like peptide-1 secretion via the G-protein-coupled receptor FFAR2. *Diabetes*, 61, 364-71.
- TRAN, T. M., FRIEDMAN, J., QUNAIBI, E., BAAMEUR, F., MOORE, R. H. & CLARK, R. B. 2004. Characterization of Agonist Stimulation of cAMP-Dependent Protein Kinase and G Protein-Coupled Receptor Kinase Phosphorylation of the  $\beta_2$ -Adrenergic Receptor Using Phosphoserine-Specific Antibodies. *Molecular Pharmacology*, 65, 196.
- UEHLING, D. E., JOSEPH, B., CHUNG, K. C., ZHANG, A. X., LER, S., PRAKESCH, M. A., PODA, G., GROULEFF, J., AMAN, A., KIYOTA, T., LEUNG-HAGESTEIJN, C., KONDA, J. D., MARCELLUS, R., GRIFFIN, C., SUBRAMANIAM, R., ABIBI, A., STRATHDEE, C. A., ISAAC, M. B., AL-AWAR, R. & TIEDEMANN, R. E. 2021. Design, Synthesis, and Characterization of 4-Aminoquinazolines as Potent Inhibitors of the G Protein-Coupled Receptor Kinase 6 (GRK6) for the Treatment of Multiple Myeloma. *J Med Chem*, 64, 11129-11147.
- UNSON, C. G., WU, C.-R., JIANG, Y., YOO, B., CHEUNG, C., SAKMAR, T. P. & MERRIFIELD, R. B. 2002. Roles of Specific Extracellular Domains of the Glucagon Receptor in Ligand Binding and Signaling. *Biochemistry*, 41, 11795-11803.
- VENKATAKRISHNAN, A. J., DEUPI, X., LEBON, G., TATE, C. G., SCHERTLER, G. F. & BABU, M. M. 2013. Molecular signatures of G-protein-coupled receptors. *Nature*, 494, 185-194.
- VOGEL, R., MAHALINGAM, M., LÜDEKE, S., HUBER, T., SIEBERT, F. & SAKMAR, T. P. 2008. Functional role of the "ionic lock"--an interhelical hydrogen-bond network in family A heptahelical receptors. *J Mol Biol*, 380, 648-55.
- WANG, Y., JIAO, X., KAYSER, F., LIU, J., WANG, Z., WANSKA, M., GREENBERG, J., WEISZMANN, J., GE, H., TIAN, H., WONG, S., SCHWANDNER, R., LEE, T. & LI, Y. 2010. The first synthetic agonists of FFA2: Discovery and SAR of phenylacetamides as allosteric modulators. *Bioorganic & Medicinal Chemistry Letters*, 20, 493-498.
- WANG, Y., LIU, J., DRANSFIELD, P. J., ZHU, L., WANG, Z., DU, X., JIAO, X., SU, Y., LI, A.-R., BROWN, S. P., KASPARIAN, A., VIMOLRATANA, M., YU, M., PATTAROPONG, V., HOUZE, J. B., SWAMINATH, G., TRAN, T., NGUYEN, K.,

- GUO, Q., ZHANG, J., ZHUANG, R., LI, F., MIAO, L., BARTBERGER, M. D., CORRELL, T. L., CHOW, D., WONG, S., LUO, J., LIN, D. C. H. & MEDINA, J. C. 2013. Discovery and Optimization of Potent GPR40 Full Agonists Containing Tricyclic Spirocycles. *ACS Medicinal Chemistry Letters*, 4, 551-555.
- WATSON, S. J., BROWN, A. J. & HOLLIDAY, N. D. 2012. Differential signaling by splice variants of the human free fatty acid receptor GPR120. *Mol Pharmacol*, 81, 631-42.
- WATTERSON, K. R., HANSEN, S. V. F., HUDSON, B. D., ALVAREZ-CURTO, E., RAIHAN, S. Z., AZEVEDO, C. M. G., MARTIN, G., DUNLOP, J., YARWOOD, S. J., ULVEN, T. & MILLIGAN, G. 2017. Probe-Dependent Negative Allosteric Modulators of the Long-Chain Free Fatty Acid Receptor FFA4. *Mol Pharmacol*, 91, 630-641.
- YANG, Z., YANG, F., ZHANG, D., LIU, Z., LIN, A., LIU, C., XIAO, P., YU, X. & SUN, J.-P. 2017. Phosphorylation of G Protein-Coupled Receptors: From the Barcode Hypothesis to the Flute Model. *Molecular Pharmacology*, 92, 201.
- YATES, C. M., CALDER, P. C. & ED RAINGER, G. 2014. Pharmacology and therapeutics of omega-3 polyunsaturated fatty acids in chronic inflammatory disease. *Pharmacology & Therapeutics*, 141, 272-282.
- ZHANG, D. & LEUNG, P. S. 2014. Potential roles of GPR120 and its agonists in the management of diabetes. *Drug Des Devel Ther*, 8, 1013-27.
- ZHOU, C., TANG, C., CHANG, E., GE, M., LIN, S., CLINE, E., TAN, C. P., FENG, Y., ZHOU, Y. P., EIERMANN, G. J., PETROV, A., SALITURO, G., MEINKE, P., MOSLEY, R., AKIYAMA, T. E., EINSTEIN, M., KUMAR, S., BERGER, J., HOWARD, A. D., THORNBERRY, N., MILLS, S. G. & YANG, L. 2010. Discovery of 5-aryloxy-2,4-thiazolidinediones as potent GPR40 agonists. *Bioorg Med Chem Lett*, 20, 1298-301.
- ZHU, S., JIANG, X., JIANG, S., LIN, G., GONG, J., CHEN, W., HE, Z. & CHEN, Y. Q. 2018. GPR120 is not required for omega-3 PUFAs-induced cell growth inhibition and apoptosis in breast cancer cells. *Cell Biol Int*, 42, 180-186.
- ZIEGLER, N., BÄTZ, J., ZABEL, U., LOHSE, M. J. & HOFFMANN, C. 2011. FRET-based sensors for the human M1-, M3-, and M5-acetylcholine receptors. *Bioorg Med Chem*, 19, 1048-54.